

Summer 2021

A Multi Physics Integrated Solution for a High-pressure Stage Turbine Efficiency and Durability

Sanjay Chopra

Follow this and additional works at: <https://scholarcommons.sc.edu/etd>



Part of the [Mechanical Engineering Commons](#)

Recommended Citation

Chopra, S.(2021). *A Multi Physics Integrated Solution for a High-pressure Stage Turbine Efficiency and Durability*. (Doctoral dissertation). Retrieved from <https://scholarcommons.sc.edu/etd/6435>

This Open Access Dissertation is brought to you by Scholar Commons. It has been accepted for inclusion in Theses and Dissertations by an authorized administrator of Scholar Commons. For more information, please contact dillarda@mailbox.sc.edu.

A MULTI PHYSICS INTEGRATED SOLUTION FOR A HIGH-PRESSURE STAGE TURBINE
EFFICIENCY AND DURABILITY

by

Sanjay Chopra

Bachelor of Science
New York Institute of Technology, 1991

Master of Science
New York Institute of Technology, 1998

Submitted in Partial Fulfillment of the Requirements

For the Degree of Doctorate in

Mechanical Engineering

College of Engineering & Computing

University of South Carolina

2021

Accepted by:

Jamil Khan, Major Professor

Tanvir Farouk, Committee Member

Chen Li, Committee Member

Je-Chin, Committee Member

Michael Foust, Committee Member

Tracey L. Weldon, Interim Vice Provost and Dean of the Graduate School

© Copyright by Sanjay Chopra, 2021
All Rights Reserved.

ABSTRACT

World electricity demand is projected to grow at an annual rate of $\sim 2.1\%$ to year 2040₁. EIA projects nearly 50% increase in world energy usage by 2050 led by growth in Asia.[28];[29]. It is predicted that the global electricity demand grows at approximately 1.6 % per year from approximately 2008 and forecasted to approximately 2035, twice the rate of primary energy demand. This raises electricity's usage in total final energy consumption from approximately 19% in 2018 to approximately 24% in 2040. Electricity demand growth is set to be particularly strong in developing economies. .[28];[29];[38]

As an enabler, to meet the aforementioned targets, market success has been and currently is the prime driver towards further enhancing the demand for the worldwide power generation industry; to advance beyond their current technological prowess and continuously drive the overall enhancement for highly efficient, carbon neutral and robust power generating equipment. Technologies aligned to the prime power generating machines, gas and steam turbines have been evolving for decades. However, it is not until relatively recently that full awareness and prime focus of addressing fuel cost, plant availability and increases in RAM (Reliability, Availability & Maintainability) and most of all addressing environmental concerns such as reduction of carbon footprint, collectively have prompted a paradigm shift in constantly challenging the status quo on turbine heat rate and the associated longevity of the Hot Gas Path components, due to harsh environments. To ensure meeting the challenges of constantly increasing the

overall thermodynamic cycle efficiency for both simple and combined cycle applications; the author applies his knowledge garnered from his academic and professional experiences, in conjunction with his in-depth research of thoroughly comprehending the pivotal challenges in the power generation realm, and hence by doing so; the author has endeavored to traverse upon an academic journey of profound understanding to mathematically integrate the necessary physics based scientific principles imbedded in the various engineering related disciplines that are directly applied into the field of turbomachinery. The author has profoundly researched and humbly applied the known scientific principles based on the fundamental laws of one-dimensional aerodynamics, thermodynamics & cycle performance, Gas dynamics, fluid mechanics, heat transfer, structural assessments of materials and the tools of mathematics and thus has generated a unique set of regression equations or rather transfer functions that unifies or rather synergistically couples the fundamental scientific principles as stated above. The unified consolidated theoretical formulation hence produced, can be applied towards predicting from a preliminary perspective, the impact of a single stage high pressure turbine's performance characteristics and simultaneously also predict from a preliminary perspective, the overall gas turbine thermal efficiency, as a function of varying engine critical to quality parameters, AK. A pivotal CTQ's. The methodology and execution approach that has been applied to establish the author's proposal has been conducted by synergizing the fundamental multi-physics-based engineering disciplines delineating specifically the high-pressure turbine stage simple cycle engine operation. The author has produced a series of multiple regression or transfer functions, capturing or rather reflecting the prime influence of the assortment of technical enablers which allows for

further investigating its impact on turbine thermal efficiency and associated component durability that directly influences the overall machine performance, life cycle of the component and finally its influence on the heat rate of the single stage simple cycle gas turbine; which is indeed a key economic factor in the commercial arena. Hence to address the gargantuan and challenging requirement to meet the ever-increasing demand for power generation; expeditious engine assessment, part evaluation and dispositioning of turbine component integrity while simultaneously sustaining optimal engine heat rate are required to be assessed.

TABLE OF CONTENTS

| | |
|---|-----|
| ABSTRACT..... | iii |
| LIST OF TABLES | x |
| LIST OF FIGURES | xi |
| LIST OF SYMBOLS | xiv |
| CHAPTER 1: INTRODUCTION | 1 |
| (1.1) Background Information..... | 2 |
| (1.2) Purpose | 5 |
| (1.3) Objective & Scope..... | 9 |
| (1.4) Assumptions & Rationale | 11 |
| CHAPTER 2: LITERATURE SEARCH..... | 17 |
| (2.1) Overview of Gas Turbine -Simple & Combined Cycle thermodynamics [1] [2] | 17 |
| (2.2) Brief overview of the Gas turbine functionality and operation | 22 |
| (2.3) High Pressure Turbine Emphasis | 24 |
| (2.4) Current challenges for the High-Pressure Turbine and proposed scope of work..... | 35 |
| CHAPTER 3: INTRODUCING THE CONTROL VOLUME APPROACH WITHIN THE GAS TURBINE | 38 |

| | |
|---|-----------|
| (3.1) High Pressure Turbine Control Volume: A Multi-Physics / synergistic approach | 38 |
| (3.2) Establishing the Region of Interest pertaining to this Dissertation | 44 |
| (3.3) Identifying and establishing a “Synergistic” approach of the key control volumes | 45 |
| (3.4) Basic Thermodynamics principles applied to region of interest: | 46 |
| (3.5) Identification of the Main Control Volume for the Stationary Component | 48 |
| (3.6) Control volume rationale and alignment to dissertation focus | 49 |
| (3.7) Basic physics-based engineering assumptions & application for each Control Volume | 51 |
| CHAPTER 4: DETAILED PHYSICS BASED MATHEMATICAL DERIVATIONS OF THE KEY CONTROL VOLUMES | 54 |
| (4.1) Physics based evaluation of the High-Pressure Turbine Conservation of energy leading to the energy balance process | 54 |
| (4.2) High Pressure Turbine Evaluation and Assessment of the Control Volumes established | 62 |
| CHAPTER 5: ESTABLISHING OVERALL SYNERGY OF HPT BASED DISCIPLINE INTEGRATION ALIGNED TO EACH KEY CONTROL VOLUME | 84 |
| (5.1) Steady 1D isentropic Flow physics derivations aligned to HPT control volumes | 85 |
| (5.2) Basic Turbomachinery assumptions-based derivations aligned to control volumes | 88 |
| (5.3) Continuing evaluation of the Gas Turbine Thermodynamics aligned to control volumes | 91 |

| | |
|---|------------|
| (5.4) Deriving the expression of the mass flow rate & flow function equations aligned to control volumes | 94 |
| (5.5) 1-D: Derivation of mean-line Aerodynamics formulations aligned to control volumes | 118 |
| (5.6) External environment: Hot Gas Path parameter derivation aligned to control volumes | 124 |
| (5.7) Internal environment: Component cooling parameter derivation aligned to control | 140 |
| CHAPTER 6: THE UNIFIED MULTI-PHYSICS HPT FORMULATION – A MULTIPLE RESPONSE SURFACE FORMULATION..... | 151 |
| (6.1) Mathematical formulations depicting overall discipline synergy for Response surface-1 stage thermal efficiency | 153 |
| (6.2) Response Surface-2: Aligning unified HPT formulation to the Stress Field | 162 |
| (6.3) Final derived Unified Multi-Physics HPT Equations explanation and application..... | 178 |
| CHAPTER 7: VALIDATION OF THE ANALYTICAL BASED UNIFIED HIGH-PRESSURE TURBINE COMPARED TO LITERATURE RESEARCH | 180 |
| (7.1) Gas Turbine Overall Thermal Efficiency (UHPT Process Vs. GT World Simple Cycle Specifications Efficiency data. [51] | 180 |
| CHAPTER 8: HIGH PRESSURE TURBINE ; UHPT PROCESS SENSITIVITY OF THE KEY PARAMETERS ASSESSMENT | 184 |
| (8.1) Sensitivity of Temperature to Cooled Turbine Stage Efficiency η_t , for various Compressor Pressure Ratio and Gas Turbine Exhaust Temperature ranges | 184 |
| CHAPTER 9: CONCLUSIONS AND REMARKS | 186 |

| | |
|---|-----|
| (9.1) Uncertainty band & Range of Parameters | 189 |
| REFERENCES | 190 |
| APPENDIX A: GAS TURBINE OVERALL THERMAL EFFICIENCY (UHPT PROCESS VS. GT WORLD SIMPLE CYCLE SPECIFICATIONS EFFICIENCY DATA- (2020 36 TH EDITION) | 197 |
| APPENDIX B: COMPARISON OF COMPRESSOR PRESSURE RATIO'S VS. HEATV RATES (BTU/KW-HR.) | 199 |
| APPENDIX C: GAS TURBINE EXHAUST TEMPERATURE VS. COMPRESSOR PRESSURE RATIO | 200 |
| APPENDIX D: COMPARISON OF THE UNCOOLED TURBINE EFFICIENCY(UHPT) η_T % VS. η_T -ADIABATIC % (BASED ON TURBINE (HPT) ISENTROPIC EQUATION-NO TURBINE COOLING) | 201 |

LIST OF TABLES

| | |
|---|-----|
| Table A.1: Gas Turbine Overall Thermal Efficiency (UHPT Process Vs. GT World Simple Cycle Specifications Efficiency data- (2020 36th Edition) | 198 |
| Table B.1: Comparison of Compressor Pressure Ratio's vs.Heatv Rates (Btu/Kw-Hr.)..... | 199 |
| Table C.1 Gas Turbine Exhaust Temperature Vs. Compressor Pressure Ratio..... | 200 |
| Table D.1 Comparison of the uncooled turbine efficiency (UHPT) η_t % Vs. η_t -Adiabatic % (Based on Turbine (HPT) Isentropic equation-No Turbine Cooling) | 201 |

LIST OF FIGURES

| | |
|--|----|
| Figure 1.1 World Energy Consumption year (1990 – 2035) [38]..... | 1 |
| Figure 1.2 World Electricity generation by fuel types [38] | 1 |
| Figure 1.3 Example of a Combined Cycle power plant [32] [41] [56] [57] | 8 |
| Figure 1.4 Components of a simple cycle gas turbine [37] | 10 |
| Figure 1.5 Schematic of a First Stage Gas Turbine High-Pressure Turbine [34] | 12 |
| Figure 1.6 Various types of cooling mechanisms [19] | 15 |
| Figure 1.7 Heat Load Vs. Cooling Effectiveness [20]..... | 15 |
| Figure 1.8 Higher TIT & RIT leads to Advanced Cooling mechanisms [39] [58] | 15 |
| Figure 2.1 Cross section of a typical Large Gas Turbine [36]..... | 18 |
| Figure 2.2 Schematic of a Gas Turbine Simple Cycle [37] | 19 |
| Figure 2.3 Key parameters from the Brayton cycle aligned to the Gas Turbine [41] | 21 |
| Figure 2.4 Example of a Combustor burner [42] | 24 |
| Figure 2.5 Coatings on blades [43] | 27 |
| Figure 2.6 Turbine Hot Section flow physics | 28 |
| Figure 2.7 The Axial Flow Turbine [34] | 29 |
| Figure 2.8 Flow Physics of the Axial Flow turbine [4] | 30 |
| Figure 2.9 The Cooling Effectiveness & Heat Load parameter depends primarily on the following factors [44]..... | 31 |

| | |
|---|-----|
| Figure 2.10 External Gas path heat transfer flow physics example [45] | 33 |
| Figure 2.11 Effect of turbine inlet pressure and temperature on coolant flow requirements [17] | 34 |
| Figure 2.12 Effect of combining effective gas path cooling and convection cooling [17]..... | 34 |
| Figure 3.1 Thermodynamic State Points reflecting overall Gas Brayton Cycle [36] | 39 |
| Figure 3.2 Enthalpy Extraction temperature Plane(EET) | 44 |
| Figure 3.3 High Pressure Turbine- Main region of focus including multiple Control..... | 49 |
| Figure 3.4 Typical Control Volume assessment for purpose of simplicity | 52 |
| Figure 4.1 Temperature Variation within the control volumes..... | 57 |
| Figure 4.2 Control Volume 3A | 63 |
| Figure 4.3 Control Volume (3B)..... | 67 |
| Figure 4.4 Control Volume (2) | 80 |
| Figure 4.5 Control Volume (effective gas path cooling Domain) | 83 |
| Figure 5.1 1D-Mean-Line Aerodynamics state points [4] | 101 |
| Figure 5.2 Description of the Velocity Triangle [4] | 106 |
| Figure 5.3 Flat Plate Boundary Layer example | 129 |
| Figure 5.4 Cylinder in cross flow boundary layer example..... | 138 |
| Figure 5.5 Airfoil Suction side Control volume; Mixing Plane..... | 146 |
| Figure 5.6 Stage 1 Nozzle Throat area assumptions..... | 147 |
| Figure 6.1 Cross section assumed for Substrate undergoing thermal stress | 163 |
| Figure 6.2 Overall Stress Field description..... | 164 |
| Figure 6.3 Depiction of Normal Strains..... | 167 |

| | |
|---|-----|
| Figure 6.4 Element in plane stress | 167 |
| Figure 7.1 Gas Turbine Overall Thermal Efficiency (UHPT Process Vs. GT World) | 180 |
| Figure 7.2 Gas Turbine Overall Thermal Efficiency (UHPT Process Vs. GT World) Simple Cycle Turbine Temperature Characteristics- aligned to Engine Heat Rate Specifications Efficiency data- (2020 36th Edition) Literature Search..... | 181 |
| Figure 7.3 Comparison of the Cooled Turbine Efficiency (UHPT Formulation) Vs. The Turbine Isentropic Formulation without Cooling & also Comparison of the UHPT (No Cooling) Vs. Turbine Isentropic Formulation without Cooling | 182 |
| Figure 7.4 Sensitivity of Control Volume Mixed Temperature, to cooled turbine stage efficiency for range of Compressor Pressure Ratio & Turbine Exhaust Temperature | 183 |
| Figure 8.1 Gas turbine – Sensitivity of Control Volume Mixed Temperature, to cooled turbine stage efficiency for range of Compressor Pressure Ratio & Turbine Exhaust Temperature..... | 184 |
| Figure 8.2 Gas turbine – Sensitivity of Mixed temperature TCV1 out, to cooled turbine stage efficiency for range of Compressor Pressure Ratio & Turbine Exhaust Temperatures- A detailed view | 185 |

LIST OF SYMBOLS

| | |
|------------|---|
| α_1 | Nozzle incidence Flow angle at the entrance of the stage 1 nozzle, at location station 1 |
| α_2 | Nozzle Flow angle at the exit of the stage 1 nozzle, at location station 2 |
| V_2 | Absolute velocity of the flow exiting the nozzle at the stationary frame of reference, at station 2. |
| v_{2R} | Relative velocity of the flow entering the rotating frame of reference at the blade incidence angle β_2 |
| β_2 | Blade incidence flow angle at the inlet conditions to the blade |
| U_2 | Axial component of the velocity at the stage 1 nozzle exit |
| v_2 | Tangential component of the velocity at the stage 1 nozzle exit |
| v_3 | Tangential component of the velocity at the stage 1 blade exit |
| T_{t1} | Absolute “total” temperature at station 1, at the inlet of the stage 1 Nozzle, A.K.A Turbine inlet temperature “TIT”. |
| T_{s1} | Static temperature at station 1, at the inlet of the stage 1 Nozzle. |
| P_{t1} | Absolute “total” pressure at station 1, at the inlet of the stage 1 Nozzle. |
| P_{s1} | Static pressure at station 1, at the inlet of the stage 1 Nozzle |
| P_{T2R} | Relative pressure at the entrance of the blade at the rotating frame of reference |
| T_{t2} | Absolute “total” temperature at station 2, at the exit of the stage 1 Nozzle |
| T_{s2} | Static temperature at station 2, at the exit of the stage 1 Nozzle. |

| | |
|------------|---|
| Tt2R | Relative Mach# at the entrance of the blade at the rotating frame of reference. |
| Pt2 | Absolute “total” pressure at station 2, at the exit of the stage 1 Nozzle. |
| Ps2 | Static pressure at station 2, at the exit of the stage 1 Nozzle |
| PT2R | Relative pressure at the exit of the blade at the rotating frame of reference |
| Tt3 | Absolute “total” temperature at station 3, at the exit of the stage 1 blade |
| Ts3 | Static temperature at station 3, at the exit of the stage 1 blade |
| Tt3R | Relative Mach# at the exit of the blade at the rotating frame of reference. |
| Pt3 | Absolute “total” pressure at station 3, at the exit of the stage 1 blade |
| Ps3 | Static pressure at station 1, at the inlet of the stage 1 Nozzle |
| PT2R | Relative pressure at the entrance of the blade at the rotating frame of reference |
| M1 | Absolute Inlet Mach# at the entrance of the stage 1 nozzle, at location station 1 |
| M2 | Absolute Exit Mach# at the throat area of the stage 1 nozzle, at location station 2 |
| M3 | Absolute Mach# at station 3, at the exit of the stage 1 blade |
| M2R | Relative pressure at the entrance of the blade at the rotating frame of reference |
| M3R | Relative pressure at the exit of the blade at the rotating frame of reference |
| β_3 | Blade incidence flow angle at the exit conditions to the blade |
| V_3 | Absolute component of the velocity at exit of the blade, at station 3 |
| U_3 | This is the axial component of the velocity at exit of the blade at station 3 |
| α_3 | Absolute Flow angle at the exit of the stage 1 blade, at location station 3, and is also termed as the swirl angle |
| H | Enthalpy of the fluid |
| U | Fluid internal energy |
| P | Fluid pressure |

| | |
|---------------------|---|
| V | Fluid volume |
| W | Work |
| h' | Total enthalpy |
| Cf | Local friction coefficient |
| St | Stanton number |
| Re _x | Reynolds number |
| q'' | Convective heat flux |
| T _s | Object surface temperature |
| T _∞ | Gas path fluid stream temperature |
| h | Convective heat transfer coefficient – cooling passages |
| Nu | Nusselt number |
| H _{gx} | Convective heat transfer coefficient – gas path flow |
| K _g | Fluid “gas” conductivity |
| ρ | Gas density Kg/m ³ |
| V _g | Gas velocity component in the x, direction; m/sec; ft/sec |
| μ | Fluid viscosity, (N * Sec)/m ² ; lb./Ft * sec |
| Pr | Prandtl number = K * μ * Cp/kgas |
| K | Dimensional Constant |
| δ | Velocity boundary thickness |
| $\frac{\dot{W}}{A}$ | Flow Flux |
| \dot{W} | Flow rate lbm/Sec |
| Φ | Flow function |
| A _m | Actual resistance flow “Mechanical” area |

| | |
|--------------------|---|
| A_t | Actual resistance flow “Throat” area |
| X | Characteristic distance |
| η_{tc} | Cooled Turbine thermal efficiency |
| η_{tuc} | Uncooled Turbine thermal efficiency |
| γ | Gamma – Fluid specific heat ratio |
| C_{pg} | Hot gas path specific heat capacity |
| C_{pc} | Coolant path specific heat capacity |
| ω | Rotation -RPM |
| r | Component radius to the engine centerline |
| β | Is defined to be the “Heat Vector |
| $\sigma_{x,y,z}$ | Stress in three dimensions |
| $\epsilon_{x,y,z}$ | Strain in three dimensions |
| σ_{thx} | Thermal Stress |
| Π_t | Turbine Pressure Ratio |
| η_t | High pressure turbine; thermal efficiency number. |

CHAPTER 1:

INTRODUCTION

World marketed energy consumption is forecasted to enhance by 53 percent from the year 2008 to the year 2035 (Figure 1.1). Total world energy utility rises from 505 quadrillion British thermal units (Btu) in 2008 to 619 quadrillion Btu in 2020 and 770 quadrillion Btu in 2035. The majority of the growth in energy consumption occurs in countries outside the Organization for Economic Cooperation and Development (non-OECD nations) where the demand for energy usage is driven by strong long-term economic growth. Energy usage in non-OECD nations increases by 85 percent in the reference case, as compared with an increase of 18 percent for the OECD economies.[38]

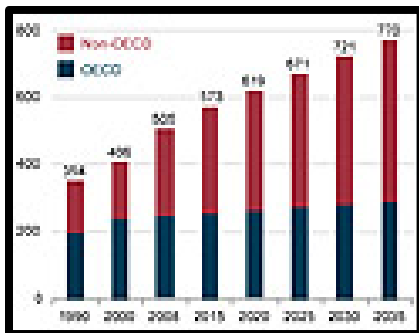


Figure 1.1 World Energy Consumption year (1990 – 2035) [38]

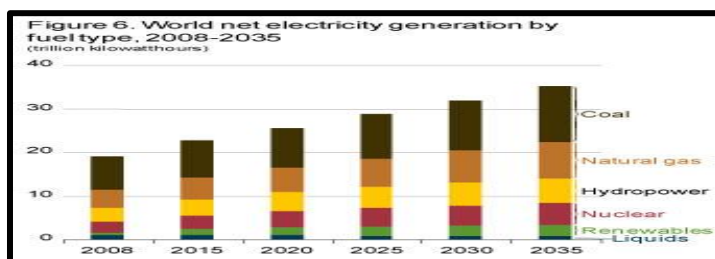


Figure 1.2 World Electricity generation by fuel types [38]

World net electricity generation increases by 84 percent in the IEO2011 Reference case, from 19.1 trillion kilowatt-hours in 2008 and was forecasted to 25.5 trillion kilowatt-hours in 2020 and is forecasted to 35.2 trillion kilowatt-hours in 2035. [38]

(1.1) Background Information

Even though the 2008-2009 global economic recessions impacted and hence decreased the rate of growth in electricity use in 2008 which resulted in negligible change in electricity use in 2009, the demand for electricity generation was resurrected in 2010, which was led by strong recoveries in non-OECD economies. Usually in OECD countries, where electricity markets are well established and mature energy consumption patterns are inherent, the corresponding growth of electricity demand is less than in non-OECD countries, whereas in non-OECD regions a large amount of potential energy demand remains pending. [29]

Total net electricity generation in non-OECD countries tends to increase by an average of 3.3 percent per year in the reference case, led by non-OECD Asia (including China and India), where annual increases average 4.0 percent from 2008 to 2035; in contrast to the net generation among OECD [46][29]

Hence to address the gargantuan and challenging requirement to meet the ever-increasing demand for power generation; expeditious assessment, evaluation and dispositioning of turbine component integrity based on the optimal engine thermodynamic performance parameters are required to be predicted. This is highly needed to evaluate and ensure executing appropriate business decisions towards maintaining the longevity of the components considering optimum quality, design for manufacturing, time to market and competitive cost.

To improve and simultaneously compete in the power generation industry, focus on technology advancements not only within the domain of a specific gas and steam turbine component are required, but applying the synergistic aspects of the various key technology enablers ranging from performance/thermodynamics, aerodynamics, secondary flows, durability, manufacturing etc., is also required and is of the utmost importance to ensure optimal overall product quality and its impact to the advancement of society by drastically reducing carbon emissions and hence addressing pollution and subsequently positively impacting the environment.

It is thus forecasted [46][30] that the next three decades will most probably experience a pronounced shift in the generation-fuel mix in favor of natural-gas and resulting in the decrease of the coal consumption – which is the most widely used fuel today, globally.

In order to address the essential energy challenges and simultaneously improve the living conditions of society in general, the key initiatives from the author’s perspective are the following:

- Address cost effective and hence affordable, carbon-neutral energy systems leading to substantial reductions in greenhouse gas emissions within the next decade.
- To achieve and successfully sustain nearly 100 percent Green, efficient, affordable, scalable energy for the entire planet.
- To successfully address carbon emissions “substantial” reduction globally before 2025.

One of the key High efficiency natural gas-fired power stations can produce up to ~70% lower greenhouse gas emissions than existing brown coal-fired generators, and less than half the greenhouse gas emissions of the latest technology black coal-fired power stations.[30][31];[46] Hence focus on combined cycle power plants accommodating both gas and steam turbines technologies will be key towards addressing our worldwide global electricity demands. It is assumed that an approximately 1 percent rise in Gas Turbine engine efficiency can address approximately fuel savings of ~ \$million over ten years, and a 1 percent enhancement in overall gas turbine efficiency saves approximately thousands of metric tons of carbon dioxide emissions a year. [46b] In places such as Asia, where the platform aligned to the LNG approach, can be costly; the savings would be much higher.” [46]. Hence advanced technologies ranging from advanced cooling designs, advanced aerodynamics, advanced alloys and coating, advanced sealing and much more will be pivotal in pioneering highly efficient world class engines and understanding the critical changes in performance parameters and its impact to the durability of the components being exposed to the harsh and ever challenging turbine flow path environment. Considering the current challenges that we “humanity” face regarding energy conservation, it is highly crucial that we produce high powered gas turbines requiring minimum amounts of fuel consumption, hence resulting in maximizing performance by considerably reducing heat rate, and simultaneously addressing our needs towards meeting global emissions reduction targets. To do so, we need to understand the coupling effects of the various technical principles that govern the fundamentals of turbine performance and synergizing these fundamental principles to generate a unified

consolidated formulation that can be applied towards preliminary predictions of the component durability as a function of engine performance parameter variations.

(1.2) Purpose

The primary purpose and focus of this dissertation is to couple and thoroughly investigate the fundamental scientific principles of cycle performance/thermodynamics, turbine aerodynamics, turbine heat transfer, turbine component structural and life evaluation, and the fundamental aspects of manufacturing & cost and eventually as stated above, to generate a unified consolidated theoretical formulation that can be applied towards predicting impact on component durability as a function of varying engine performance parameters. The methodology and execution approach to be applied to establish the author's proposed approach is to consolidate the fundamental physics-based equations delineating the turbine operation and subsequently to then generate a single or a series of multiple regression or transfer equations, hence capturing the influence of the various technical disciplines and investigating its impact on turbine component durability. Hence the primarily goal of this dissertation is to couple or synergize the parameters involving the simple cycle gas turbine efficiency along with the turbine mean-line aerodynamics, component durability, turbine thermodynamics and hence realizing the limitations of the various technology enablers that directly influence the overall \$/Kw-Hr of a power plant. To improve and simultaneously compete in the power generation industry, focus on technology advancements not only within the domain of a specific gas turbine component /discipline but coupling of the various key technology enablers ranging from performance, aerodynamics, durability etc. is of the utmost importance.

- Based on the author's reading various articles on this subject matter; the next three decades will see a pronounced shift in the generation-fuel mix in favor of gas and away from coal, the most widely used fuel today worldwide.
- High efficiency natural gas-fired power stations can produce high percentages of lower greenhouse gas emissions than existing brown coal-fired generators, and less than half the greenhouse gas emissions of the latest technology black coal fired power stations. Hence sustainable focus on gas turbine technologies will be key towards addressing our global electricity needs. [31],[46]

Therefore, advanced technologies ranging from cooling, aerodynamics, advanced alloys and coating, sealing and much more will be key in pioneering highly efficient world class engines.

- Considering the current challenges that we face regarding energy conservation, it is highly crucial that we produce high powered gas turbines requiring minimum amounts of fuel consumption, hence resulting in maximizing performance and efficiency targets. To do so, we need to understand the coupling effects of the various technical principles that govern the fundamentals of gas turbine performance.
- The focus of this dissertation as iterated earlier, is to couple the fundamental scientific principles of cycle performance, turbine aerodynamics, turbine heat transfer, turbine structural and the fundamental aspects of manufacturing & cost, and establish multiple regression or transfer equations, hence capturing the effect of the various technical disciplines and investigating its impact on gas turbine efficiency and component durability. Hence the primarily goal for this dissertation

is to utilize the generated response surface transfer functions and apply it toward garnering a preliminary understanding of the related physics pertaining to the simple cycle gas turbine efficiency and component durability.

Brief introduction to the Simple & Combined Cycle: To generate electricity by utilizing as much as useful energy as thermodynamically possible a combined cycle approach, which is accommodating two or more thermodynamic cycles operating together off the same source of heat, hence converts the energy released from the heat input into useful and applicable mechanical energy and is what ultimately drives the generator for electricity production. The principle within this validated concept for combined cycles applications, is that the exhaust of the gas turbine (Brayton cycle) is used as the input-heat source for the steam turbine (Rankine Cycle); hence with the extraction the useful energy from the heat source it finally increases the system's overall efficiency. A typical Combined Cycle Gas Turbine (CCGT) plant and can potentially achieve an approximate thermal efficiency of 60%, and higher, in contrast to a simple steam cycle power plant which is limited to efficiencies of lower percentages than the Gas Turbine applications, and on the other hand, a single cycle steam power plant is limited to efficiencies from 35 to 42%. [46] [49b]

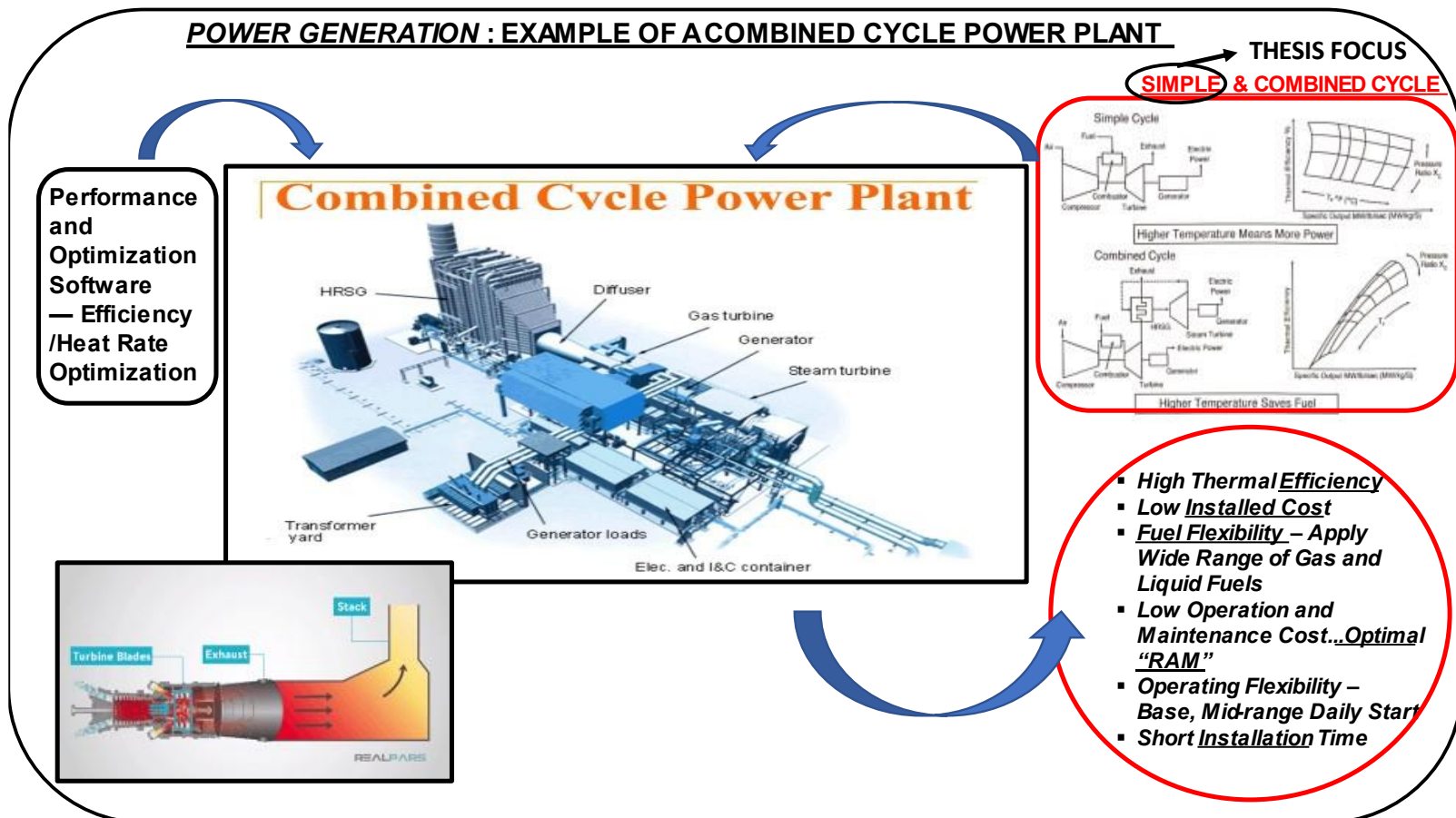


Figure 1.3 Example of a Combined Cycle power plant [32][41][56][57]

Simple Cycle: The simple cycle (SC) delineates the most fundamental thermodynamic based [9] operating cycle of gas turbines with a proven fleet around the globe of potentially outputting a thermal efficiency ranging from approximately 15 to 45 percent. The thermal efficiency of a SC is defined as the ratio of useful shaft energy to fuel energy input [9]. The application of the Simple cycle gas turbines is predominantly for shaft horsepower applications without taking advantage or benefit of having any recovery of exhaust gases emanating from the last stage blade annulus exhaust. For example, simple cycle gas turbines are used by electric utilities for generating amounts of electricity during certain emergency related occasions or during fluctuating peak demand periods.

(1.3) Objective & Scope

This dissertation will delineate the synergy or the coupling of the multiple disciplines involving principles of thermodynamics, aerodynamic velocity diagrams, heat transfer and structural assessments and hence integrate it to the efficiencies and power output of the simple cycle mode, including a single stage high pressure turbine module. The control volume established in this dissertation, is focused primarily on the High-Pressure Turbine- single stage application, simple cycle Gas Turbine, with only the Stage1 Nozzle cooled.

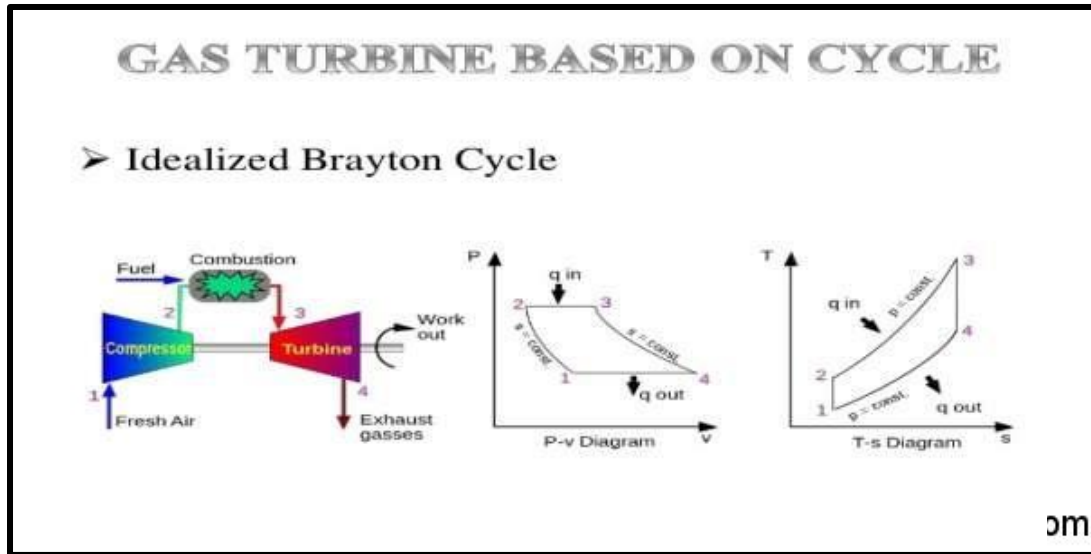


Figure 1.4 Components of a simple cycle gas turbine [37]

Figure 1.4 highlights the key components of a simple cycle gas turbine. The compressor module heats and compresses the air drawn in from the atmosphere which is subsequently heated by the addition of fuel in the combustion chamber which is termed as the Air to Fuel ratio. This hot air and combustion gas mixes to operate the expander or a.k.a turbine, thus producing substantial energy to generate required shaft power to the mechanical generator while simultaneously providing required energy to the compressor. The power produced by the expander and consumed by a compression process is directly proportional to the absolute or total temperature of the combustion gases passing through the overall simple gas turbine annulus. It is beneficial operating the turbine (expander) at the highest possible gas path temperature as long as it meets the demands of the applied materials from a high temperature sustainability point of view and also economically speaking from a cost effectiveness and manufacturability aspect. The higher temperature and high-pressure ratios yield higher turbine efficiency and specific power. Hence in summary, the generic trend in gas turbine advanced technology has been towards a goal of having a combination of higher temperatures and pressures. Even though with the key

advancements in high temperature and pressure ratio gas turbines results in increasing the overall manufacturing cost of the gas turbine; however. due to the associated benefits of the corresponding power output and higher efficiency ultimately yields an overall net gain from an economic benefits perspective. The aforementioned discussion provides a Segway to the importance of enhancing the simple cycle thermal efficiency at the lowest cost possible, which leads to the thorough and detailed understanding of the physics of the various key disciplines playing a critical role in gas turbine multi-physics operation hence leading towards coupling the thermal efficiency to the multiple disciplines into one unique mathematical expression or into a robust transfer function.

(1.4) Assumptions & Rationale

Given the engine inlet thermo dynamic conditions, such as the supply pressure and combustion exit temperature AKA the Turbine inlet temperature (prior to the region mating with the stage 1 nozzle-see Figure 1.5) TIT, RPM, and also the stage 1 vane exit angle “alpha”, based on the physics related to the velocity triangles the characteristics of the turbine stage, such as the fluid flow path pressure, Mach number, temperature and inlet and exit velocity triangles, control volume interface temperatures, heat loads etc. are subsequently computed.

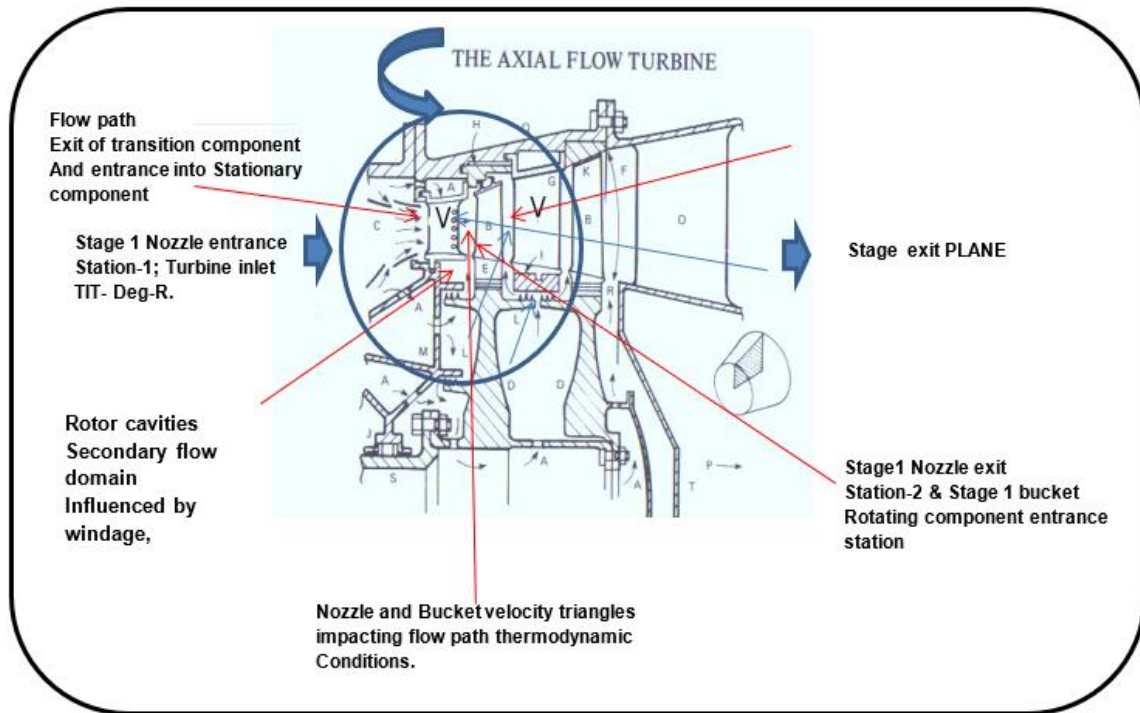


Figure 1.5 Schematic of a First Stage Gas Turbine -High Pressure Turbine [34]

On calculating the pressure ratio across the stage 1 nozzle based on the thermodynamic fluid properties computed earlier, and with the assumed alpha angle, and throat area, one can then compute from the flow physics based compressible flow formulation, the mass flow rate passing through the turbine annulus.

As the stage I nozzle may limit the flow through the entire turbine, one can assume that devoid of any leakages; this mass flow rate will be the turbine flow rate passing through the assumed control volume single stage application.

Now the stage annulus area AN^2 , is computed, along with the stage loading and flow coefficient. Subsequently the number of stages is then calculated. Once we have the number of stages, then the turbine length which is a function of the stages, the assumed typical axial chords of the airfoils, and the wheel spacing is then computed. Computing of the annulus and number of stages etc. is beyond the scope of this dissertation.

The idea is to then apply the impact of the thermodynamics, aerodynamics, heat transfer, compressible flow aspects and durability targets into the overall turbine efficiency equation, which is derived from the steady flow energy process, and subsequently evaluate the overall high-pressure turbine and gas turbine efficiency and associated heat rates, and then compare it to the open literature for comparative assessment purposes.

At this stage of the process, we have coupled the turbine efficiency, power output, and turbine mass flow rate with the station thermodynamic parameters and the overall flow path preliminary single stage simple cycle formulation based on the control volume selected.

Knowing the external heat transfer coefficient and the gas path stage by stage pressure and temperature values, the heat load into the component can be then evaluated to assess the need for cooling the component and determining the extent of the cooling technologies required via the assessment of the internal heat transfer coefficient by using the physics for the heat load parameter, cooling efficiencies, and the overall cooling effectiveness formulations. Next by applying the Fourier's law of heat conduction, from a one-dimensional perspective, we can then compute the temperature of the external surface of the component hot spots and also the temperature differential " ΔT " across the resistance which is comprised of the component wall thickness and also included within is the insulated thermal barrier coatings if applicable.

From the component temperatures resulting from the preliminary process mentioned above, we can now from a one-dimensional perspective calculate the thermal stress induced in the component and subsequently the low cycle fatigue life of the component

based on the assumed material properties and the component wall temperature differential.

At this stage of the process, we have coupled the component durability to the thermodynamic flow path properties.

Now from the preliminary computational assessment conducted in the steps proposed above, the intent is now to generate a regression equation or a transfer function that can relate the thermal efficiency to the pertinent independent variables or influential factors directly related to the key gas turbine engine parameters.

Application of the multiple control volume approach will be conducted to generate the proposed transfer function that finally can be used towards predicting the high-pressure stage and overall gas turbine thermal efficiencies based on the various engine operating parameters. On deriving the required transfer or regression equations/functions, a sensitivity process may be conducted to evaluate the maximum range of the control volume parameters that can positively influence turbine efficiency and associated gas turbine heat rate etc. and simultaneously ensure the longevity and durability of the components with the required heat load and cooling effectiveness parameters, resulting from which, the required advanced technologies could be then deduced as per the resulting heat load and cooling effectiveness parameters (as shown as an example in the figures below.). Generating the advanced technologies is beyond the scope of this dissertation.

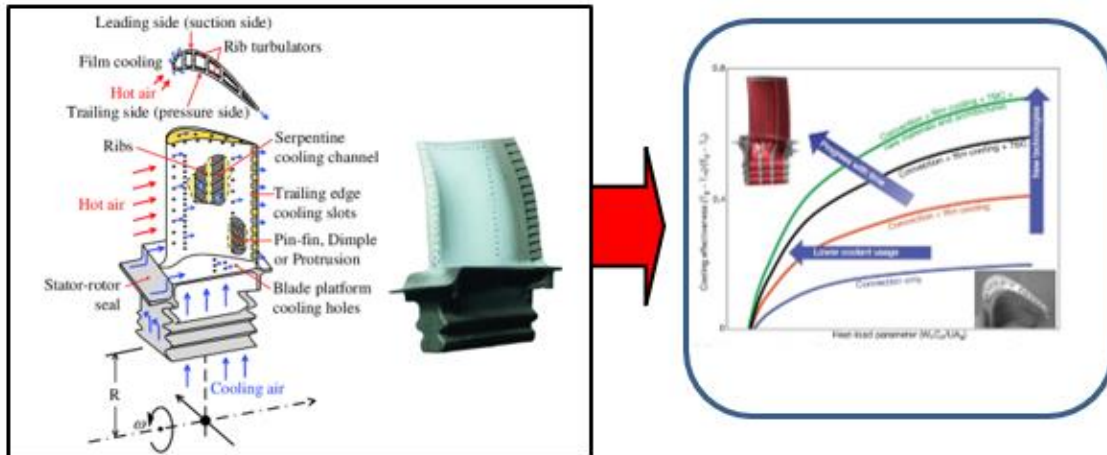
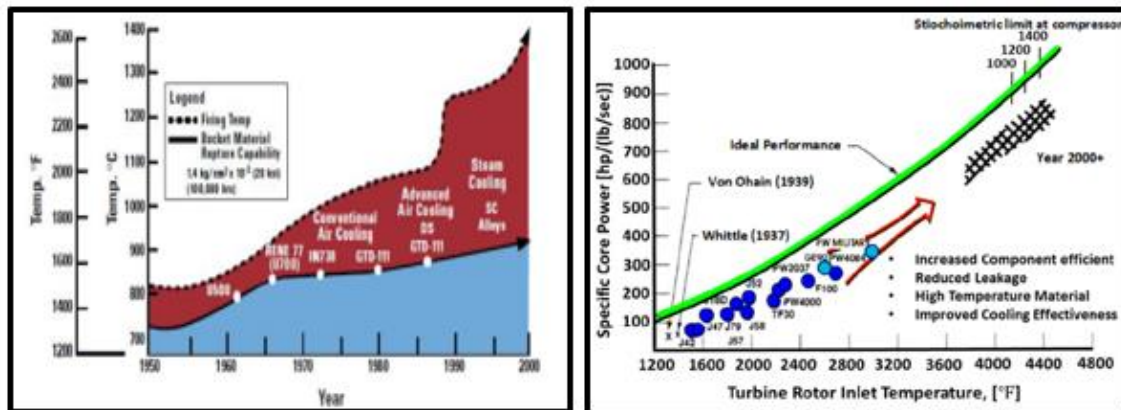


Figure 1.6 Various types of cooling mechanisms [19] Figure 1.7 Heat Load Vs. Cooling Effectiveness [20]



manages to circumvent the tripping of the gas turbine it is then that the power plant is considered as reliable based on its power output.

The key and essential parameters aligned to the Reliability and availability of the gas turbine in both simple and combined cycles are important to maintain, to ensure cost effective electricity generation for the powerplant owner. Hence increasing forced outages detrimentally impacts overall cost effectiveness of the power plant.

Hence in alignment with this dissertation, full comprehension of the land-based gas turbine physics and its operating mechanisms influenced by the various scientific disciplines is indeed extremely vital so to ensure continuous component durability while maintaining low heat rates.

CHAPTER 2:

LITERATURE SEARCH

(2.1) Overview of Gas Turbine -Simple & Combined Cycle thermodynamics [1]

[2]

The example of an internal combustion engine that utilizes the working fluid medium “air” is a depiction of a gas turbine that works on the fundamental principles of the Brayton Cycle thermodynamics. Gas turbines have been used for electricity generation for many years. There are two basic types of gas turbines - aero derivative and industrial as their name suggests, aero derivative units are aircraft jet engines modified to drive electrical generators. These units have a maximum output of approximately 40 MW. Aero derivative units can produce full power within approximately few minutes after starting up. They are not suitable for base load operation. Industrial gas turbines range in sizes up to more than approximately 260 MW. Depending on size, startup can take from approximately few minutes to approximately an hour to produce full output. Over the last ten years there have been major improvements to the sizes and efficiencies of these gas turbines such that they are now considered an attractive option for base-load electricity generation. Industrial gas turbines have a lower capital cost per kilowatt installed than aero derivative units and, because of their more robust construction, are suitable for base load operation.

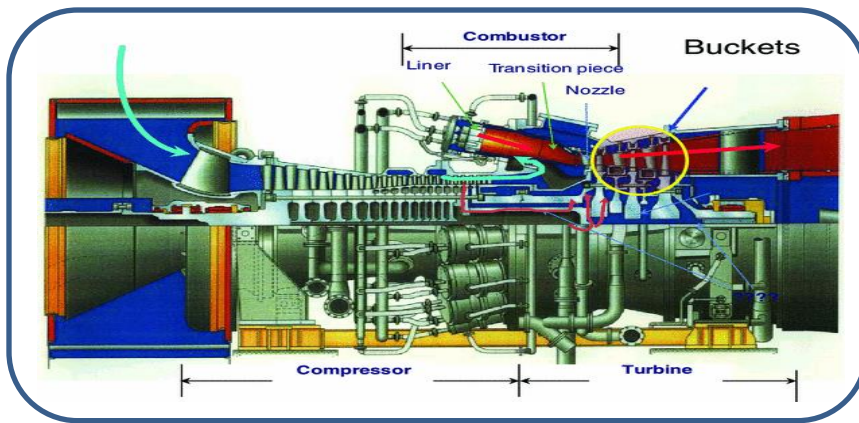


Figure 2.1 Cross section of a typical Large Gas Turbine [36]

Gas Turbine Thermodynamics of a Simple Cycle: In reference to the figure below “Schematic of a Gas Turbine Simple Cycle”, it is shown that, from state point (1), [11] the ambient air enters the module that is the axial flow compressor, at an average standard atmospheric condition of approximately 60 degrees Fahrenheit and at approximately 14.696 atmospheric pressure absolute. At this state (1), the air entering the compressor module undergoes a compression in order to increase its pressure. While the air is in compression the associated air temperature is increased thus finally at the end of the compression state both the air temperature and its pressure are much higher than what it was at the entrance conditions at state (1).

The compressed air enters the combustion module at state point (2). At this state point (2), fuel is introduced or rather injected and mixed with the compressed air conditions and at this state point (2) combustion occurs. The combustion process is assumed in this dissertation to be at a fairly constant pressure hence assuming $\Delta P/P$ across the combustor is negligible or very small.

At state point (3), the products of the reactants from the combustion process enters the High-Pressure turbine at a mixed temperature condition. Here, in the turbine module the combustion gases at mixed temperature conditions expand while the thermal energy of the fluid, a gaseous state is converted into useful work. The air is first accelerated in the stationary vanes and then passed along to the rotational blades where the kinetic energy of the gas is then converted into useful work. Approximately it is assumed from an average condition that 40%-50% of the work that is generated in the turbine module is applied towards driving the compressor module while the remainder of the energy is assumed to drive the output shaft, devoted to the network.

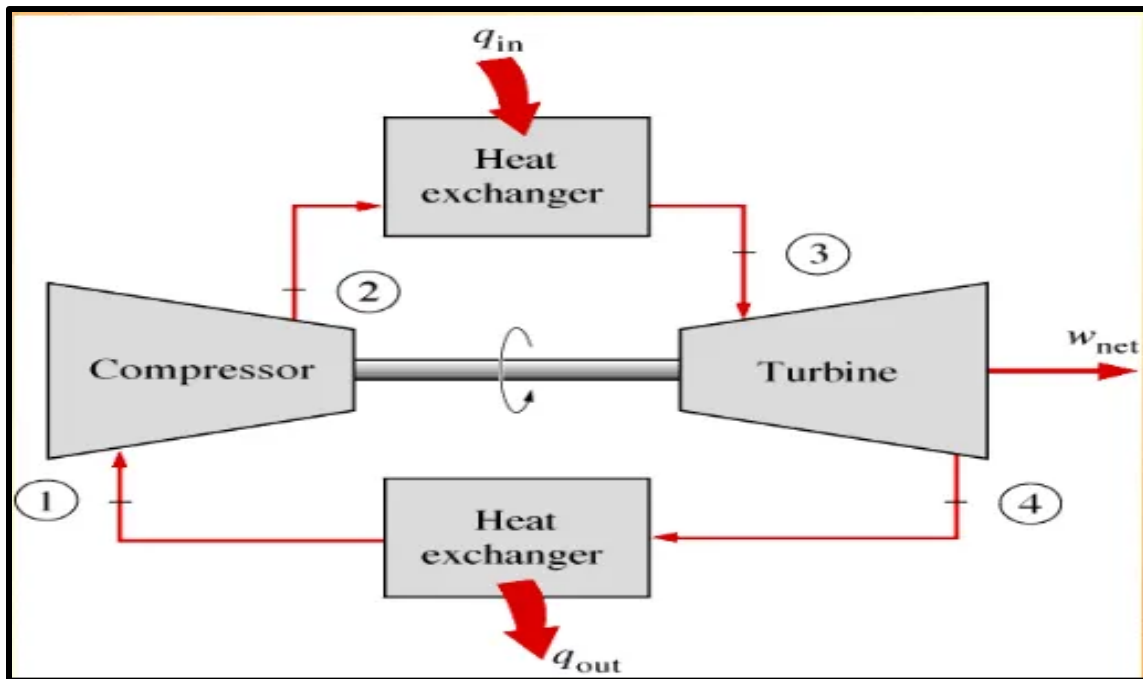


Figure 2.2 Schematic of a Gas Turbine Simple Cycle [37]

Brief Summary of the Performance Characteristics- Power Output: In general, the power output from the gas turbine is influenced by the following mechanisms:

- (1) The energy provided by the turbine and used by the air compressor if less energy is used to compress the air, more energy is available at the output shaft.

- (2) The enthalpy or the temperature of the hot gas leaving the combustors - increased enthalpy or temperature generally results in increased power output.
- (3) The temperature of the high-pressure turbine flow exit or exhaust gas - reduced temperature generally results in increased power output or greater work accomplished.
- (4) The overall mass flow through the gas turbine including fuel and compressor air combination - in general, higher mass flows result in higher power output.
- (5) The pressure differential or the pressure difference -in pressure across the inlet air filters, silencers and ducts - a decrease in overall delta- pressure loss increases power output.
- (6) There is also an improvement in reducing the pressure across the exhaust gas silencers, ducts and stack - a decrease in overall pressure loss increases power output.
- (7) Increasing the overall fluid pressure of the air entering or leaving the compressor - an increase in overall fluid or air pressure increases power output.

Importance of understanding the Brayton cycle in terms of the Gas Turbine key performance parameters.

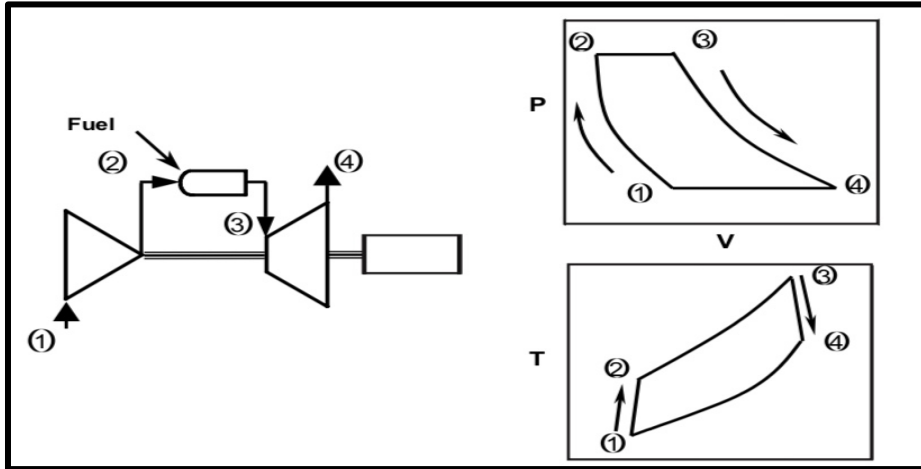


Figure 2.3 Key parameters from the Brayton cycle aligned to the Gas Turbine [41]

In reference to the schematic above in Figure 2.3; the fundamental and key parameters that can be derived from the Brayton cycle and directly aligned to the gas turbine efficiency are the overall cycle pressure ratio and turbine module inlet temperature. The pressure ratio of the cycle is defined as the pressure at the compressor discharge pressure conditions, divided by the compressor inlet pressure conditions. In this dissertation it is also assumed that as the pressure losses through the combustion process is minor (negligible) hence compressor discharge pressure is the pressure also at the inlet of the high pressure turbine module and as this dissertation is focused on the simple cycle single stage turbine with no downstream low pressure turbine, hence the exhaust conditions at the turbine exit is approximately at atmospheric pressure conditions, hence this allows for the assumption that the pressure ratio across the compressor is approximately equivalent to the pressure ratio across the one stage turbine. Whereas the highest air temperature that is achieved in the Brayton thermodynamic cycle is at the exit combustor conditions i.e., inlet to the turbine nozzle plane. The total or the absolute temperature across the nozzle is constant as there is no work done across the

nozzle. However, in an open loop system that this dissertation is based on, the turbine nozzle is cooled and considering that this coolant is ejected into the main gas stream hot gas path hence this mixing influences the overall gas path absolute temperature by decreasing the hot gas path temperature and hence decreasing its inherent thermal energy prior to work being done in the turbine rotational frame of reference. The author leverages his graduate academic background from various texts [4] to generate the overall mathematical coupling of the essential physics with the One-dimensional aero dynamic based coupling studies. [4] for the state points aforementioned.

(2.2) Brief overview of the Gas turbine functionality and operation

Gas turbines use the hot gas produced by burning a fuel to drive a turbine. They are also called combustion turbines or combustion gas turbines. The main components of a gas turbine are an air compressor, several combustors (also called burners) and a turbine. The air compressor compresses the inlet air (raises its pressure). Fuel is mixed with the high-pressure air in burners and burnt in special chambers called combustors. The hot pressurized gas coming out of the combustors is at very high temperatures. This gas then passes through a turbine, giving the turbine energy to spin and do work, such as turn a generator to produce electricity. As the turbine is connected to its compressor, the compressor can use (about ~50%) of the turbine's energy because some of its heat and pressure energy has been transferred to the turbine, the gas is cooler and at a lower pressure when it leaves the turbine. It is then either discharged up a chimney (often called a stack) or is directed to a special type of boiler, called a Heat Recovery Steam Generator (HRSG), where most of the remaining heat energy in the gas is used to produce steam in a combined cycle operation.

Different sections of a Gas Turbine:

Air Compressor: The air compressors used in gas turbines are made up of several rows of rotational components. Each row of these rotating components compresses and push the fluid onto the next row of the rotating blades. As the air becomes more and more compressed, the sizes of these rotating parts also become smaller from row to row in the direction of the flow field. The row of largest blades is at the left end of the compressor, starting from the inlet, and maybe after the variable guide vanes, and with the smallest blades to the right, upstream of the compressor discharge location or thermodynamic state point.

Fuel Application: Gas turbines can operate on a variety of gaseous or liquid fuels, including liquid or gaseous fossil fuel, for example such as crude oil, heavy fuel oil, natural gas, methane, distillate and "jet fuel" (a type of kerosene used in aircraft jet engines); when natural gas is used, power output and thermal efficiency of the gas turbines is higher than when using most liquid fuels.

Inlet Air: The air coming into the compressor of a gas turbine must be devoid and clean of impurities (such as dust and smoke) which could erode or cohesively become an intrinsic part of the components within the compressor or turbine, resulting in tremendous reduction of the power and efficiency of the gas turbine. The power and efficiency ratings of a gas turbine are usually based on the inlet air being at ISO conditions of 15° C and 65% relative humidity. If the inlet air that is being introduced into the gas turbine is hotter and drier than ISO conditions, then this results in the power of the gas turbine to decrease and also impacts the overall Gas Turbine thermal efficiency.

Burners and Combustors: [42] The overall compressed working fluid and the added or required fuel content is mixed in burners. These burners are attached to chambers called combustors. The fuel & air mixture is fired close to the exit tip of the burners, then subsequently allowed to fully burn in the combustors. The temperature of the gas in the combustors and entering the turbine can reach up to extremely high temperature ranges. Ceramics, which are heat resistant materials, or good insulators are used to line the inside walls of the combustors.

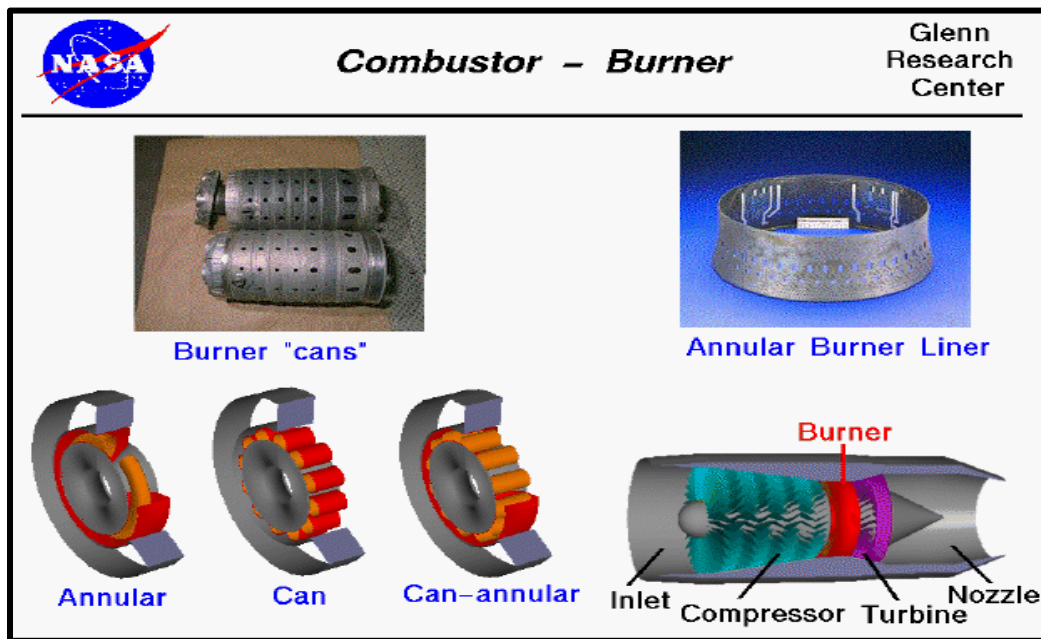


Figure 2.4 Example of a Combustor burner [42]

(2.3) High Pressure Turbine Emphasis

Turbine-The Work Horse: The Axial flow turbine (also called the "power" turbine) consists of several rows of blades (the "moving" blades) that are fastened to the rotating shaft of the turbine. A row of "fixed" blades is located after each row of the "moving" blades. These fixed blades are attached to the casing of the turbine and do not rotate. As the hot gas from the combustors passes through the moving and fixed blades of the

turbine, energy is transferred from the hot gas to the turbine, causing it to rotate. This energy transfer reduces the pressure of the gas and causes the gas to become cooler as it passes through the turbine.

The blades of the turbine become larger from row to row to accommodate the expansion of the gas as its pressure reduces. The moving blades in the turbine are subjected to extreme temperature (from the hot gas exiting the combustors) and stress (from the combination of their rotation and the pressure of the hot gas). The efficiency of the gas turbine improves if the hot gas temperature rises. The gas path flowing through the axial flow turbines is proposed to be adiabatic in nature, since the heat losses are minuscule as compared to the overall work outputs. Now note as the gas path flow is proposed to be adiabatic hence for a provided pressure differential, the second law of thermodynamics is applicable to depict that the overall maximum work can be obtained if the turbine is defined as isentropic.[13]

Turbine -Hot Gas Path Material Introduction: New materials and techniques used to manufacture the turbine blades have resulted in a significant increase in operating temperatures. Currently, turbine blades are made from exotic Super alloys that retain their strength at the high temperatures experienced in the turbine. Ceramic blades offer the possibility of still higher operating temperatures. However, materials to withstand the higher temperatures are usually more expensive than those that can withstand lower temperatures.[6] The materials for the turbine blades (and other components of the turbine) are therefore selected to give a balance between hot gas temperature (and efficiency) and material selection (and cost). Research into better (and cheaper) materials for these high temperature, high stress duties is ongoing. Various coatings for turbine

blades have been developed as another way to minimize this high temperature damage to the blades

Turbine Materials Desirable properties:

- (a) High creep and rupture strength
- (b) Resistance to corrosion, oxidation and sulfur content
- (c) Good fatigue strength & low thermal expansion and high thermal conductivity

Material Options and considerations: Typical basic properties of gas turbine materials are: (a) Strength and ductility: Component should have high strength and also should withstand large plastic strains before rupture. Ductility is required as it allows large deformations before rupture (b) Fatigue: Fatigue failure occurs when the Component experiences excessive cyclic loads. High Cycle Fatigue is caused by vibratory load distributions. HCF cracks will usually nucleate at specific locations of material inhomogeneities. The hot components of the turbine, particularly the rotating components, are also subject to "creep" i.e., temperature and time dependent failure. Metals at excessively high temperature & high overall and local stress fields gradually morph their metallurgical properties and plastically deform ("creeps"). This deformation could result in the rotating parts touching the stationary parts with possible catastrophic conclusions to the overall engine frame. The high-pressure turbine components are subjected to thermal conditions causing creep and hence are regularly inspected and tested. Advanced materials researched based Coatings on high pressure components have tremendous advantages to overall blade low cycle fatigue life and also decreases the amount of cooling consumption applied, thus increasing overall turbine performance, and associated component durability aspects on a sustainable level.

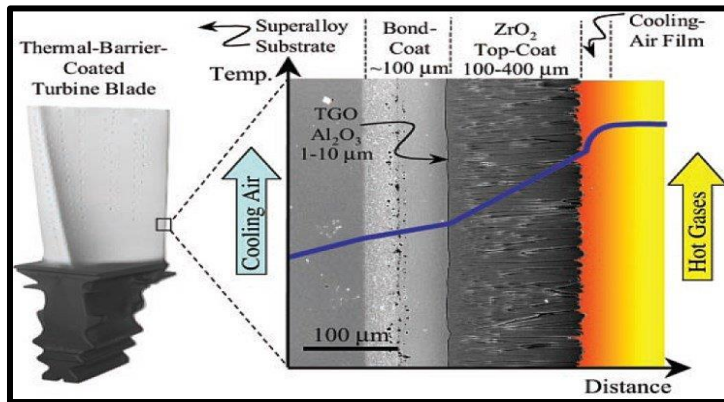


Figure 2.5 Coatings on blades [43]

Turbine “Hot Gas Path” Physics of the flow stream: Gas properties change through a turbine stage. Through the first stage stationary component the total pressure decreases; this is attributed to frictional losses and various aerodynamic losses. The total temperature across the stationary component is assumed to be constant based on negligible heat transfer. The static pressure decreases across the stage 1 nozzle, and also across the first stage blade, the total pressure and the total temperature decreases a lot. Even though the static pressure across the first stage blade decreases, but not as much as the decrease across the first stage vane, the amount of the static pressure drops across both the first stage vane and blade is the measure of the stage reaction.

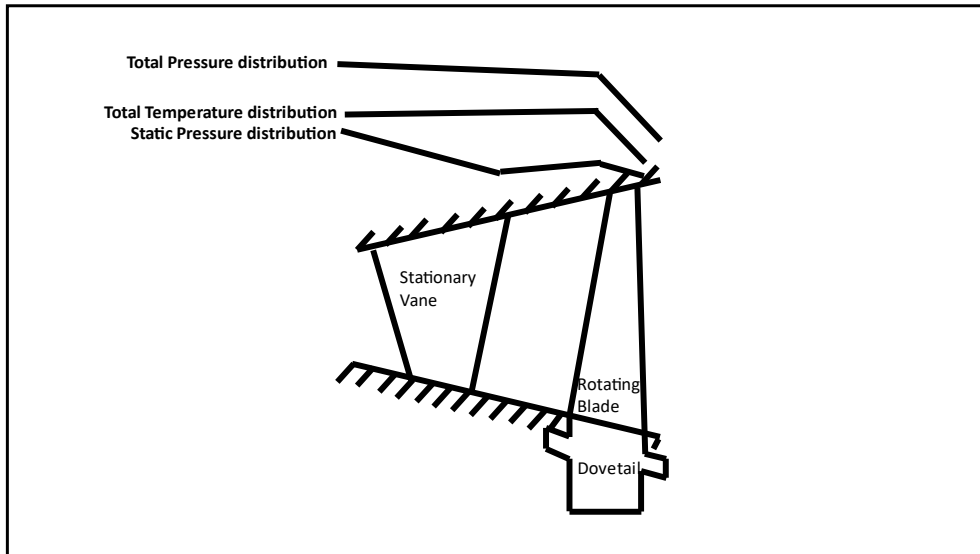


Figure 2.6 Turbine Hot Section flow physics

Typical Gas Turbine Airfoil Physics -Brief summary

- Gas turbine working fluid inlet temperature and thermal properties
- Gas turbine working fluid turbine inlet pressure properties
- Gas turbine working fluid turbine inlet flow rate
- Gas turbine rpm, and turbine shaft power
- Gas turbine flow function, flows with source conditions
- Gas turbine inlet & exit velocity (Mach#), and exhaust pressure
- Stage loading & Zweifel number
- Component geometrical dimensions
- Annulus area & shaft speed
- Temperature limitations on yield strength, ductility and material oxidation limits

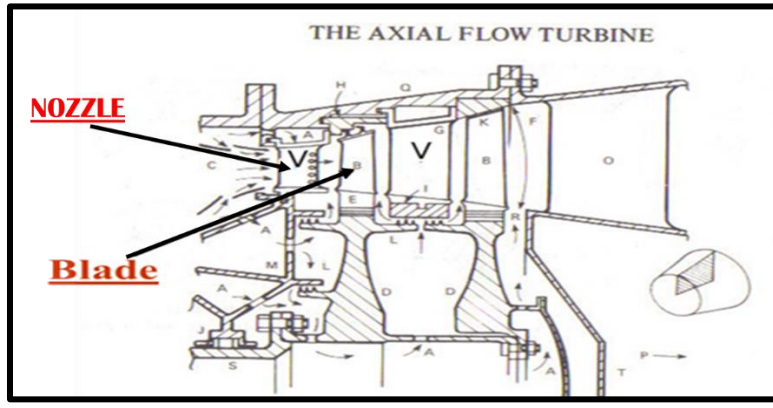


Figure 2.7 The Axial Flow Turbine [34]

The Figure 2.7 depicts the magnitude and direction of the gas velocities within the stage on a cylindrical surface the gas is accelerated across the stator, while the gas static pressure is decreased, and the tangential velocity of the working fluid is increased in the direction of rotation. The rotor decreases the tangential velocity in the direction of rotation, and the resulting tangential forces are exerted by the fluid onto the rotor blades and a resulting torque is produced on the output shaft. In many axial flow turbines, the hub and tip diameters vary little through a stage, and the hub to tip ratios approaches unity. There is little variation in static pressure from root to tip.

In order to assess the state point temperatures and pressures; the author leverages his graduate academic background from various texts [4] to generate the overall mathematical coupling of the essential physics with the One-dimensional aero dynamic based evaluations. [4] for the state points aforementioned.

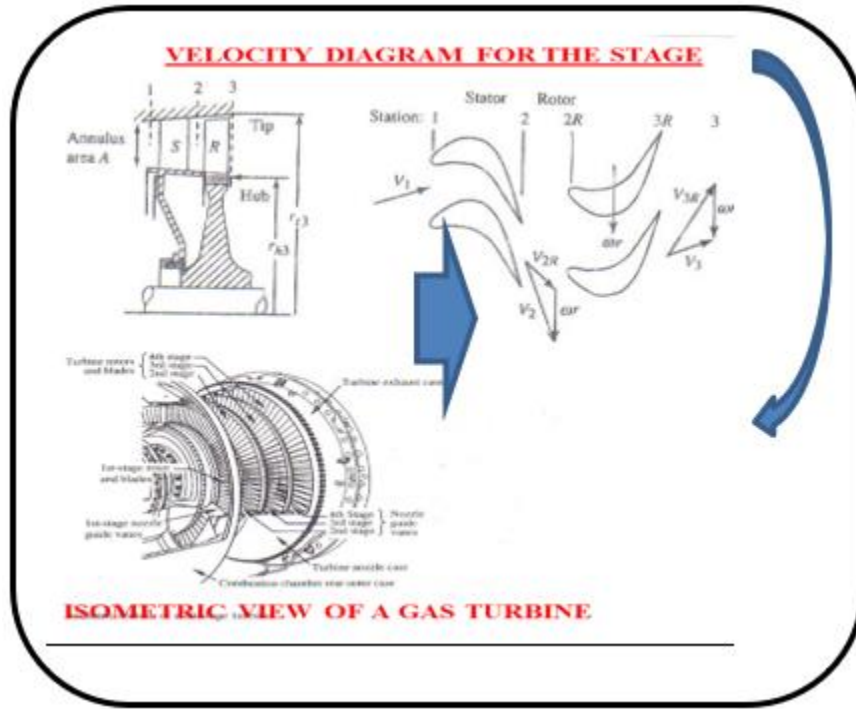


Figure 2.8 Flow Physics of the Axial Flow turbine [4]

Turbine component Heat Transfer design fundamentals: One of the major challenges is ensuring maintenance of the durability of the hot gas path components. Hence, coupling of heat transfer mechanisms required to maintain the thermal and structural integrity of the component to the performance benefits is of the utmost importance.

Increases in pressure ratio and firing temperature, depending on which cycle (simple or combined) will require an in-depth understanding of the outlining physics of cooling [6], material science, stress analysis, aerodynamics [4] and thermodynamics, hence maintaining component reliability. This dissertation introduces and provides an in-depth assessment of the importance of the multi-physics approach within the single stage of the high-pressure turbine module. The performance of any gas turbine airfoil can be depicted in terms of the “cooling effectiveness” of the design system Cooling effectiveness [6] is

defined as the ratio of the difference between the turbine gas path flow maximum localized temperature, considering recovery effects, and the maximum blade metal temperature to the difference between gas path flow maximum local temperature and the coolant medium temperature.[19]

Internal Cooling brief introduction: Cooling effectiveness measures the heat transfer performance of the turbine airfoil cooling system as the fraction of the total potentially available temperature reduction achieved in cooling the metal.[19], however cooling does introduce losses within the Gas Turbines [20];[21]

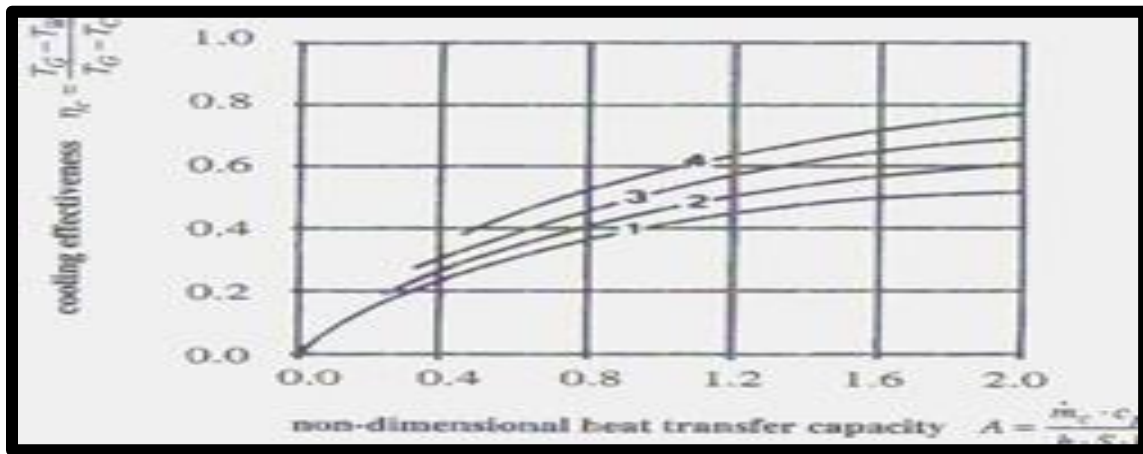


Figure 2.9 The Cooling Effectiveness & Heat Load parameter depends primarily on the following factors [44]

- (a) length of the path along which the heat must flow through the metal external wall to the internal wall
- (b) Internal surface area per unit external surface area available to remove the heat by the coolant medium
- (c) Thermal conductivity of the coolant boundary layer
- (d) overall coolant flow rate

External Gas Path Heat Transfer: Airfoil heat transfer coefficients are obtained by including the application of the energy equation into the boundary layer calculation [8] using empirical correlations in locations where the boundary layer calculations do not yield reasonable results. On vane shrouds, and blade platforms, the application of CFD is mostly used to obtain the external heat transfer coefficients and validated with testing. The author is leveraging from literature research while associating the mathematical equations to conduct the derivations aligned to the control volume under consideration.[10][17][8]

The simplified Navier Stokes equations [8] also known as the Prandtl's boundary layer formulations based on steady flow assumptions are the following: Detail equations of motion in vector form will be discussed in the subsequent chapters.

$$\frac{\partial u}{\partial x} + \frac{\partial v}{\partial y} = 0$$

$$u \frac{\partial u}{\partial x} + v \frac{\partial u}{\partial y} = -\frac{1}{\rho} \frac{dp}{dx} + \nu \frac{\partial^2 u}{\partial y^2}$$

There are five main flow regimes defined in the external heat transfer domain:[17]; [18]

- (1) Leading edge stagnation region
- (2) Separation and reattachment region caused by the pressure fluctuations near the leading edge
- (3) A laminar boundary layer region
- (4) A region of laminar to turbulent boundary layer transition
- (5) A region of fully turbulent boundary layer flow field

High vorticity strength regions increase the external heat transfer coefficient. End wall contouring Schemes have been proposed by certain investigators, to decrease the external heat transfer coefficient.

Flat Plate and Leading-edge external heat transfer Correlation leveraged from Reference [10] [17] and mathematically adjusted by the author, with parameters reflecting the control volume is as follows. Detail derivations are shown in the subsequent chapters.

- $h_g = \left(\frac{K_g}{X}\right) (0.0296)(Pr^{1/3}) \left[\sqrt{\frac{\gamma g c}{RT_g}} \right] (P1_a) \left\{ \frac{M}{[1 + (\frac{\gamma-1}{2})M^2]^{\gamma+1/2(\gamma-1)}} \right\} (X/\mu) [17]$
- $h_g \left(\frac{L}{e}\right) = a [(1.14) \left(\frac{K_g}{D}\right) \left\{ \sqrt{\frac{\gamma g}{RT_g}} (Pt) \frac{M}{[1 + \frac{\gamma-1}{2}(M)^2]^{\gamma+1/2(\gamma-1)}} (X/\mu) \right\}^{0.5} [(Pr)^{0.4} (1 - |\varphi|/90)^3] [17]$

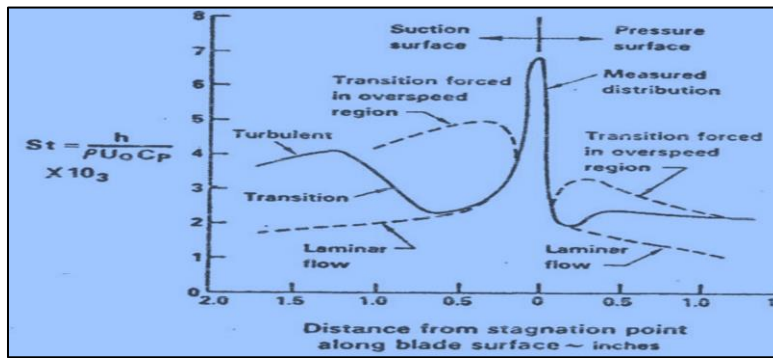


Figure 2.10 External Gas path heat transfer flow physics example [45]

Because of limited internal cooling passage size within the cooling circuitry cavities in a typical turbine airfoil; there is a restriction/limitation to the amount of cooling air available, as well as a limit also on the supply source pressure; it is apparent that there is a limitation to the capabilities of plain convection cooling. The Figure 2.11 below shows

the effect of turbine inlet pressure and temperature on coolant flow requirements. There is a highly non-linear increase in cooling air consumption for typical convection cooling, as pressure and temperature increases

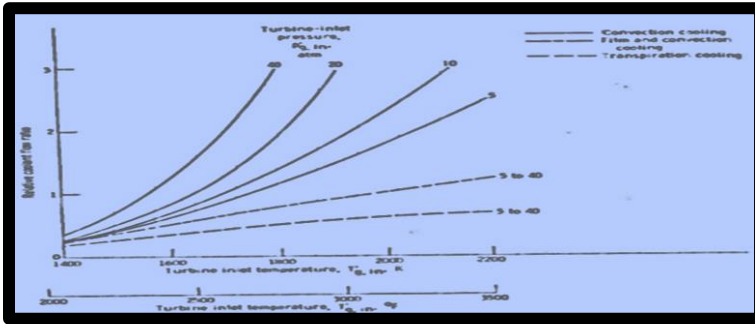


Figure 2.11 Effect of turbine inlet pressure and temperature on coolant flow requirements [17]

Effect of combining effective gas path cooling and convection cooling:[17] As turbine inlet temperatures increase, the pure convection cooling needs to be augmented by effective gas path cooling techniques to reduce the metal temperatures, and reduce cooling air Consumption, hence extracting lower amounts of air from the compressor.

Figure 2.12 below shows that combined effective gas path and convection cooling techniques yields a significantly lower wall temperature than does either effective gas path or convection cooling alone.

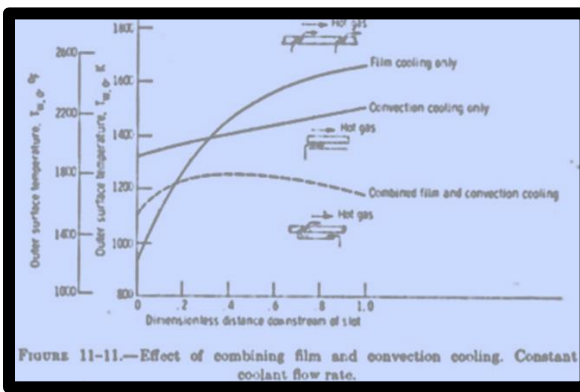


Figure 2.12 Effect of combining effective gas path cooling and convection cooling [17]

The above Figure 2.12 attests to the fact that ensuring coupling of the heat transfer mechanisms to the overall thermal efficiency thermodynamic based mathematical expression is of the utmost importance to ensure a thorough understanding of the impact of the multi-disciplinary approach and its evaluation on the overall turbine single stage thermal efficiency

(2.4) Current challenges for the High-Pressure Turbine and proposed scope of work

The key challenges within the High-Pressure gas turbine are for the associated components to sustain the high temperatures emanating out of the combustor. While considering the hot gas path temperatures detrimentally impacting the parts and diminishing its longevity; simultaneously maintaining the HPT stage efficiencies is also extremely vital in order to ensure a well-balanced system based robust design. Hence in order to do so, as aforementioned it is pivotal to couple or rather integrate the key physics based disciplines and better understand the overall synergistic aspect of thermodynamics, aerodynamics, material properties, conduction and convection heat transfer , component stress evaluations influencing the life cycle of the component under consideration and in doing so to ensure that the overall stage efficiency is maintained to be at optimum as the stage efficiency influences the overall cycle efficiency and ultimately the fuel consumption. From an economic perspective the overall life cycle cost of the part or rather the component, is a strong criterion to justify the overall “ROI- Return of investment” of the product, both from a durability and heat rate perspective. In order to avoid a long period of time in ascertaining the risks of not meeting the targeted stage

efficiency and component durability requirements, it is essential to ensure identifying expeditiously the risks of the aforementioned challenges.

In order to mitigate the risks a quick computation to address a preliminary understanding of the key requirements is indeed essential and hence the author of this dissertation has proposed through rigorous derivations an integrated “synergistic” approach of computing the pivotal High Pressure turbine stage efficiency and associated component durability; as a function of coupling all the necessary key disciplines ranging from thermodynamics, mean line aerodynamics, external gas path and internal heat transfer, component geometrical resistances and associated stress fields .

Further literature research for coupling the overall physics into one consolidated and synergistic formulation; based on the authors research the following materials were referenced:

[23] Modeling and performance of gas turbine cycles with various means of blade cooling; Kristin Jordal; May2001 Doctoral Thesis, Division of Thermal Power Engineering; Dept. of Heat and power engineering; Lund University, Sweden. Here in this referenced material, the author identifies a method simulating the cooled GT, however, the author does not couple the overall scientific principles into one equation for the stage thermal efficiency or the durability as conducted by UHPT function.

[52] Land based Gas Turbines for Power Production; Kurt Hansen, Prof; Lakshmi Kantha, ASEN 5063; December 15th, 2009. Here in this referenced material, the author identifies the LBGT efficiency and power generation calculations. However, the author does not couple the overall scientific principles into one equation for the stage thermal efficiency or the durability as conducted by UHPT function.,

[53] Design Study for Single Stage High Pressure Turbine of Gas Turbine Engines; Ajoko, Tolumoye John Department of Mechanical/Marine Engineering, Faculty of Engineering, Niger_Delta University, Wilberforce Island, Bayelsa State, Nigeria. Here in this referenced material, the author identifies Analysis for the prediction of Turbine efficiency. The author applies the isentropic efficiency of the component for the engine's performance, by using Smith's chart correlation method of turbine efficiency prediction. Smith's correlated turbine efficiency chart, measurements from stage loading coefficient ($\Delta H/U^2$) and flow coefficient (V_a/U) are connected and traced to the efficiency correlation curves, however, the author does not couple the overall scientific principles into one equation for the stage thermal efficiency or the durability as conducted by UHPT function

[15][13] In these references, the effect of cooling on Turbine Efficiency is considered briefly, and the author of this dissertation, based on having studied these references in graduate classes, has leveraged a certain amount of physics from this reference material. However, this reference material does not consider the overall synergy of the flow function with the one dimensional aero dynamic parameters, including velocity triangles and associated parameters in the relative frame of reference[3], effective gas path cooling effectiveness and the detailed coupling of the control volume approach involving fluid temperature differentials and pressure losses within, interface temperatures including overall resistances for the substrate and thermal barrier coatings, as conducted in this dissertation.

CHAPTER 3:
INTRODUCING THE CONTROL VOLUME APPROACH WITHIN THE
GAS TURBINE

**(3.1) High Pressure Turbine Control Volume: A Multi-Physics / synergistic
approach**

The region of interest specifically attributed to the prime focus for this dissertation is the High-Pressure Turbine. Prior to proceeding into the details related to the Multi-Physics synergistic approach, the author believes that the importance of evaluating the overall Gas Brayton cycle including the major components such as the compressor, combustor(heat adder) and turbine (expander), into the overall thermodynamic cycle assessment is essential, and hence from literature and academic, and professional background , the author provides a Segway into the main control volume aligned to the prime focus for this dissertation, by evaluating the overall thermodynamic cycle.

Thermodynamic Cycle performance evaluation: Considering that this dissertation reflects the preliminary assessments for aspects of the high-pressure turbine, hence from the derivations involving the overall Gas Brayton cycle, the author will extract and align the necessary thermodynamic mathematical expression specifically aimed towards the prime focus of this dissertation, incorporating the main measures of the performance parameters of the Brayton Cycle.

- (i) Specific Power
- (ii) Thermal Efficiency

In addition, the two main cycle characteristics are the Gas Turbine compressor pressure ratio and the other being the Turbine Inlet to compressor inlet temperature ratio.

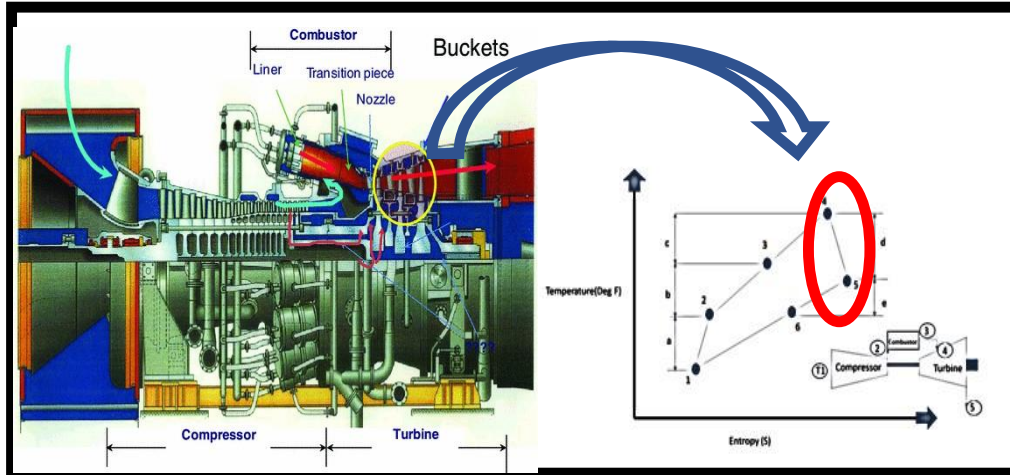


Figure 3.1 Thermodynamic State Points reflecting overall Gas Brayton Cycle [36]

- Points: 1-2-3-4-5-6 => Are thermodynamic state points
- State (1-2) "a" = This is where the compression work on the fluid occurs
- State (2-4) "b + c" = This is where the heat is added to the cycle through the module called the combustor
- State (4-5) "d" = This is where the turbine work occurs
- State (5) "e" This is where the exhaust gases emanating out of the last stage of the turbine.
- Now the Gas Turbine net power is defined by the following known mathematical equation: [12]
- $W_{net} \Rightarrow [\text{Turbine Power} - \text{Compressor Power}]$ 3-1
- $\text{Specific Power} = [W_{net} / (\dot{w}_c \bar{C}_{p_c} T_{01})]$ 3-2

Or -

- $SP = \text{Specific Power} = \{[\text{Turbine Power} - \text{Compressor Power}]/$
 $(\dot{w}_c \bar{C}_{p_c} T_{01})$ 3-3

- $\text{Turbine Power} = \dot{w}_t (h_{04} - h_{05})$ ** 3-4

- $\text{Compressor Power} = \dot{w}_c (h_{02} - h_{01})$ 3-5

**Differentiation of the enthalpies are ascertained from higher state to lower state.

Now: Referencing Figure 3.1; we obtain the following:

- $\dot{w}_t (h_{04} - h_{05}) \equiv \dot{w}_t \bar{C}_{p_t} (T_{04} - T_{05})$ 3-6

- $\dot{w}_c (h_{02} - h_{01}) \equiv \dot{w}_c \bar{C}_{p_c} (T_{02} - T_{01})$ 3-7

Hence, resulting in the following mathematical expression:

- $SP = \{[\dot{w}_t \bar{C}_{p_t} (T_{04} - T_{05}) - \dot{w}_c \bar{C}_{p_c} (T_{02} - T_{01})]/ (\dot{w}_c \bar{C}_{p_c} T_{01})\}$ 3-8

- $SP = \frac{\dot{w}_t \bar{C}_{p_t} (T_{04} - T_{05})}{\dot{w}_c \bar{C}_{p_c} T_{01}} - \frac{\dot{w}_c \bar{C}_{p_c} (T_{02} - T_{01})}{\dot{w}_c \bar{C}_{p_c} T_{01}}$ 3-9

- $SP = \frac{\dot{w}_t \bar{C}_{p_t} (T_{04} - T_{05})}{\dot{w}_c \bar{C}_{p_c} T_{01}} - \frac{(T_{02} - T_{01})}{T_{01}}$ 3-10

And as the Gas Turbine Brayton Cycle Thermal efficiency is defined as:

- $\eta_{\text{thermal}} = \text{Specific Power} / \text{Specific Heat Addition}$ 3-11

Now in the aforementioned equation we need derive the Heat Addition term. The energy or rather the enthalpy that is added in the Brayton cycle is via the combustor hence referring to the Temperature – Entropy Diagram the heat addition term is defined to be the following:

- $\text{Heat added into cycle} = \dot{w}_{\text{comb}} (h_{04} - h_{02})$ 3-12

Or

- $\dot{w}_{\text{comb}} (h_{04} - h_{02}) = \dot{w}_{\text{comb}} \bar{C}_{p_{\text{comb}}} (T_{04} - T_{02})$ 3-13

Now the specific heat addition is defined as:

$$\bullet \quad \dot{Q} = \text{Heat Addition} / (\dot{w}_c \bar{C}_{p_c} T_{01}) = \frac{\dot{w}_{\text{comb}} \bar{C}_{p_{\text{comb}}} (T_{04} - T_{02})}{(\dot{w}_c \bar{C}_{p_c} T_{01})} \quad 3-14$$

Therefore, the Gas Turbine (Gas Brayton) overall cycle thermal efficiency is defined as the following: Note the author based on academic research and professional experiences gained over the years is assuming that the assessment the author has conducted is for an adiabatic gas turbine (no cooling) comparison to a cooled turbine where it is assumed that the overall gas turbine and its major components undergo a “steady flow process” which signifies that its inlet and exit pressures are constrained or rather fixed, which leads to the fact that this idealized process is reflecting an Isentropic process between the inlet and exit of the control volume which in this case is the high pressure turbine region where for multiple stages the work extraction or output decreases in enthalpy from the inlet to exit thermodynamic state points.

$$\bullet \quad \eta_{\text{thermal}} = \frac{SP}{\dot{Q}} = \frac{\left\{ \frac{\dot{w}_t \bar{C}_{p_t} (T_{04} - T_{05})}{\dot{w}_c \bar{C}_{p_c} T_{01}} - \frac{(T_{02} - T_{01})}{T_{01}} \right\}}{\dot{w}_{\text{comb}} \bar{C}_{p_{\text{comb}}} (T_{04} - T_{02}) / (\dot{w}_c \bar{C}_{p_c} T_{01})} \quad 3-15$$

Now we extract from the aforementioned overall GT Brayton cycle However as stated previously, for the focus of this dissertation the region of interest is the high-pressure turbine (HPT), Hence the adiabatic efficiency for the high-pressure turbine is defined to be as the following:

$$\bullet \quad \eta_{\text{thermal}} = \frac{\text{Actual energy output}}{\text{Ideal energy output}} \quad 3-16$$

Building mathematically and based on laws of thermodynamics, referencing Figure 3.1:

$$\text{For a given turbine pressure ratio } \Pi_t = (P_{t5}/P_{t4})^{\gamma-1/\gamma} \quad 3-17$$

$$\text{Actual turbine work per unit mass} = (h_{t4} - h_{t5}) \quad 3-18$$

$$\text{Ideal turbine work} = (h_{t4} - h_{t5a}) \text{ (Where a = isentropic expansion)} \quad 3-19$$

Now substituting the enthalpies for temperatures per unit mass yields the following:

$$\text{Actual Process: } (h_{t4} - h_{t5}) = C_p(\Delta t) = C_p(T_{t4} - T_{t5}) \quad 3-20$$

$$\text{Ideal (Isentropic Process)} = (h_{t4} - h_{t5a}) = C_p(\Delta t_a) = C_p(T_{t4} - T_{t5a}) \quad 3-21$$

Therefore, Actual temperature leaving turbine = T_{t5} & the Ideal temperature leaving the turbine = T_{t5a}

Further mathematical computation yields the following:

$$\frac{(h_{t4} - h_{t5})}{(h_{t4} - h_{t5a})} = \frac{(T_{t4} - T_{t5})}{(T_{t4} - T_{t5a})} = \frac{\text{Actual energy output}}{\text{Ideal energy output}} = \frac{1 - T_{t5}/T_{t4}}{1 - T_{t5a}/T_{t4}} \quad 3-22$$

As we know that:

$T_{t5}/T_{t4} = (P_{t5}/P_{t4})^{\gamma-1/\gamma}$; hence further substitution yields the following:

$$\frac{(h_{t4} - h_{t5})}{(h_{t4} - h_{t5a})} = \frac{1 - T_{t5}/T_{t4}}{1 - (P_{t5}/P_{t4})^{\gamma-1/\gamma}} \quad 3-23$$

Hence the Turbine “HPT” isentropic efficiency without cooling streams can be defined as the following and therefore we have now the following equation reflecting the region of interest aligned to this dissertation and referring to the Figure 3.1

$$\eta_t = \frac{\text{Actual energy output}}{\text{Ideal energy output}} = \frac{(h_{t4} - h_{t5})}{(h_{t4} - h_{t5a})} = \frac{1 - T_{t5}/T_{t4}}{1 - (P_{t5}/P_{t4})^{\gamma-1/\gamma}} \quad 3-24$$

The author now based on his academic research; here forth applies the above equation for Turbine efficiency η_t , by taking into account the cooled turbine physics [15] implementation reflecting the mixing of the two streams mixing, i.e., gas path stream and the cooling stream, and from the turbine work expands the aforementioned equation even further as depicted below.

$\eta_t - \text{thermal} =$

$$\frac{\text{Work Actual (Two streams)} = \{C_{pgt}[T_{t_4} - T_{t_5}] + C_{pc}[EET - T_{t_4}(P_{t_5}/P_{t_4})^{\frac{\gamma-1}{\gamma}}]\}}{\text{Work Ideal (Two streams)} = \{C_{pgt}(T_{t_4})[1 - (P_{t_5}/P_{t_4})^{\frac{\gamma-1}{\gamma}}] + \{C_{pc}(EET)[1 - (P_{t_5}/P_{t_4})^{\frac{\gamma-1}{\gamma}}]\}} \quad 3-25$$

This equation 3-25, above is the fundamental thermodynamic High pressure turbine efficiency formulation, including the cooled turbine reflecting the mixing of the two streams, however it now requires further physics based implementation; to be converted to the mass fractions pertaining to the related physics specifically for the HPT region, considering the mixing of the two streams i.e. pertaining to the gas path flow fluid stream, diluted with the coolant emanating from the defined control volume and mixing with the gas path stream hence resulting in a lower total temperature at station 2, which is at the exit plane of the stage 1 nozzle or A.K.A Firing Plane. Hence, the author will generate the ratio of the mass fraction of the two mixing streams and based on the control volume analysis reflecting the mixed temperature computations via an energy balance to generate the overall Total temperature at station 2. This computation will be depicted in the following sections.

The author references Gas Turbine World 2020 Performance Specifications- 36th edition, public domain magazine to later in this dissertation, to compare the results from the Unified High Pressure Turbine formulation. [51]. Now that we have specifically identified the actual region or rather the control volume of the focused area, we now proceed into the identification and evaluation of the High-Pressure Control Volume multi-physics approach.

(3.2) Establishing the Region of Interest pertaining to this Dissertation

The author commences the assessment of the dissertation focus with the known scientific mathematical formulations of the thermodynamic discipline applied to the Single Stage high pressure Gas Turbine: Evaluation of the control volume for the component Cooling configuration coupled with turbine flow thermodynamics and flow path mean line aerodynamics. Hence the author has chosen for this particular dissertation to focus on the major region of interest encapsulated within the single stage high pressure turbine which incorporates the stationary component and the rotating component, defined as the stage 1 nozzle and stage 1 bucket respectively and where the trailing edge plane of the stage 1 nozzle (EET) basically defines the temperature at the

“Enthalpy extraction” plane [41] i.e., station 2 as per Figure 3.2

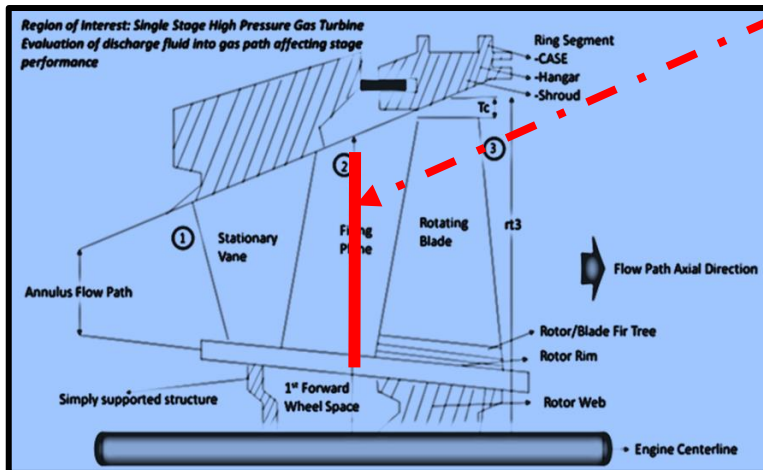


Figure 3.2 Enthalpy Extraction temperature Plane (EET)

(3.3) Identifying and establishing a “Synergistic” approach of the key control volumes

Fundamental Physics based mathematical derivations

- (i) The thermodynamics assessment has been conducted earlier as aforementioned.
- (ii) As we proceed into the dissertation in order to ascertain the gas path boundary conditions the author applies his academic knowledge in deriving the one-dimensional aerodynamic parameters. A velocity diagram aligned to the stage analysis is conducted at the mean radius and the author assuming isentropic conditions; gas path flow properties have been derived at the specific thermodynamics cycle state points (1, 2&3) of Figure 3.1
- (iii) Derivation resulting from the velocity diagram and the author’s derivations of the external gas path heat transfer parameters will also be ascertained to establish external heat loads. And from the cooling aspects of the cavity within the control volume selected; the author will ascertain through detail assessment and evaluation the derivation of the fluid coolant temperature exiting out of the effective gas path cooling rows based on the authors systematic control volume analysis.
- (iv) The assumption here is that the overall coolant medium “effective gas path cooling” is assumed to be applicable to the stationary high-pressure turbine component within an open loop system and hence the amount of cooling air emanating out of the stationary component and into the flow path alters influences and hence alters the enthalpy or the firing temperature of the flow entering the first

stage rotating component. This location is termed as the firing plane as also captured in Figure 3.1

(v) In a typical conventional gas turbine engine, the first stage stationary component the air used toward cooling is provided from the discharge air exiting out of the compressor i.e., compressor discharge air. And hence when this coolant is emitted through the effective gas path cooling row holes into the flow path results in a mixed-cup temperature hence reducing the enthalpy of the gas path by reducing the firing temperature which inevitably reduces the stage performance and overall engine performance as well.

(vi) Gas turbine performance is greatly driven by the gas path temperature upstream of the high-pressure rotating component i.e., the first stage blade.

(vii) The intent of this dissertation is to synergize the overall physics based fundamental disciplines of the thermodynamics, mean line aerodynamics, external and internal heat transfer aspects, ascertaining the thermal and the structural integrity or the durability of the component and align it to the overall HPT Stage efficiency.

(3.4) Basic Thermodynamics principles applied to region of interest

The author had conducted the thermodynamics assessment for the overall Gas Turbine Brayton Cycle, however as mentioned previously the primary focus of this dissertation is the high-pressure turbine hence This section will depict the initiation of the construction of the fundamental physics based mathematical equations capturing the proposed multi-physics coupled approach addressing the gas turbine single stage high pressure region focused on the stationary nozzles and rotating buckets.

Referring to the High-Pressure cross-section in Figure 3.1

Where:

- State (1) = Inlet conditions to the high-pressure stage stationary vane 1
- State (2) = Exit conditions of the high-pressure stage stationary vane-1 & entrance to the stage 1 rotating frame of reference i.e., stage 1 rotating blade.
- The plane upstream of the rotating stage 1 blade is also referred as the Enthalpy Extraction Temperature Plane (EET)
- State (3) = Exit conditions of the high-pressure stage 1 rotating frame of reference i.e., stage 1 rotating blade.

The thermodynamic and aerodynamic derivations of each stage or state points will be conducted as we progress into the dissertation as the thermodynamic parameters will be defined as the external gas path boundary conditions which are required to ensure the overall synergy of the multi physics aspects are well evaluated.

Note: As the intent of the dissertation is to also synergize or rather couple the effective gas path cooling effects into the high-pressure stage efficiency hence from a thermodynamic efficiency perspective If there was no coolant ejecting from the stationary component between stations (1) & (2), Then the physics dictates

that($Tt_2 = Tt_1$) 3-26

However due to material limitations and not being able to withstand high skin temperatures due to its fatigue and yield limitations, hence the material due to its durability requirements undergoes a process of cooling details of which is beyond the objective and scope of this dissertation. However, this coolant when ejected into the flow

or gas path the component is imbedded into; then based on the laws of thermodynamics and based on the physics influenced by the recovery effects [40], hence ($T_{t2} \neq T_{t1}$)

3-27

T_{t2} at station 2; is defined as the mixed-cup temperature resulting from the mixing of the two fluid streams as per the following definitions:

- (a) Fluid stream T-Recovery (Gas Path temperature)
- (b) Coolant temperature being ejected into the flow or gas path as effective gas path temperature which mixes with the Gas Path temperature.

A mass enthalpy balance or a control volume process is conducted as depicted in the Figure 3.1, below reflecting or rather representing the mixing of the two aforementioned streams in the gas path. This physics-based control volume approach conducted with the necessary mathematics, depicts a bulk or average estimated assessment reflecting the coupling of the state points thermodynamic conditions , one dimensional mean line aerodynamics, external gas path boundary layer conditions, component geometric resistances, material properties of the resistances, fluid properties of both the external gas path and the internal cooling medium, internal cooling heat transfer turbulence promoter mechanisms, all coupled into the high pressure turbine stage1 thermal efficiency which once derived will also be applied towards the component stress field relationships to determine the effectiveness of the part durability.

(3.5) Identification of the Main Control Volume for the Stationary Component

Volumes reflecting the Stationary Component and including the region of the firing plane along with the rotating component gas path exit temperature, assuming the only component that is cooled is the stationary component.

Now to proceed progressing toward conducting an overall mass enthalpy balance on

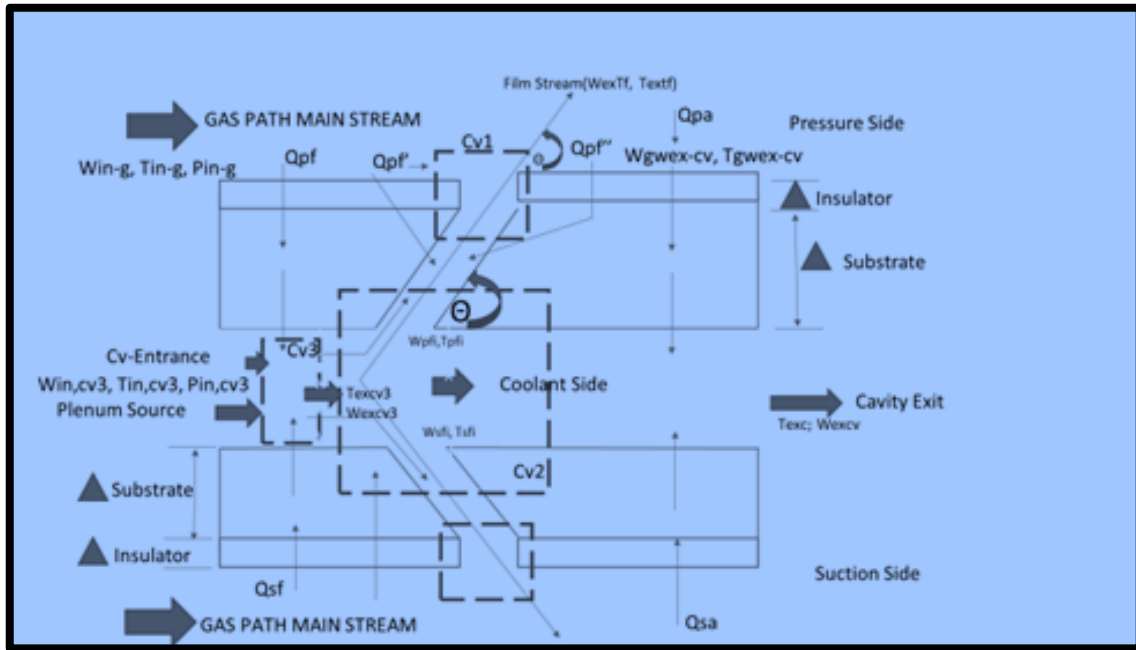


Figure 3.3 High Pressure Turbine- Main region of focus including multiple Control control volume (CV₁). It should be noted that the other various control volumes as depicted in the Gas Path control volume CV₁ need to be evaluated in order to ascertain the ultimate conditions in control volume CV₁.

(3.6) Control volume rationale and alignment to dissertation focus

The overall Figure 3.3 depicts and captures the fundamental physics and associated multi-physics aspects of a typical gas turbine stationary vane including the pressure and suction side of the components under consideration and couples the physics of the internal, external regions of the component being assessed.

Having the thorough comprehension of the associated synergy between the physics related to the component and its environment is extremely essential in order to generate the thermodynamic properties of the mixing region of control volume CV₁

Explanation of the Applied Physics for each control volume.

Control Volume (CV-1): This reflects the region of the external gas path and is subjected to the following parameters.

- (i) The energy entering the control volume from the upstream gas path
- (ii) The energy entering the control volume from the coolant conduits or effective gas path cooling, or effusion holes or transpiration holes, whichever could be the choice of the cooling process that can be accommodated by the control volume process and corresponding heat pick up as the coolant traverses in its journey towards its destination i.e., emanating into the flow path.
- (iii) The steady state balanced mixed-cup energy exiting out of the control volume CV_1

Control Volume (CV-2): This control volume is subjected to the following parameters.

- (i) The energy of the coolant medium within the cavity entering CV_2 from CV_3

This signifies that if the cavity is cooled by any turbulence promoting cooling scheme device, it is then the heat picked up of the coolant upstream of CV_2 that now enters CV_2 from CV_3

- (ii) The energy of the main gas stream through the resistances from both the pressure and suction side upstream and downstream of the of the component under consideration related to CV_2 .
- (iii) The energy of the coolant medium within the cooling configuration considering the energy transfer resulting in heat pick up, and subsequently exiting out of CV_2 for the overall component representing both the pressure and suction sides respectively.

- (iv) Assuming that the downstream of CV_2 is the location of the cavity exit; the energy exiting out of CV_2

Control Volume (CV-3): (CV_3) This control volume is subjected to the following parameters:

- (i) The energy of the coolant entering from the source. This could be the compressor exiting temperature or any other source of cooling medium related to an open cycle gas turbine Brayton Cycle thermodynamic process.
- (ii) The energy of the main gas or flow path stream through the resistances from both the pressure and suction of the associated component upstream of CV_2
- (iii) The energy of the coolant exiting out of the CV_3

(3.7) Basic physics-based engineering assumptions & application for each

Control Volume

Let us now dwell into the physics of the typical control volume-based energy balance derivation assessment and evaluation. Assume the typical control volume is analogous to an enclosed structure as depicted for purposes of simplicity in Figure 3.2. The authors key objective here is to develop and derive the fundamental mathematical formulations depicting the overall energy balance required to compute the entrance and exit conditions of each of the control volumes established. Hence based on the following Figure 3.3, the basic physics-based assumptions are as follows toward assessing the fluid exit temperature emanating out of the control volume.

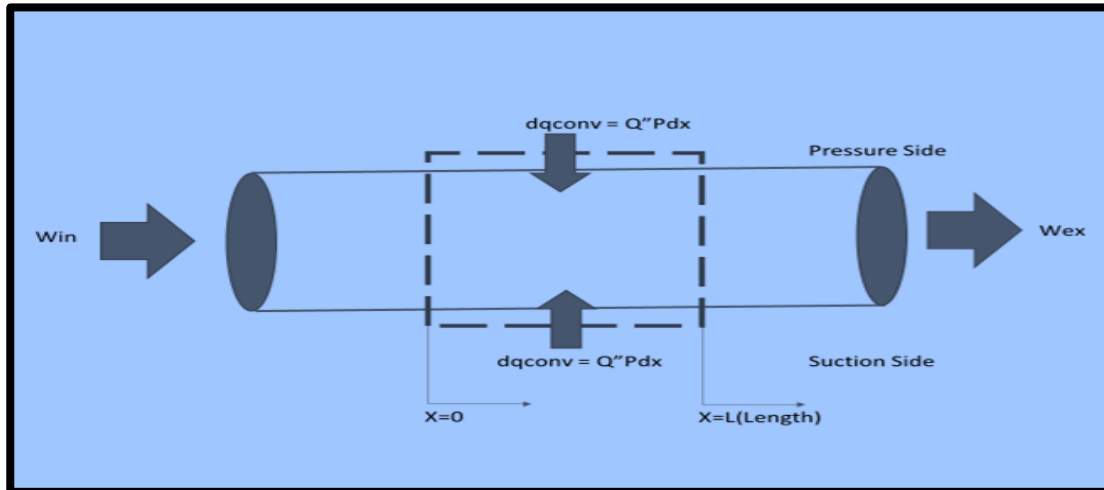


Figure 3.4 Typical Control Volume assessment for purpose of simplicity

- (i) The entrapped fluid within the structure is assumed to be completely enclosed.
- (ii) Based on Non-adiabatic conditions the average or the mean fluid temperature differs along the length of the inner side dimension of the structure from $X=0$ to $X=L$
- (iii) Energy is entrained into the fluid based on the source from both sides of the structure.
- (iv) The heat transfer mode to transfer the energy from both sides of the structure is through the process of conduction through the resistances and subsequently converted into the fluid that is entrapped within the structure.
- (v) The inner walls of the structure that is wetted by the fluid is assumed to experience a surface temperature that results from the thermal evaluations reflecting the resistances in series, from adjacent control volume conditions.

Note: The equation of continuity which is based on the conservation of mass and the energy balance equation which is also aligned to the conservation of energy is applied.

The equation of continuity states that if we assume a fluid particle of extremely small volume $d\tau$ and associated density ρ at time t , then the mass of this fluid particle is prohibited to change as it moves about and mathematically it can be depicted as per the mathematical expression:[55]

$$\frac{d}{dt}(\rho d\tau) = 0 ; \text{ This expression is one form of the continuity equation or also}$$

known as the conservation of mass. Assuming that no particles of the fluid can be created and destroyed within the control volume, hence the mass of the fluid particles can only get larger by flowing through the boundary.

Hence by applying Gauss's theorem [55]

$$\int_{(v)} \left(\frac{\partial \rho}{\partial t} + \bar{V} (\rho q) \right) d\tau = 0$$

Hence the selected control volume can be replaced by any closed surface, thus this yields at every point the mathematical expression which is another form of the continuity equation

$$\frac{\partial \rho}{\partial t} + \bar{V} (\rho q) = 0$$

Hence from a physics-based perspective the expression can simply be expressed as

$\dot{W}_{in} = \dot{W}_{out}$ => Applicable to the given control volume under consideration

CHAPTER 4:
DETAILED PHYSICS BASED MATHEMATICAL DERIVATIONS OF THE
KEY CONTROL VOLUMES

**(4.1) Physics based evaluation of the High-Pressure Turbine Conservation of
energy leading to the energy balance process**

$$[\dot{W}_{in}(cv_3)\dot{T}_{in}(cv_3) + \dot{Q}_{px}(cv_3) + \dot{Q}_{sx}(cv_3) - \dot{W}_{exit}(cv_3)\dot{T}_{exit}(cv_3) = 0] \quad 4-1$$

Where:

- $\dot{Q}_{px}(cv_3) = \dot{Q}/A) p = \Delta t / (\sum R)$ pressure side 4-2

- $\dot{Q}_{sx}(cv_3) = \dot{Q}/A) s = \Delta t / (\sum R)$ suction side 4-3

From the authors heat transfer academic background and leveraging from open literature text books, the physics based mathematical tool the author is applying to compute the respective control volume temperature rise with the assumption that after computing the corresponding resistance temperatures , the author holds the internal surface temperature of the respective control volume constant in the lateral direction as the author assumes that there is negligible change of temperature in the lateral direction and majority of the temperature change is across the resistances in the “through wall direction”. Taking this into consideration, the author now generates the energy balance applying the Log-Mean temperature difference to calculate fluid exit temperature rather than a mathematical average based fluid temperature rise as the author assumes the fluid temperature rise in non-linear from inlet to outlet of the respective control volume.

In the presiding Figure 3.3 the author applies the conservation of energy to the differential control volume and uses the definition of the bulk temperature.

The bulk fluid temperature at the given region of the cross -section is defined as the thermal energy transported by the fluid as the fluid transitions across the regional area of the associated cross section.

The rate at which this transition occurs is defined to be “ \dot{E}_t ”.

The process in which \dot{E}_t is evaluated is by mathematically integrating the product of the mass flux (ρu) and also by conducting the integration of the internal energy per unit mass ($C_v * T$) across the region under consideration of the given cross-sectional area.

Mathematically this is expressed as the following:[10]

$$[\dot{E}_t = \int_{AC} (\rho u * C_v * T) da] \quad 4-4$$

From the literature research [10] based on the fundamental laws of Physics the definition of the mean temperature is the following:

$$\dot{E}_t = \dot{W} C_v T_w \quad 4-5$$

Where:

T_w = Bulk fluid temperature within the enclosure.

Through the algebraic manipulation the following yields:

$$\bullet \quad T_w = \frac{\dot{E}_t}{\dot{W} C_v} \quad 4-6$$

Now note that: "

$\bullet \quad \dot{W} = \rho V A \rightarrow$ Which is the continuity equation Which can also be written as

$$\bullet \quad \dot{W} = \rho u A \quad 4-7$$

$$\text{Now as defined earlier} \rightarrow [\dot{E}_t = \int_{AC} (\rho u * C_v * T) da] \quad 4-8$$

Hence:

$$\bullet \quad T\dot{W} = \frac{\{\int_{AC} (\rho u \cdot C_v \cdot T) da\}}{W C_v} \quad 4-9$$

Therefore, now we have the following mathematical expression:

$$dq_{conv} + \dot{W}(C_v T_w + p v) - [\dot{W}(C_v T_w + p v) + \dot{W} \left\{ \frac{d}{dx} (c_v T_w + p v) \right\} = 0 \quad 4-10$$

-or-

After mathematical simplification yields:

$dq_{conv} = \dot{W} d(C_v T_w + p v) \rightarrow$ This mathematical equation represents that the convection heat transfer rate must be equally balanced to the rate at which the specific thermal energy of the fluid increases and in addition to the overall net rate at which the specific work is used up or expended in pushing the fluid across or through the region of the defined control volume.

Now assume that the fluid being pushed through the control volume (cv) is an ideal gas and the specific heat at constant pressure C_p is assumed to be a constant, then we have the following:

$$\bullet \quad [dq_{conv} = \dot{W} C_p dT_w] \quad 4-11$$

Hence to better understand and thus to evaluate the axial variation of the temperature “ T_m ” we have the following mathematical approach.

$$\bullet \quad \frac{dT_w}{dx} = \frac{q'' s(P)}{W C_p} = \frac{P}{W C_p} * h(T_s - T_w) \quad 4-12$$

If $T_s > T_w$; then the process or mode of heat transfer occurs from the inner wall surface allowing T_m to increase in magnitude in the axial direction which then allows the inner wall temperature to be greater than the temperature of the fluid.

Hence as aforementioned the control volume we have considered assumes that within that control volume the corresponding inner wall surface temperature once calculated applying the Fourier law of heat conduction, is held constant for further assessment via an iterative process.

- T_s = Inside CV Surface temperature

Now we shall introduce the physics-based mathematics of the Log-Mean temperature difference approach and also depict its derivation and application to the control volume analysis the author has introduced to address the objective at hand. With this in mind the author based on researching and leveraging academic background shall derive the fundamental mathematical equations expressing the axial distribution of the difference between $(T_s - T_{mf})$, {where T_{mf} is a bulk fluid temperature}. decays exponentially, with respect to the control volume approach under consideration and along the axial traversing distance. Application of the Log-Mean temperature difference method of approach to each control volume:

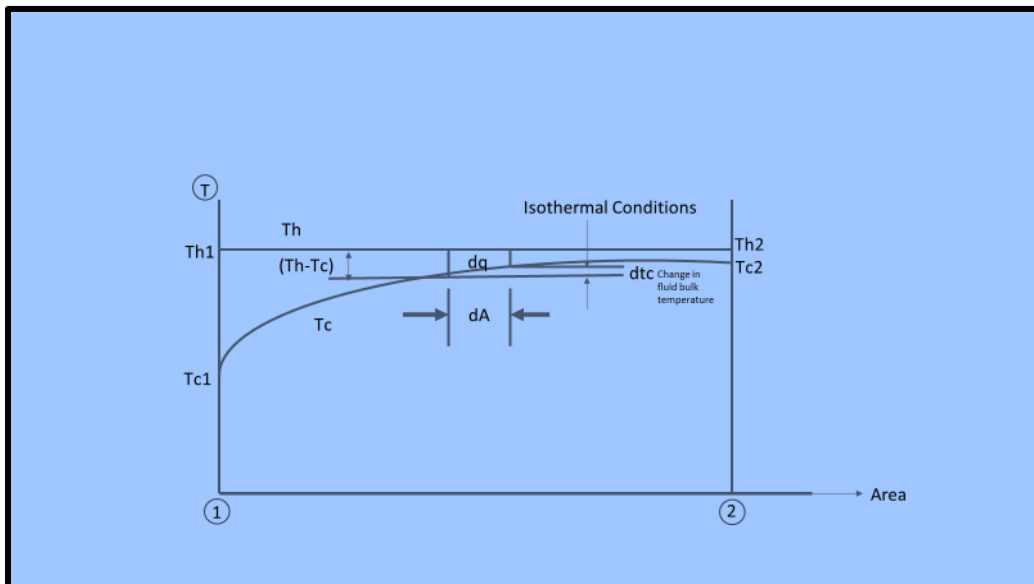


Figure 4.1 Temperature Variation within the control volumes

Assumptions and considerations:

Temperature variation of the fluid in the respective control volume under consideration.

Heat transferred through an element of area (dA) can be written also as:

- $dq = uAdT = \dot{W}C_p dT_c$ 4-13

Where:

- $U = \frac{1}{\sum R} = \frac{1}{\frac{1}{hc}} = hc \rightarrow$ which is the convective cooling coefficient. 4-14

- $dT = (T_h - T_c)$ 4-15

Hence:

- $dq = (hc)dA (T_h - T_c)$ 4-16

Now the heat load that is lost or expended from the wall inner surface is equivalent in energy that is gained by the fluid wetting the wall inner surface. Note the inner wall surface implicitly includes the physics of the external gas path heat transfer, geometry of the resistances, thermodynamics and the aerodynamics boundary condition.

Hence this can be mathematically expressed as the following:

- $[dq = (hc)dA (T_h - T_c) \equiv \dot{W}C_p dT_c]$ 4-17

Where:

- $dT_c \Rightarrow$ This is the increase of the fluid bulk temperature over the element of area as shown in the figure (4.1) as Area (dA)

Therefore, as shown previously:

- $[dq = (hc)dA (T_h - T_c) \equiv (\dot{W}C_p)dT_c]$ 4-18

Which in turn now becomes through mathematical manipulations:

- $dt_c = \frac{dq}{\dot{W}C_p}$ 4-19

And:

- $(T_h - T_c) = \frac{dq}{hcdA}$ 4-20

Now as:

- $dT = (T_h - T_c)$ 4-21

Then:

- $hc\left(\frac{da}{\dot{W}C_p}\right) = \frac{dt_c}{(T_h - T_c)}$ 4-22

Where:

- $dt_c \Rightarrow$ Is defined and referred to as the Log-Mean temperature difference.
- $T_c \Rightarrow$ variable fluid temperature. A.K.A T_w
- $T_h \Rightarrow$ constant

Now as we have mathematically defined $\Delta T = (T_h - T_c)$ 4-23

Hence differentiating ΔT which mathematically is shown as the following:

- $d(\Delta T) = (T_h - dT_c) \equiv -dT_c$ 4-24

Therefore:

- $dT_c = -(T_h - T_c) \equiv (T_c - T_h)$ 4-25

Hence:

- $d(\Delta T)/\Delta T = -[hc(dA)/\dot{W}C_p]$ 4-26

Therefore as:

- $\frac{d(T_h - T_c)}{(T_h - T_c)} = -\frac{hc(dA)}{\dot{W}C_p}$ 4-27

Hence this equation above is defined mathematically as a separable differential equation.

$$\text{Let } \Delta T = T_h - T_c \quad 4-28$$

Then:

$$\bullet \quad \frac{d(\Delta T)}{\Delta T} = - \frac{hc(dA)}{\dot{W}C_p} \quad 4-29$$

Performing the integration on both sides of the above equation:

$$\bullet \quad \int_a^b \frac{d(\Delta T)}{\Delta T} = - \left[\frac{hc}{\dot{W}C_p} \right] \int_a^b dA \quad 4-30$$

$$\text{Where the limits of the integration are as follows: } a=1; b=2. \quad 4-31$$

Now by Performing the integration on both sides of the above equation yields:

$$\bullet \quad [\ln(\Delta T)]_1^2 = - \left[\frac{hc}{\dot{W}C_p} \right] (A) \quad 4-32$$

$$\bullet \quad \ln((\Delta T_2) - \ln((\Delta T_1) = - hc(A)/ \dot{W}C_p \quad 4-33$$

Now leveraging from the identity of Logarithms:

$$\text{We have: } \left[\ln P - \ln Q \equiv \ln \left(\frac{P}{Q} \right) \right] \quad 4-34$$

$$\bullet \quad \ln \left[\frac{\Delta T_2}{\Delta T_1} \right] = - hc(A)/ \dot{W}C_p \quad 4-35$$

Now:

$$\bullet \quad \Delta T_2 = T_{c2} - T_h \equiv -T_{c2} + T_h \quad 4-36$$

&

$$\bullet \quad \Delta T_1 = -T_{c1} + T_h \quad 4-37$$

$$\bullet \quad \ln \left[\frac{-T_{c2} + T_h}{-T_{c1} + T_h} \right] = - hc(A)/ \dot{W}C_p \quad 4-38$$

Now by taking natural logs on both sides we get the following:

$$\bullet \quad \frac{-T_{c2} + T_h}{-T_{c1} + T_h} = e^\alpha ; \quad \text{Where } \alpha = - hc(A)/ \dot{W}C_p \quad 4-39$$

Hence:

- $\frac{-T_{c2} + T_h}{-T_{c1} + T_h} = e^{-hc(A)/\dot{W}C_p}$ 4-40

The above mathematically derived equation represents the log-mean temperature varying exponentially. However, the equation derived is still not in the typical expression of the delta-log hence the following mathematical steps is applied to derive the delta-Tm-Log.

Now the following equation below as stated previously:

- $dq = hc(dA) (T_h - T_c) \equiv \dot{W}C_p dT_c$ can also be written down as subsequent it being integrated:
- $q = hc(Ac)(T_h - T_c) = \dot{W}C_p(T_{c2} - T_{c1})$ 4-41

Where:

LMTD which is the Log-Mean temperature difference is termed as: $(T_h - T_c) = \Delta t_{lm}$

Now:

- $hcAc(\Delta t_{lm}) \equiv \dot{W}C_p(T_{c2} - T_{c1})$ 4-42

Or

- $hc(Ac)/\dot{W}C_p = (T_{c2} - T_{c1}) / \Delta t_{lm}$ 4-43

Now substituting the above equation into the previous derived equation- 4-38 as shown again below:

- $\ln \left[\frac{-T_{c2} + T_h}{-T_{c1} + T_h} \right] = -hc(A)/\dot{W}C_p$ 4-44

Yields:

- $\ln \left[\frac{-T_{c2} + T_h}{-T_{c1} + T_h} \right] = (T_{c2} - T_{c1}) / \Delta t_{lm}$ 4-45

Now to formulate the above equation in terms of the Log-Mean temperature

difference:

$$\bullet \quad \Delta t_{lm} = \frac{(T_{c2} - T_{c1})}{\ln \left[\frac{-T_{c2} + T_h}{-T_{c1} + T_h} \right]} \quad 4-46$$

The above equation is applied to ensure the appropriate fluid heat pickup within the control volume is assessed.

Hence finally in terms of heat load the corresponding heat load formulation is defined as the following in terms of the established control volumes.

$$\bullet \quad Q = -hc(A) \left\{ \frac{(T_{c2} - T_{c1})}{\ln \left[\frac{-T_{c2} + T_h}{-T_{c1} + T_h} \right]} \right\} \quad \text{or} \quad Q/A = (hc) \left\{ \frac{(T_{c2cv3ex} - T_{c1cvin3})}{\ln \left[\frac{-T_{c2cv3ex} + T_h}{-T_{c1cvin3} + T_h} \right]} \right\} \quad 4-47$$

(4.2) High Pressure Turbine Evaluation and Assessment of the Control Volumes established

Now proceeding forward, we now assess each control volume as identified and described in the preceding section; CV (1-3) is now evaluated towards ascertaining the temperature or rather the mixed-cup temperature exiting out of CV₁

Therefore, we commence our detailed assessment, which is basically the heart of this dissertation with CV₃, which is taken as control volume that establishes the inlet boundary conditions to the effective gas path cooling region.

Now we conduct the mass and energy balances assuming that the mixing chamber CV₃ is a steady flow system.

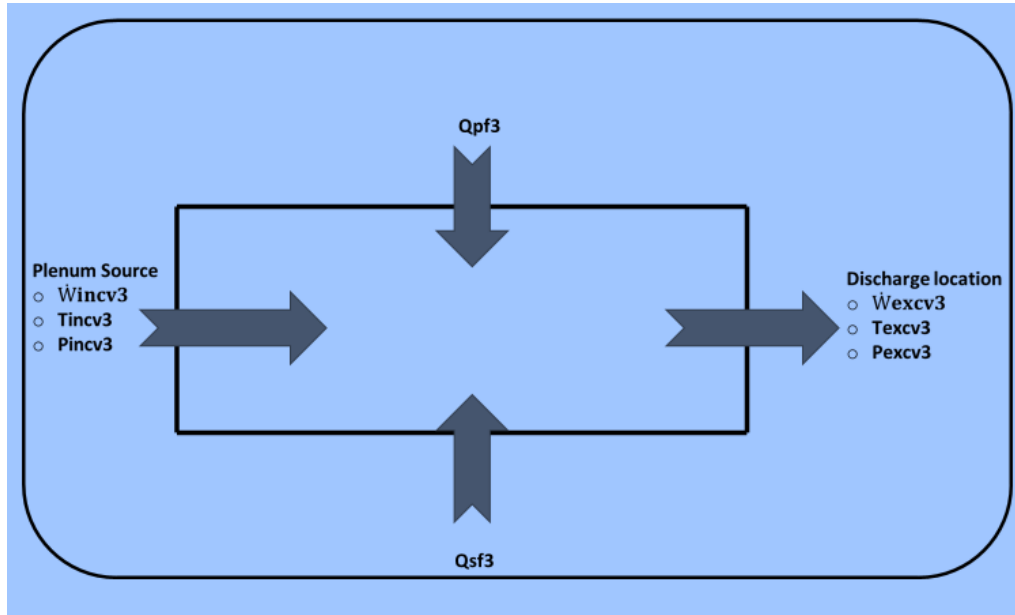


Figure 4.2 Control Volume 3A

Where:

- **Q_{pfcv-3}** => This represents the heat load entering from the source that is the flow path through the multiple resistances and into the coolant medium. This energy enters from the pressure side of the component under consideration and associated with the pressure side boundary conditions.
- **Q_{sfcv-3}** => This represents the heat load entering from the source that is the flow path through the multiple resistances and into the coolant medium. This energy enters from the suction side of the component under consideration and associated with the suction side boundary conditions.
- **\dot{W}_{incv-3} ; T_{incv-3} ; \dot{W}_{excv-3} ; T_{excv-3}** ; These parameters are described as the Inlet& Outlet Mass flow rate & Temperature conditions.

From applying the physics of mass balance hence based on the Conservation of mass theory

- $\dot{W}_{in\text{cv}3} - \dot{W}_{ex\text{cv}3} = 0$ 4-48

OR:

- $\dot{W}_{in\text{cv}3} = \dot{W}_{ex\text{cv}3}$ 4-49

And now from applying the physics of energy balance hence based on the

Conservation of energy theory:

- $[\dot{E}_{in}(\text{cv}3) - \dot{E}_{ex}(\text{cv}3) = \Delta E \text{ System}] = 0$ 4-50

Where:

- $\dot{E}_{in}(\text{cv}3) - \dot{E}_{ex}(\text{cv}3) \Rightarrow$ This is defined as the rate of net energy transfer by heat, work, and mass transfer 4-51
- $\Delta E \text{ System} \Rightarrow$ This is defined for the steady state conditions as the rate of change in the internal kinetic energy, potential energy, gravitational energy and also can be the quantum energy at the sub-atomic range but for this dissertation the author will not dwell too profoundly into the quantum state physics of the sub-atomic regions and will leave this aspect to the authors next Ph.D. dissertation initiative.

Thus:

- $\dot{E}_{in}(\text{cv}3) - \dot{E}_{ex}(\text{cv}3) = 0$; as $\Delta KE \ \& \ \Delta PE \equiv 0$ 4-52

Hence:

- $\dot{E}_{in}(\text{cv}3) = \dot{E}_{ex}(\text{cv}3)$ 4-53

Now we make the initial assumption that the flow rate in CV₃ is based on a typical

duct flow situation

- $\dot{W}_{in\text{cv}3}(\text{hincv}3) + Q_{pfcv3} + Q_{sfcv3} - \dot{W}_{ex\text{cv}3}(\text{hexcv}3) = 0$ 4-54

Now we let:

- $Q_{pfcv3} + Q_{sfcv3} = Q_{totalcv3} = Q_{Tcv3}$ 4-55

Hence:

- $\dot{W}_{incv3}(\dot{h}_{incv3}) + \dot{Q}_{Tcv3} - \dot{W}_{exc3}(\dot{h}_{exc3}) = 0 \Rightarrow$ This is the Energy Balance equation 4-56

Therefore:

- $\dot{Q}_{conv} = \dot{H}_{avg}(A_s)\Delta T_{lm} \Rightarrow$ This mathematical expression is the total heat transfer rate equation. Where ΔT_{lm} has been derived and defined earlier.

Now we proceed in combining the previously derived energy balance equation with the derived heat transfer rate equation and we obtain the following mathematical formulation specifically for Control Volume CV₃

Now we shall conduct and derive the energy balance for the identified control volume

- $\dot{Q}_{conv} = \dot{W}_{incv3}(C_p)(T_{W,exc3} - T_{W,incv3})$ 4-57

Which can also be depicted as the following mathematical expression:

- $\dot{Q}_{conv} = \dot{H}_{avg}(A_s)\Delta T_{lm} = \dot{Q}_{Tcv3}$

This is the control volume rate equation 4-58

- $\dot{W}_{incv3}(C_p)(T_{exc3} - T_{incv3}) = \dot{H}_{avg}(A_s)\Delta T_{lm} \Rightarrow$ This is the mathematical expression for the cold side or coolant side assessment of the control volume under consideration 4-59

Now:

- $\{\Delta T_{lm} = \frac{(\Delta T_{exc3} - \Delta T_{incv3})}{\ln(\Delta T_{exc3} / \Delta T_{incv3})}\}$ 4-60

Now to convert the above equation to be aligned to the focus of the control volume being assessed, based on the aforementioned mathematical evaluations we now have the following expression in terms of the parameters reflecting the control volume under consideration.

$$\bullet \quad \Delta T_{lm} = \frac{(T_{hs} - T_{exc3}) - (T_{hs} - T_{inc3})}{\ln \left[\frac{T_{hs} - T_{exc3}}{T_{hs} - T_{inc3}} \right]} \quad 4-61$$

Where “s” is reflecting the inner control volume wall surface temperature.

Hence: $\text{Havg}(As)\Delta T_{lm} \Rightarrow$ Can now be written down as:

$$\bullet \quad \text{Havg}(As)(\Delta T_{lm}) \equiv (As) \left\{ \frac{(T_{hs} - T_{exc3}) - (T_{hs} - T_{inc3})}{\ln \left[\frac{T_{hs} - T_{exc3}}{T_{hs} - T_{inc3}} \right]} \right\} \quad 4-62$$

After furthermore mathematical manipulation yields:

$$\bullet \quad \dot{W}_{inc3}(C_p)(T_{exc3} - T_{inc3}) = \text{Havg}(As) \left\{ \frac{(T_{hs} - T_{exc3}) - (T_{hs} - T_{inc3})}{\ln \left[\frac{T_{hs} - T_{exc3}}{T_{hs} - T_{inc3}} \right]} \right\} \quad 4-63$$

Now at this point we determine the process of obtaining the exit conditions of the control volume CV_3

Hence based on the above earlier derived mathematical expression The following is the Nomenclature:

- $\text{Havg}(As) \Rightarrow$ This is referenced as the control volume inner wall surface heat transfer “Havg” multiplied by the wetted surface area (As)
- $\dot{W}_{inc3} \Rightarrow$ Mass flow rate into (CV_3)
- $C_{p-avg} \Rightarrow$ Specific heat rate (average) based on fluid properties of control volume CV_3
- $T_{exc3} \Rightarrow$ This is the fluid exit temperature for CV_3 including heat pick up.
- $T_{inc3} \Rightarrow$ This is the fluid inlet temperature for CV_3
- $T_{hs3} \Rightarrow$ This is the inner cooled wall CV_3 surface temperature

Further illustration of control volume (3) ; let’s call it Control Volume (3B)

Control volume CV-3B can be illustrated as follows:

Where:

- T_1, T_2, T_3 = The interface layer surface temperature
- \dot{W}_{in} = Flow rate entering the control volume

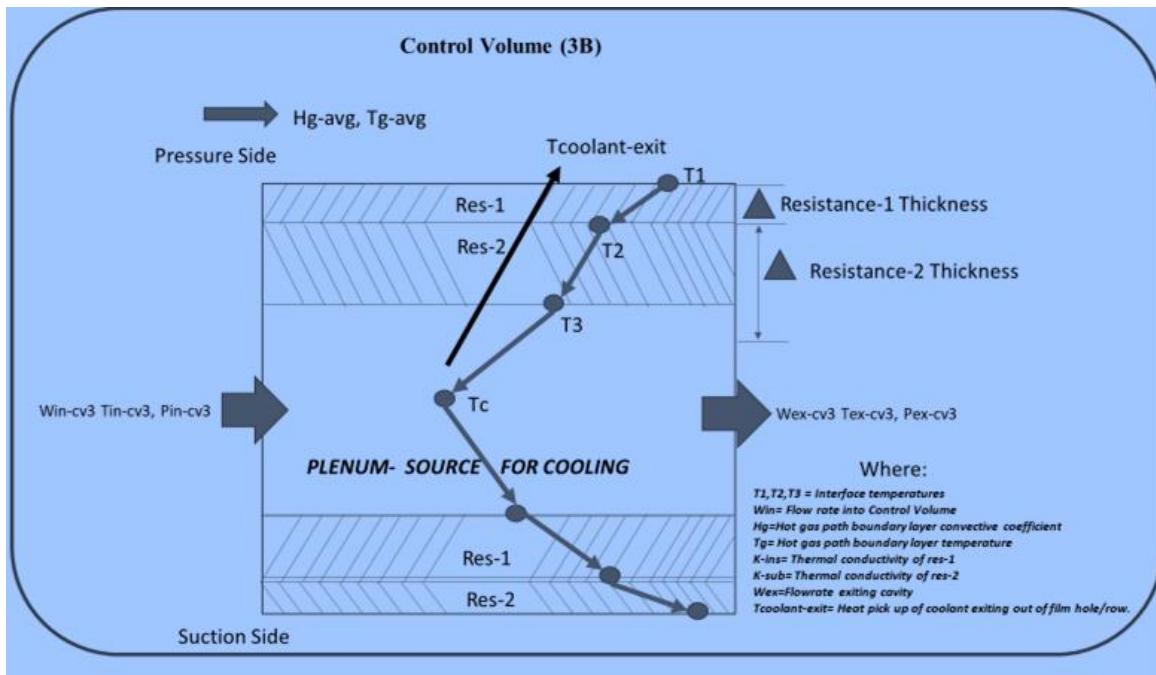


Figure 4.3 Control Volume (3B)

- H_g = External hot side path heat transfer coefficient
- T_g = External hot side path fluid temperature
- K = Interface property Conductivities
- \dot{W}_{ex} = Flow rate exiting out of the control volume

Now to solve for $CV_3 - T \dot{W}_{ex} CV_3$; we need to ascertain the values of the remainder of the parameters and explain its rationale and logic.

Therefore:

- \dot{W}_{in} = This is the plenum or the source-based conditions and is a given input into the control volume - CV_3 .

Now we resolve for the synergy or the interdependency / coupling of the inner wall material temperature and the associated coolant side heat transfer coefficient.

Physics based Mathematical Analysis is as follows: In reference to the established control volume as per Figure 3.3; an energy balance is applied relating to the energy being conducted from each of the faces of the control volume selected.

i.e., Energy being conducted in the left section of the control column selected + heat generated within the element part of the control volume which equates to the differential variation of the internal energy + the total energy that is conducted exiting out of the right face.

Hence, by combining all the energies with respect to each of the faces of the selected control volume, and defining the following parameters as follows:

Where:

\dot{q} = energy that is being generated per unit volume

c = specific heat of the applied material

ρ = the density of the applied material under consideration

hence by combining the overall parameters we get the following mathematical description of the overall process:

$$-kA \frac{\partial T}{\partial x} + \dot{q}A dx = \rho c \frac{\partial T}{\partial \tau} dx - A \left[k \frac{\partial T}{\partial x} + \frac{\partial}{\partial x} \left(k \frac{\partial T}{\partial x} \right) dx \right]$$

Or the above expression can also be written down as per the following expressions which is also the one-dimensional heat conduction equation.

$$\frac{\partial}{\partial x} \left(k \frac{\partial T}{\partial x} \right) + \dot{q} = \rho c \frac{\partial T}{\partial \tau}$$

For purposes of this dissertation, it is assumed there is no heat generation and hence the above expression is now written down as the following:

$\frac{d^2T}{dx^2} = 0$; which is defined as the steady state with no heat generation, and also can be

written as; $\dot{q} = -kA \frac{\partial T}{\partial x}$

Where:

- \dot{q} = is the heat transfer rate
- $\frac{\partial T}{\partial x}$ = the temperature gradient in the flow direction of the heat flux vector
- k = thermal conductivity of the material under consideration

Fourier's law of heat conduction states that the heat flow rate through the process of conduction through the material under consideration is directly proportional to the temperature potential difference and inversely proportional to the overall resistances.

In mathematical terms the differential equation depicting the Fourier's law of heat conduction is as aforementioned is the following:

- $q = -KA \frac{dT}{dx}$ 4-64

Performing the separation of variables:

- $qdx = -KA dT$; which can also be written as $\Rightarrow \frac{q}{A(dx)} = -KdT$ 4-65

Integrating both sides of the above equation with the defined limits yields:

- $\frac{q}{A} \int_{x1}^{x2} dx = - \int_{Tg}^{Twf} KdT$ 4-66

- Let $(Tg - Twf) = \Delta t$ 4-67

Hence this leads to the following known mathematical expression:

- $\frac{q}{A} = \frac{\Delta t}{\Sigma R}$ 4-68

Now considering the aforementioned mathematically derived expression is applied to a composite wall. Based on the Fourier's law of heat conduction- The overall resistance

to the heat flow is assumed to be directly proportional to the material thicknesses (metal & insulation layers); and is inversely proportional to the inverse of the External Gas path heat transfer coefficient, The substrate metal wall thickness/ The substrate metal wall - Conductivity; The insulation layer thickness/ Insulation property- Conductivity and directly proportional to the heat flux vector.

For the purpose of this dissertation the author conducts a simplification for assessing the one-dimensional heat transfer, hence Simplifying this equation the Fourier's Law of heat conduction is as follows:

$$(i) \frac{q}{A} (\text{Heat Flux Vector}) = \frac{(T_g - T_{wf})}{\sum R} \quad 4-69$$

Where Resistances are defined as =>

$$(ii) \left\{ \left(\frac{1}{Res_1} \right); \left(\frac{\Delta x}{K} Res_2 \right); \left(\frac{\Delta x}{K} Res_3 \right); \left(\frac{1}{Res_4} \right) \right\} = \sum R \quad 4-70$$

Where:

(iii) T_{wf} => The cold side fluid medium bulk temperature

Hence: The differential equations for the interface temperature across the control volume resistances can be solved from the following equation based on cartesian co-ordinates

$$\frac{\partial}{\partial x} \left(k \frac{\partial T}{\partial x} \right) + \frac{\partial}{\partial y} \left(k \frac{\partial T}{\partial y} \right) + \frac{\partial}{\partial z} \left(k \frac{\partial T}{\partial z} \right) + \dot{q} = \rho c \frac{\partial T}{\partial \tau} \quad 4-71$$

From the above differential equation depicting the overall system, we can now write by solving for the one-dimensional aspects and negating the heat generation term, the required interface temperatures for each resistance within the respective control volumes and assuming recovery effects within the boundary layer.

Where:

$$T1 = \left\{ \left[\frac{T_t}{\left(1 + \frac{(\gamma-1)M^2}{2}\right)} \right] + \left[1 + \frac{(\gamma RM^2)}{2C_p} \right] \right\} - \left[\frac{-KA \frac{dT}{dx}}{\left[\left(\frac{Kg}{X} \right) (0.0296) (Pr^{1/3}) \left[\sqrt{\frac{\gamma g c}{RT_g}} \right] (P1_a) \left\{ \frac{M}{\left[1 + \left(\frac{\gamma-1}{2} \right) M^2 \right]^{\gamma+1/2(\gamma-1)}} \right\} (X/\mu) \right]} \right]$$

4-72

$$T2 = \left\{ \left[\frac{T_t}{\left(1 + \frac{(\gamma-1)M^2}{2}\right)} \right] + \left[1 + \frac{(\gamma RM^2)}{2C_p} \right] \right\} - \left[\frac{-KA \frac{dT}{dx}}{\left[\left(\frac{Kg}{X} \right) (0.0296) (Pr^{1/3}) \left[\sqrt{\frac{\gamma g c}{RT_g}} \right] (P1_a) \left\{ \frac{M}{\left[1 + \left(\frac{\gamma-1}{2} \right) M^2 \right]^{\gamma+1/2(\gamma-1)}} \right\} (X/\mu) \right]} \right] - \left[\frac{-KA \frac{dT}{dx}}{\left[\frac{\Delta x}{K} (\text{Resistance}-1) \right]} \right]$$

4-73

$$T3 = \left\{ \left[\frac{T_t}{\left(1 + \frac{(\gamma-1)M^2}{2}\right)} \right] + \left[1 + \frac{(\gamma RM^2)}{2C_p} \right] \right\} - \left[\frac{-KA \frac{dT}{dx}}{\left[\left(\frac{Kg}{X} \right) (0.0296) (Pr^{1/3}) \left[\sqrt{\frac{\gamma g c}{RT_g}} \right] (P1_a) \left\{ \frac{M}{\left[1 + \left(\frac{\gamma-1}{2} \right) M^2 \right]^{\gamma+1/2(\gamma-1)}} \right\} \left(\frac{X}{\mu} \right) \right]} \right] - \left[\frac{-KA \frac{dT}{dx}}{\left[\frac{\Delta x}{K} (\text{Resistance}-1) \right]} \right] - \left[\frac{-KA \frac{dT}{dx}}{\left[\frac{\Delta x}{K} (\text{Resistance}-2) \right]} \right] \quad 4-74$$

- T1, T2 & T3 => Are the control volume interface temperatures.
- Twf = Bulk temperature of the fluid

As mentioned previously Thscv3= Inner wall cooled side surface temperature =

T3. Hence:

$$\{Thscv3 = T1 - Hg \left(\left\{ \left[\frac{T_t}{\left(1 + \frac{(\gamma-1)M^2}{2}\right)} \right] + \left[1 + \frac{(\gamma RM^2)}{2C_p} \right] \right\} - T1 \right) [(\Delta x/K_{Ins}) + (\Delta x/K_{Wall})] \} \quad 4-75$$

Note: Thscv3 = Tsurface of the control volume assessment and for analysis purposes, once magnitude is determined then it is assumed to be held constant for calculations

pertaining to the flow exit temperature for the respective control volume under consideration.

In addition, also note the author assumes that the average substrate temperature is also applied to the inner surface wall temperature for the effective gas path cooling hole as it is assumed that the surface area for CV₃ dominates over surface area for CV₂

Assuming the system is a planar geometrical feature and in addition the author assumes that the lateral conduction is negligible and through wall conduction is pivotal hence, based on the energy balance across the overall system of resistances the heat flux vector is equivalent throughout the entire series of resistances.

Mathematically this is depicted as the following:

$$\bullet \quad \left(\frac{Q}{A}\right)_{\text{Hot}} = \left(\frac{Q}{A}\right)_{\text{Cold}} \quad 4-76$$

Or in other words:

$$\bullet \quad [\text{ENERGY IN} = \text{ENERGY OUT}] \quad 4-77$$

The energy or the enthalpy garnered from the external gas path is equivalent to the energy lost to the internal coolant side fluid medium.

Now we solve for the exit temperature “Tw_{excv3}” = T_{excv3} out of the control volume (cv₃):

To compare or rather derive a mathematical expression for “Tw_{excv3}” = f (x₁, x₂, x₃, etc.) The author proposes the following approach:

Identify the known quantities:

- Inlet conditions into cv₃ are known and that is the following:
- W_{incv3}; Tw_{cv3}; P_{incv3}, Cp_{avg-cv3}

- On conducting the one-dimensional Fourier's law of heat conduction and associated convection assessment and evaluation the "HAs" for cv3 can then be ascertained and the corresponding "Thscv3" can also be termed as a known quantity through application of the one-dimensional heat conduction equation as derived earlier.
- From the aforementioned rationale the only unknown is now "Twexcv3"

Now we conduct the mathematical analysis for the chosen control volume under consideration. Let's expand the following equation earlier derived for CV₃, and hence yields

Let:

$$\dot{W}_{incv3}(C_p)T_{excv3} - \dot{W}_{incv3}(C_p)T_{incv3} = \overline{Hc}(As) \left\{ \frac{(T_{hs} - T_{excv3}) - (T_{hs} - T_{incv3})}{\ln \left[\frac{T_{hs} - T_{excv3}}{T_{hs} - T_{incv3}} \right]} \right\}$$

4-78

$$\dot{W}_{incv3}(C_p)T_{excv3} - \dot{W}_{incv3}(C_p)T_{incv3} = \overline{Hc}(As) \left\{ \frac{[-T_{excv3} + T_{incv3}]}{\ln \left[\frac{T_{hs} - T_{excv3}}{T_{hs} - T_{incv3}} \right]} \right\}$$

4-79

Where in order to simplify we let:

$$\ln \left[\frac{T_{hs} - T_{excv3}}{T_{hs} - T_{incv3}} \right] = \mathfrak{N} \quad 4-80$$

From the fundamentals of mathematics, we know that as per the Natural log's mathematical expressions we have:

$$\left[\ln \left(\frac{a}{b} \right) = \ln(a) - \ln(b) \right] \text{ , hence yields the following after further expansion}$$

and substituting the parameter "N" 4-81

- $\dot{W}_{incv3}(C_p)T_{excv3} - \dot{W}_{incv3}(C_p)T_{incv3} = HAs \left\{ \left(-\frac{T_{Wexcv3}}{\bar{m}} + \frac{T_{Wincv3}}{\bar{m}} \right) \right\}$ 4-82

- $\dot{W}_{incv3}(C_p)T_{excv3} - \dot{W}_{incv3}(C_p)T_{incv3} = HAs \left(-\frac{T_{excv3}}{\bar{m}} \right) + HAs \left(\frac{T_{incv3}}{\bar{m}} \right)$ 4-83

Now as aforementioned earlier:

- $\ln \left[\frac{T_{hs} - T_{excv3}}{T_{hs} - T_{incv3}} \right] = \bar{m} \equiv \ln(T_{hs} - T_{excv3}) - \ln(T_{hs} - T_{incv3})$ 4-84

Thus:

- $HAs \left\{ \left(-\frac{T_{excv3}}{\bar{m}} \right) + HAs \left(\frac{T_{incv3}}{\bar{m}} \right) \right\} \equiv \{ HAs (-T_{excv3}) / \ln(T_{hs} - T_{excv3}) - \ln(T_{hs} - T_{incv3}) \} + \{ HAs(T_{incv3}) / \ln(T_{hs} - T_{excv3}) - \ln(T_{hs} - T_{incv3}) \}$ 4-85

- $T_{Wexcv3} \left\{ \frac{HAs}{\bar{m}} + (\dot{W}_{incv3})(\bar{C}_p) \right\} = \frac{HAs}{\bar{m}} (T_{Wincv3}) + (\dot{W}_{incv3})(\bar{C}_p)(T_{Wincv3})$ 4-86

Now from the above equation we recognize that this equation is a transcendental equation, and hence through the process of mathematical iteration between the L.H.S and R.H.S of the derived equation; we try to solve for T_{excv3} , and we obtain the following mathematical expression:

Hence: Solving for T_{excv3} , through the process of mathematical iteration between the L.H.S and R.H.S of the derived equation the fluid temperature emanating out of control CV_3 is obtained.

Once we include the values of the known parameters then the only parameter that is remaining unknown to be solved for is the parameter “ T_{excv3} ” Hence after substitution

of the values of the known parameters we can then solve for “Texcv3” through the process of mathematical iteration between the L.H.S and R.H.S of the derived equation.

Therefore: As it is assumed that there are no bleed holes or inlets in CV₃; except the source; Hence from the laws of continuity the following is true:

$$(i) \quad \dot{W}_{excv3} = \dot{W}_{incv3} \quad 4-87$$

$$(ii) \quad T_{wexcv3} = \frac{\left\{ \frac{H_{As}}{\dot{m}} (T_{incv3}) + (\dot{W}_{incv3}) (\overline{C_p}) (T_{incv3}) \right\}}{\left\{ \frac{H_{As}}{\dot{m}} + (\dot{W}_{incv3}) (\overline{C_p}) \right\}} \quad 4-88$$

Note: The author has deduced then rigorous control volume assessments the following parameter “ η ” which incorporates the overall Gas Path and coolant side synergy or coupling effects aligned to CV₃.

Inlet conditions to CV₂:

Note: Here the author assumes that the only exit from CV₂ is the inlet to the effective gas path cooling configuration for both the suction and pressure side bleeds (effective gas path holes). However, for this dissertation and confirming to simplicity the author assumes a bulk average of the two streams (pressure & suction) and consolidates the effective gas path as one stream entering and exiting out of CV₂:

Hence, entering the control volume CV₂ are the following parameters derived from exit conditions of CV₃, and are the following:

- \dot{W}_{excv3}
- T_{wexcv3}
- P_{excv3}

Now we proceed to evaluate the fluid pressure conditions required for the respective control volume under consideration.

The other essential parameter yet to be derived is the exit pressure emanating out of CV₃, and the following physics based on the authors academic and professional understanding is applied referencing open literature based fundamental physics on how to evaluate the exit pressure emanating out of CV₃. The following assumptions & corresponding physics based mathematical computations are conducted, based on solving the momentum equation.

For CV₂: As per the continuity relationship and based on the assumption that the flow within the CV₃ is steady hence from the system-based conservation of mass theory:[7];[14]

$$\bullet \quad (d\dot{W}/dT)_{\text{System}} = 0 = d/dt \left(\int_{\text{cs}} \rho dV \right) + \left(\int_{\text{cs}} \rho \mathbf{V} \cdot \mathbf{n} \right) dA \quad 4-89$$

Here the author references open literature textbooks [7];[14] applied from academic experience, Note the above equation is the integral mass conservation law for a control volume which is deformable, however we will make the assumption that CV₃ is a fixed volume hence the following mathematical expression is applied:

$$\bullet \quad \int_{\text{cv}} (\partial \rho / \partial t) dV + \int_{\text{cs}} \rho (\mathbf{V} \cdot \mathbf{n}) da = 0 \quad 4-90$$

Where for steady state conditions:

$$\bullet \quad \int_{\text{cv}} \left(\frac{\partial \rho}{\partial t} \right) dV = 0 \quad 4-91$$

&

$$\bullet \quad \int_{\text{cs}} \rho (\mathbf{V} \cdot \mathbf{n}) da = 0 \quad \Rightarrow \text{This states that in the condition of steady state flow, the associated mass flow entering \& exiting the CV}_3 \text{ must by definition be fully balanced}$$

$$\bullet \quad \Sigma(\rho_i * V_i * A_i)_{\text{in}} = \Sigma(\rho_i * V_i * A_i)_{\text{out}} \quad 4-92$$

The above equation is the representation of the steady flow mass conversation relation.

For the following assumptions related to the control volume under consideration that the associated flow is at steady flow conditions, hence the continuity equation can be described as the following:

$$\rho \bar{v} = \frac{w}{A} = k \text{ this is the Continuity Equation}$$

Differentiating the continuity equation, we get the following mathematical expression

$$\frac{d\rho}{\rho} + \frac{d\bar{v}}{\bar{v}} = 0$$

Now by introducing the Steady Flow Energy Equation, and also including the Force Momentum Equation, and also considering that the inner wall of the control volume is subjected to the frictional force “ τ ” the general Momentum equation derived is the following:

Starting with the equating the forces in the axial direction, (as the author assumes that the axial direction is the direction of motion) to the rate of change of momentum in the direction of motion across the overall control volume boundaries.

$$A\{p - (p + \partial p)\} - \tau_o P dx = w\{(\bar{v} + \partial \bar{v}) - \bar{v}\}$$

P = denoted to be the overall perimeter of the control volume under consideration.

$$-dp - \left(\frac{\rho \left[\frac{0.046}{Re^{0.2}} \right] \bar{v}^2}{2} \right) \frac{P}{A} dx = \left(\frac{w}{A} \right) d\bar{v}$$

Note: The flow velocity as well as the flow temperature will differ as the fluid flows along the prescribed boundaries of the control volume under consideration. As the flow velocity differs so will the associated fluid Mach number. To decipher the change of the

fluid properties we can leverage the physics of combining the state equation with the momentum equation.

Now to ensure we have the mathematical equation for the pressure loss of the fluid traversing the control volumes. Hence from the state equation, continuity relationships and including the steady flow energy equation and momentum equation [14][50]; with assuming fully developed flow conditions, the following mathematical expression has been derived by the author as per the control volume under consideration.

$$\begin{aligned}
 & \frac{1}{2}(P_2^2 cv3ex - P_1^2 cvin3) - (V_1^2 / R \left\{ \frac{(Tc_2 cv3ex - Tc_1 cvin3)}{\ln \left[\frac{-Tc_2 cv3ex + Th}{-Tc_1 cvin3 + Th} \right]} \right\}) P_1^2 cv3 \\
 & * \log_e(P_2^2 cv3ex / P_1^2 cvin3) \\
 & = \frac{1}{2} \left(\frac{0.046}{\left(4 * \frac{W}{\text{perim} * \mu} \right)^{0.2}} \right) \left(\frac{P}{A} \right) P_1^2 cv3in / R \left\{ \frac{(Tc_2 cv3ex - Tc_1 cvin3)}{\ln \left[\frac{-Tc_2 cv3ex + Th}{-Tc_1 cvin3 + Th} \right]} \right\} * V_1^2 (x_2 - x_1) \quad 4-93
 \end{aligned}$$

Hence from Eq 4-93, the Delta-P or the pressure differential can be mathematically depicted as the following based on the control volume under consideration.

Let

$$\begin{aligned}
 a1 &= \frac{1}{2} \left(\frac{0.046}{\left(4 * \frac{W}{\text{perim} * \mu} \right)^{0.2}} \right) \left(\frac{P}{A} \right) P_1^2 cv3in / R \left\{ \frac{(Tc_2 cv3ex - Tc_1 cvin3)}{\ln \left[\frac{-Tc_2 cv3ex + Th}{-Tc_1 cvin3 + Th} \right]} \right\} \\
 a2 &= V_1^2 (x_2 - x_1) + \left\{ - (V_1^2 / R \left\{ \frac{(Tc_2 cv3ex - Tc_1 cvin3)}{\ln \left[\frac{-Tc_2 cv3ex + Th}{-Tc_1 cvin3 + Th} \right]} \right\}) P_1^2 cv3 \right. \\
 a3 &= \log_e(P_2^2 cv3ex / P_1^2 cvin3) \}
 \end{aligned}$$

Therefore, the overall mathematical expression is the following:

$$(P_2^2 cv3ex - P_1^2 cvin3) = \sqrt{(a1)(a2)(a3)} \quad 4-94$$

Solving the above equation 4-94 above via an iteration approach for R.H.S = L.H.S will yield the desired Pressure at the exit location of the control volume.

Where:

- $P_{1cvin3} = P_{incv3} \Rightarrow$ known parameter at the inlet of cv3 plenum-total pressure conditions, and here the author assumes this to be Compressor discharge conditions, assuming negligible losses from compressor exit to intended control volume.

- $P_{2cv3ex} = P_{excv3} =$ Exit pressure out of the control volume

- $Perim =$ Duct or control volume equivalent perimeter

- $T =$ Fluid temperature in control volume based on Log Mean differential. Which

$$\text{is } \frac{(T_{c2cv3ex} - T_{c1cvin3})}{\ln \left[\frac{-T_{c2cv3ex} + T_h}{-T_{c1cvin3} + T_h} \right]} \quad 4-95$$

- $f =$ friction factor for the smooth duct.

- $D_h =$ Hydraulic diameter $= 4A_c/P$ 4-96

- $\dot{W} =$ Flow rate $\left(\frac{\text{lbm}}{\text{Sec}} \right)$

- $\rho =$ Density of the fluid

- $g_c =$ Gravitational acceleration

- $\mu =$ Fluid viscosity, $(\text{N} \cdot \text{Sec})/\text{m}^2$; $\text{lb.}/\text{Ft} \cdot \text{sec}$

- $X =$ Duct length

- $\left(\frac{P}{A} \right)^{-1} = (A/P) =$ hydraulic Depth of the control volume. [47] 4-97

- On further obtaining the delta-P “ Δp ” CV_3 we can then compute the values for P_{excv3} knowing P_{incv3} & associated Δp .

We now commence our assessment with the subsequent control volume – Control volume-CV₂: This control volume is taken as a system mixing chamber. We now conduct the mass and energy balances assuming that the mixing chamber is a steady flow system.

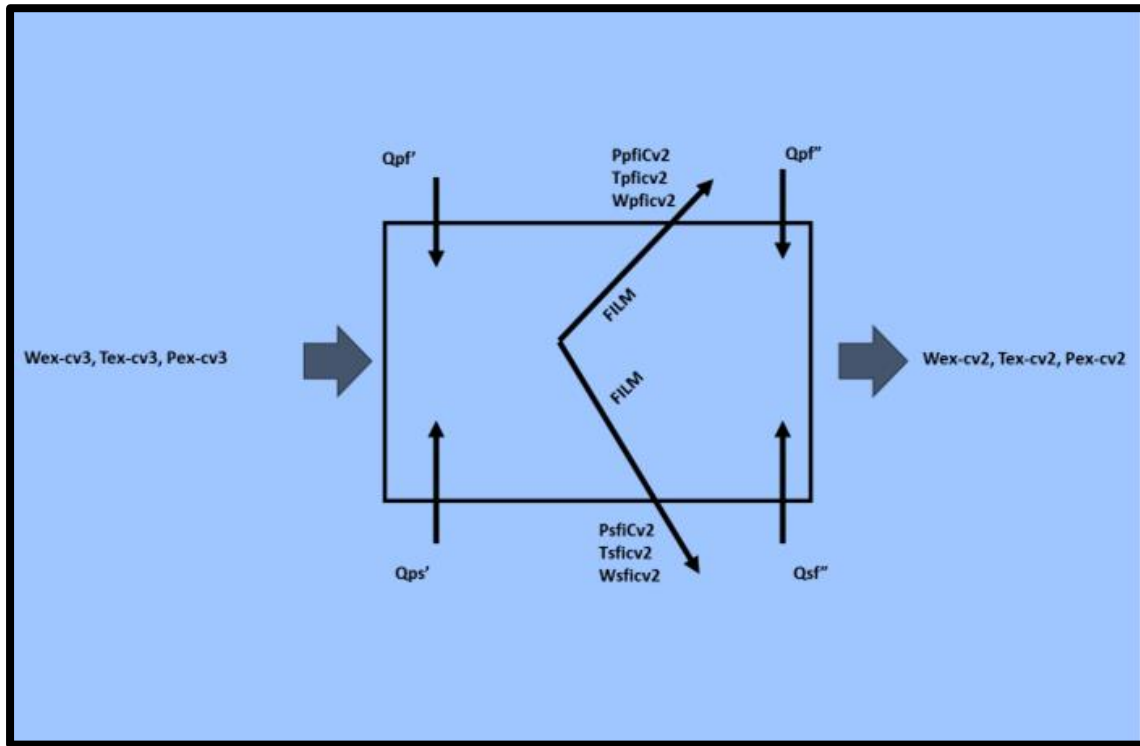


Figure 4.4 Control Volume (2)

Where:

- $T_{excv3}, P_{excv3}, \dot{W}_{excv3} \Rightarrow$ Temperature, pressure and mass flow rates exiting out of CV₃ and entering CV₂
- $Q_{pf}; Q_{sf} \Rightarrow$ Heat flux vectors generated from the hot gas path accumulating from the both the pressure and suction side of the component under consideration and primarily focused on the areas upstream of the coolant “effective gas path” ejection rows and downstream of the areas already considered in CV₃ evaluation.

- Q_{pf} ; $Q_{sf} \Rightarrow$ Same as defined above but for the regions downstream of the effective gas path rows. Additional extremely essential assumptions are as follows:
- If it is assumed that the area related to the energy generated from the HGP (pressure & suction) being absorbed into CV_2 , is negligible for the region upstream of the coolant ejection rows; then the following applies:
- $Q'_{pf} \& Q'_{sf} = 0 \Rightarrow$ Note this is an extremely essential assumptions as the author is assuming that as also mentioned earlier that the CV_3 surface area is dominating over surface area of CV_2 , hence the average substrate temperature is being applied for effective gas path cooling hole inner surface metal temperature. Now the other option is to actually, similar to the CV_3 , conduct the overall conduction and convection assessment and ascertain the effective gas path cooling inner wall temperature, but for this dissertation the assumption aforementioned is satisfactory on a bulk assessment perspective.

And note that this signifies that all (region upstream of the coolant ejection) heat fluxes are already considered within CV_3 .

This results in the mass balance of CV_3 as follows:

$$\bullet \quad \dot{W}_{excv3} - (\dot{W}_{pficv2} + \dot{W}_{sficv2}) = \dot{W}_{ocv2} \quad 4-98$$

-Or-

$$\bullet \quad \dot{W}_{excv3} - \dot{W}_{pfi - cv2} - \dot{W}_{sfi - cv2} - \dot{W}_{o - cv2} = 0 \quad 4-99$$

This results in the mass balance of CV_2 as follows:

Known quantities

- $\dot{W}_{excv3} \rightarrow$ This is known from $cv3$

- $\dot{W}_{pfi-cv2} \rightarrow$ Knowing the pressure ratio across the effective gas path hole/row, mass flow rate along with the assumed hole area can be computed.
- $\dot{W}_{sfi-cv2} \rightarrow$ Similar logic and rationale as $\dot{W}_{pfi-cv2}$

Now based on the aforementioned quantities \dot{W}_{o-cv2} can be determined.

Therefore: The coolant ejection effective gas path row inlet conditions are the following:

Assuming the inlet and other conditions pertaining to the effective gas path hole/row in CV₁:

Note:

- Pressure inlet to effective gas path cooling row is the static pressure computed as the exit pressure based on flow ejection out of CV₃
- Temperature inlet to effective gas path cooling row is the temperature computed as the exit temperature based on flow ejection out of CV₃
- The gas path pressure at effective gas path cooling row exit plane has already been computed previously in the aerodynamic section during the evaluation of the mean-line average conditions, hence now we have defined the overall pressure ratio across the coolant ejection rows.

The following methodology is applied in computing the coolant ejection “effective gas path cooling rows” mass flow rates.

The following analysis will now provide the foundation for deriving the following relationships.

- (i) Mass flow rate through / ejected out of coolant ejection regions
- (ii) Heat pick-up of fluid through coolant ejection regions

- (iii) Fluid outlet temperature ejected out of coolant ejection regions
- (iv) Assumption is made on the coolant ejection geometrical effectiveness

We shall now introduce an additional “intermediate” control volume which is coupled to the rest of the control volumes and is defined as the control volume for the coolant ejection region.

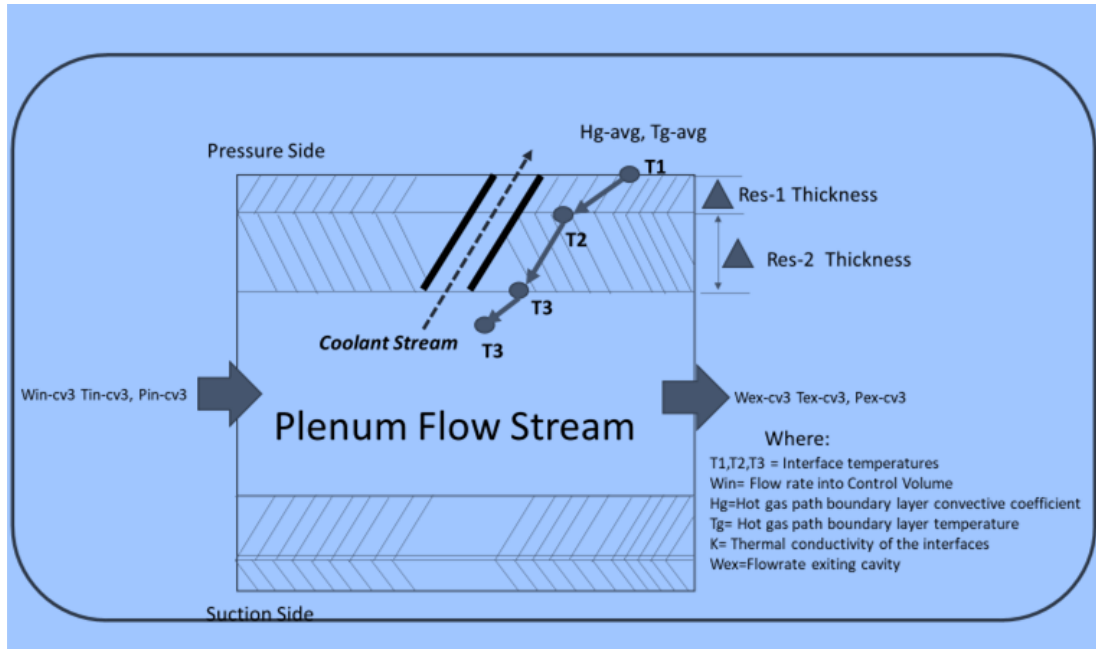


Figure 4.5 Control Volume (effective gas path cooling Domain)

CHAPTER 5:
ESTABLISHING OVERALL SYNERGY OF HPT BASED DISCIPLINE
INTEGRATION ALIGNED TO EACH KEY CONTROL VOLUME

The primary objective is now to derive the physics based mathematical expressions to obtain the flow rate ejected or rather emanated from the coolant ejection regions, considering the assumed known and derived boundary conditions.

Note at this point the corresponding heat transfer mechanisms imposed on the cold side of the substrate-metal wall is entirely unknown and requires defining. Hence, we shall now introduce the smooth duct conditions at this region.

At this point of my dissertation a Segway is provided for the application toward the synergy between the mean-line aerodynamics based parameters.

Note during the evaluation of the single stage high pressure turbine velocity triangle, the associated thermodynamic properties at each state point will be derived as a mathematical expression for pressure variation for each state point.

Hence, from the aforementioned explanation applying the hot gas path static pressure evaluated on the external fiber of the stationary component and by also knowing the supply conditions at the entrance of the coolant ejection regions resulting from the previous control volume analysis; we now derive the physics based mathematical formulations to further evaluate the corresponding flowrates across the coolant ejection regions. Hence the following assessment is being conducted primarily for the respective

control volumes and also for the control volume that resides the effective gas path cooling aspects.

(5.1) Steady 1D isentropic Flow physics derivations aligned to HPT control volumes

Our next physics based mathematical formulations for the compressible flow related pressure ratio and Mach number relationship is now depicted through derivation. In order to do so the author relies on the second law of thermodynamics and entropy concepts.

Hence, the following process is commenced as referenced from the second law of thermodynamics and entropy concepts.

When we consider a thermodynamic reversible process, we usually assume that in this process all of the energy in the form of heat added into a system can be transferred into applied work. However, this is not the case. The reason being is as follows:

Note the first law of thermodynamics focuses upon the portion of the energy (heat) that is transferred into applied work, whereas the second law of thermodynamics focused on the actual quantity of the energy (heat) that is transferred into applied work.

For a closed system undergoing a cyclic transformation where heat per unit mass (δQ_R) is obtained reversibly at absolute temperature. Here the author again leverages his academic studies to derive the following mathematical expressions:

Mathematically this is defined as the following:

$$\bullet \quad \oint \frac{\delta Q_R}{t} = 0 \quad [7] \quad 5-0$$

Where:

$$\bullet \quad Q = \text{Heat}$$

R= Reversible process

- $\oint = \text{Cyclic}$
- $T = \text{Absolute temperature}$
- $\frac{\delta Q_R}{t} \Rightarrow$ This is a thermodynamic property of the system under consideration and termed as “s” the system entropy by Clausius. 5-1
- $\oint \frac{\delta Q_R}{t} = 0 \Rightarrow$ Leads to $dS \equiv \frac{\delta Q_R}{t}$ [7] 5-2

Therefore, if the assumption is now made that the system undergoes an isentropic or a reversible process then this leads to the following mathematical description:

- $dS \geq \frac{\delta Q}{t} \Rightarrow$ This equality determines that the system is undergoing a reversible process. 5-3

At this point we shall now introduce the known concept of the thermodynamics of the steady one-dimensional flow process.

Hence the known mathematical expression for the steady state one dimensional flow [14] of any fluid is the following:

Steady State flow:

- $Q + h_1 + 1/2(V_1^2) + gZ_1 = W + h_2 + 1/2(V_2^2) + gZ_2$ 5-4

Where:

- $Q \Rightarrow$ Heat (Energy) added into the fluid
- $H \Rightarrow$ Enthalpy of the fluid
- $Z \Rightarrow$ Height applied in the potential energy term
- $W \Rightarrow$ Work term

Finally, the mathematical expression is the following with the assumption:

$g(Z_2 - Z_1) \Rightarrow$ This term is negligible for fluids of small density

$$\bullet \quad Q + h_1 + 1/2(V_1^2) + gZ_1 = W + h_2 + 1/2(V_2^2) + gZ_2 \quad 5-5$$

$$\bullet \quad Q + h_1 + 1/2(V_1^2) = W + h_2 + 1/2(V_2^2) \quad 5-6$$

From the perspective of this dissertation in the control volume of effective gas path cooling hole cv (effective gas path cooling) a stationary hole in the stage1 nozzle; there is no work extraction, hence Work term =0

Therefore, based on aforementioned assumption; now we make the assumption that if the fluid flowing through the orifices that provide effective gas path cooling does not contribute towards any work and is basically semi-adiabatic which is translated as negligible heat transfer then for all practical purposes the physics based mathematical expression is as follows:

$$\bullet \quad \delta Q = \delta W = 0 \quad 5-7$$

Then:

$$\bullet \quad h_1 + \frac{V_1^2}{2} = h_2 + \frac{V_2^2}{2} \quad 5-8$$

$$\text{If: } h_i = C_{pi} * t_i \quad 5-9$$

Then:

$$\bullet \quad C_{p1}t_1 + \frac{V_1^2}{2} = C_{p2}t_2 + \frac{V_2^2}{2} \quad 5-10$$

Assume: $C_p \equiv$ Specific heat is constant between state points (1-2)

Then mathematically we have now the following:

$$\bullet \quad C_{p1}t_1 + \frac{V_1^2}{2} = C_{p2}t_2 + \frac{V_2^2}{2} = C_{pt} + 1/2(V^2) \quad 5-11$$

Note:

- K Constant
- $V_1^2/2$ & $V_2^2/2 \rightarrow$ These are the Kinetic energy terms

- $C_{pt} \rightarrow$ Is the Internal energy term

Based on the author's experience and education the kinetic energy is aligned to the directed motion of the molecules in the gaseous fluid. Whereas the internal energy C_{pt} is aligned to the Brownian motion or the erratic random movement of the molecules in the gaseous fluid.

(5.2) Basic Turbomachinery assumptions-based derivations aligned to control volumes

This section will deal mainly with the derivation of the Mach# and associated pressure ratios and flow function. This is highly required so as to assess the flow conditions within each control volume established. Now the aforementioned energy equation derived earlier from the steady state flow process, basically is assumed to reflect the interaction of the energy inherent within the fluid molecules.

Based on the references studied we now make the assumption of the following:

$$\text{ENERGY RATIO} = \text{Random Motion/ Directed Motion} \quad 5-12$$

Now we introduce the concept of the Mach number; which is the ratio of the flow velocity passing a boundary to the local speed of sound in air.

$$\text{Hence: } M = \frac{V}{a} = \frac{\text{Flow Velocity}}{\text{Acoustic Velocity}} \quad 5-13$$

$$\text{Where: } a = \text{The acoustic velocity} = \sqrt{\gamma g c R T_s} \quad 5-14$$

And now combined with the definition of specific heat:

$$\bullet \quad C_p = (T) = \frac{\gamma R}{(\gamma - 1)} \rightarrow \text{This is the ideal gas assumption.} \quad 5-15$$

Now if:

$$\bullet \quad C_p = \gamma R / (\gamma - 1) \text{ \& } a = \sqrt{\gamma g c R T_s} \text{ Then ; } a^2 = \gamma g c R T_s \quad 5-16$$

- Hence now substituting the terms of C_p & a into the aforementioned steady state flow equation

- $\{ C_{p1}t_1 + (V_1^2)/2 = C_{p2}t_2 + (V_2^2)/2 = C_{pt} + 1/2(V^2) = K \text{ Constant} \}$ 5-17

yields the following mathematical expression:

- $\{[(\gamma R)/(\gamma - 1)]t_1 + 1/2(V_1^2) = [(\gamma R)/(\gamma - 1)]t_2 + 1/2(V_2^2) = [(\gamma R)/(\gamma - 1)]t + V^2/2 = K\}$ 5-18

Further mathematical manipulation yields the following:

- As: $a^2 = \gamma R T_s$ 5-19

Hence:

- $\frac{a_1^2}{(\gamma-1)} + \frac{V_1^2}{2} = \frac{a_2^2}{(\gamma-1)} + \frac{V_2^2}{2} = \frac{a^2}{(\gamma-1)} + \frac{V^2}{2} = K$ 5-20

This can also be written down as:

$$[\{V_1^2/2 + a_1^2/(\gamma - 1) = V_2^2/2 + a_2^2/(\gamma - 1) = a^2/(\gamma - 1) + V^2/2\} = K]$$

5-21

Where: $K = \text{Constant}$

Now applying the formulation for Mach #; we have the following

As $M\# = V/a$ or $V = M\# (a)$; Hence on substitution into the above equation

yields

Let: $M\# = M$

- $\frac{1}{2}(M_1 a_1)^2 + \frac{a_1^2}{(\gamma-1)} = \frac{1}{2}(M_2 a_2)^2 + \frac{a_2^2}{\gamma-1} = \frac{a^2}{(\gamma-1)} + \frac{1}{2}(Ma)^2 = K$ 5-22

- $a_1^2 \left[\frac{M_1^2}{2} + \frac{1}{(\gamma-1)} \right] = a_2^2 \left[\frac{M_2^2}{2} + \frac{1}{(\gamma-1)} \right] = a^2 \left[\frac{M^2}{2} + \frac{1}{(\gamma-1)} \right] = K$ 5-23

Now note that:

- $\frac{M_1^2}{2} + \frac{1}{(\gamma-1)} = \frac{(\gamma-1)M_1^2+2}{2(\gamma-1)}$ 5-24

Finally, this yields the following:

$$\frac{M_1^2}{2} + \frac{1}{(\gamma-1)} \text{ Proved} \quad \text{5-25}$$

Now by multiplying throughout by $(\gamma - 1)$; we have the following expression:

- $(\gamma - 1) \left\{ (a_1^2 \left(\frac{1}{2}(M_1)^2 + \frac{1}{(\gamma-1)} \right) = a_2^2 \left(\frac{1}{2}(M_2)^2 + \frac{1}{(\gamma-1)} \right) = a^2 \left(\frac{1}{2}(M)^2 + \frac{1}{(\gamma-1)} \right) \right\} = K$ 5-26

Which further breaks down to the following:

- $(\gamma - 1)a_1^2 \left[\frac{1}{2}(M_1)^2 + 1/(\gamma - 1) \right] = (\gamma - 1)a_2^2 \left[\frac{1}{2}(M_2)^2 + 1/(\gamma - 1) \right] = (\gamma - 1)a^2 \left[\frac{1}{2}(M)^2 + 1/(\gamma - 1) \right] = K$ 5-27

Hence after further algebraic evaluation; now we have the Physics based

mathematical expression:

- $a_1^2(\gamma - 1) \frac{1}{2}(M_1)^2 + a_1^2 = a_2^2(\gamma - 1) \frac{1}{2}(M_2)^2 + a_2^2 = a^2(\gamma - 1) \frac{1}{2}(M)^2 + a^2 = K$ 5-28

Or

- $a_1^2 [1 + (\gamma - 1) \frac{1}{2}(M_1)^2] = a_2^2 [1 + (\gamma - 1) \frac{1}{2}(M_2)^2] = a^2 [1 + (\gamma - 1) \frac{1}{2}(M)^2] = K$ 5-29

The equation derived above is based on the acoustic velocity (a); M# & Specific heat ratio (γ). Hence this aforementioned derived equation is also a form of the energy equation and applicable if the assumption is made that C_p is constant i.e., independent of the gas temperature variation or assume it negligible.

To convert the equation depicting or make it a function of absolute temperature “t”;
M# & γ ; the following mathematical arrangement yields.

As aforementioned; $a = \text{The acoustic velocity} = \sqrt{\gamma g_c R T_s} = a^2 = \gamma R T$. Hence
following similar mathematical manipulation yields:

$$\bullet \quad (\gamma R t)_1 [1 + (\gamma - 1) \frac{1}{2} (M_1)^2] = (\gamma R t)_2 [1 + (\gamma - 1) \frac{1}{2} (M_2)^2] = (\gamma R t) [1 + (\gamma - 1) \frac{1}{2} (M^2)] = K \quad 5-30$$

Now dividing the above equation by γR yields the following mathematical expression:

$$\bullet \quad [t_1 ((1 + \frac{1}{2}(\gamma - 1)(M_1)^2)) = t_2 ((1 + \frac{1}{2}(\gamma - 1)(M_2)^2)) = t (1 + \frac{1}{2}(\gamma - 1)(M)^2) = K] \rightarrow \text{This equation is also a form of the energy equation.} \quad 5-31$$

(5.3) Continuing evaluation of the Gas Turbine Thermodynamics aligned to control volumes

The next step in this process assumes that the overall process is an isentropic process hence in a perfect gas that experiences an isentropic change of state then based on the physical laws the author has been educated with is that the associated pressure and corresponding temperature is interdependent by the following relationship.

Therefore: From the thermodynamic state (1) – (2) in which is inherent an isentropic change.

Hence

$$\bullet \quad \frac{t_2}{t_1} = \left(\frac{p_2}{p_1} \right)^{\frac{(\gamma-1)}{\gamma}} \quad 5-32$$

Where:

t_2 & p_2 indicates that the states have reached isentropic conditions due to the behavior of the molecules of the gas.

Now by leveraging that the following physics based mathematical expression earlier stated above,

$$\bullet \quad \frac{t^{2'}}{t^1} = \left(\frac{p^{2'}}{p^1} \right)^{\frac{(\gamma-1)}{\gamma}} [7] \quad 5-33$$

And as previously defined, now apply the physics-based understanding of the stagnation pressure.

As the stagnation or total pressure I that pressure inherent within the fluid where the velocity or rather the dynamic head $V^2/2gc = 0$, hence as explained previously with the process being isentropic for a perfect gas the total pressure and corresponding total temperature are interdependent and therefore: Since the flow process is isentropic for an assumption of a perfect gas hence the stagnation pressure P and the stagnation temperature T are related by the following mathematical expression:

$$\bullet \quad \frac{P}{p} = \left(\frac{T}{t} \right)^{\gamma/(\gamma-1)} \quad 5-34$$

Where P & T Are identified as the total conditions at static point. Now we also know that from the definition of stagnation temperature is when/ where the fluid velocity is zero. Therefor if we assume the fluid (medium) is a perfect gas and is brought to an abrupt halt within an isentropic process, so that its associated velocity is zero hence also ensuring the fluid Mach # is also zero; then in this state condition the stagnation or total temperature can be derived by leveraging the following derivations of the form of the energy equation and this yields the following:

$$\bullet \quad [T = t (1 + (\gamma - 1) \frac{1}{2}(M)^2)] = [T/t = 1 + (\gamma - 1) \frac{1}{2}(M)^2] \quad 5-35$$

Now at this point we have the two most recent physics based mathematical expressions derived:

$$(i) \quad \frac{P}{p} = \left(\frac{T}{t}\right)^{\gamma/(\gamma-1)} \quad 5-36$$

$$(ii) \quad \left[\frac{T}{t} = 1 + \frac{(\gamma-1)}{2}(M^2)\right] \quad 5-37$$

By direct substitution of the following:

- T/t into P/p yields:
- $\frac{P}{p} = \left[1 + \frac{1}{2}(\gamma - 1)(M^2)\right]^{\gamma/(\gamma-1)} \rightarrow$ This expression is identified as the pressure ratio across the resistance. 5-38

Where:

- P = Total or absolute conditions of the state point (pressure)
- p = Static pressure of the fluid stream
- M = Mach number of the fluid stream
- γ = Specific heat ratio

The entire purpose of having derived the compressible flow related pressure ratio equation across the respective control volumes, is to derive a physics based mathematical expression toward ascertaining the flow function and their associated mass flow rates required to emanate through the intended control volume associated with the insulation via effective gas path cooling holes hence making the following section critical toward deriving the overall flow function equation used to compute the mass flow rate through the resistance based on known pressure ratios

The aforementioned derived equations provide the Segway toward the physics based mathematical analysis of defining the essential equations to obtain the expression of the mass flow rate emanating through a resistance which in this case is the effective gas path cooling hole.

(5.4) Deriving the expression of the mass flow rate & flow function equations

aligned to control volumes

Starting with the earlier derived mathematical expression for the pressure ratio, hence from the earlier derived function we have the following:

- $\frac{P}{P_0} = [1 + \frac{1}{2}(\gamma - 1)(M^2)]^{\gamma/(\gamma-1)} \rightarrow$ This expression is identified as the pressure ratio across the resistance.[7] 5-39

Now we proceed to derive the mathematical function for the isentropic mass flow rate:

From the continuity equation:

- $\dot{W} = (\rho VA)t$ 5-40

Where:

- $t=At$ Throat conditions
- $At=$ Throat area
- $(\rho)t =$ Density at t'
- $Vt=$ Velocity at t'

Now from the physics related to the governing equations associated with the isentropic flow of a perfect gas we have the following:

The ideal gas equation of state:

$$P = \rho R t \quad [9] \quad 5-41$$

$$(i) \quad \Rightarrow \left[\rho = \frac{P}{RT} \right] \quad [9] \quad 5-42$$

Where:

- $R =$ gas constant

- P= Absolute pressure
- T= Absolute temperature
- R air = 1716 ft²/ (S² R=deg)
- $P = \rho RT$
- $C_v = du/dt \Rightarrow u = C_v(t)$ { Constant volume specific heat }
- $C_p = dh/dt \Rightarrow h = C_p(t)$ { Constant pressure specific heat }

Hence from the previous derived mathematical expressions, the total temperatures and pressures can be written as the following:

$$T = t \left\{ 1 + \frac{\gamma-1}{2} M^2 \right\} = K \quad 5-43$$

$$P = p \left\{ 1 + \frac{\gamma-1}{2} M^2 \right\}^{\frac{\gamma}{\gamma-1}} = K \quad 5-44$$

$$\rho_o = \rho \left\{ 1 + \frac{\gamma-1}{2} M^2 \right\}^{\frac{1}{\gamma-1}} = K \quad 5-45$$

Where:

t, p & ρ are static thermodynamic properties for the state points.

Therefore:

As:

$$P/p = 1 + \left[\frac{\gamma-1}{2} \right] M^2 \quad 5-46$$

Hence from the above equation solving for the M# yields:

$$(P/p)^{(\gamma-1)/\gamma} = 1 + \left[\frac{\gamma-1}{2} \right] M^2 \quad 5-47$$

& hence:

$$M^2 = \left[\frac{(P/p)^{(\gamma-1)/\gamma} - 1}{\gamma/2} \right] \quad 5-48$$

This yields the mathematical expression for Mach number as:

- $M = \pm \sqrt{\frac{2}{\gamma-1} \left\{ \left(\frac{P}{p} \right)^{(\gamma-1)/\gamma} - 1 \right\}}$ 5-49

- Where: P = Plenum supply conditions & p = Sink conditions.

Our next step is to derive the flow function which is identified as a dimensionless parameter.

Again as per the continuity equation we have:

- $\dot{W} = \rho V A$

& as previously defined:

- $P = \rho R T \rightarrow$ State equation

Hence:

- $\rho = \frac{P}{RT}$

Multiplying both sides by “V”

- $\rho V = \frac{PV}{RT}$

Now as the Flow Flux is as follows:

- $\frac{\dot{W}}{A} = \rho V$

or

- $\frac{\dot{W}}{A} = \rho V = \frac{PV}{RT}$

As we are aware of the following from previous assessment:

- $V = \text{Velocity} = (M\#)(a)$ 5-50

Where: “a” is the acoustic velocity

Therefore:

- $\frac{\dot{W}}{A} = \rho V = \frac{PV}{RT} = \left(\frac{P}{RT} \right) (Ma)$ 5-51

- $a = \sqrt{\gamma g c R T}$ 5-52

- $\left(\frac{P}{RT}\right)\left(\frac{M}{a}\right) = (P/RT)(M)(\sqrt{\gamma g c R T})$ 5-53

- $\left(\frac{P}{RT}\right)\left(\frac{M}{a}\right) = (P/RT)(M)(\sqrt{\gamma g c})(\sqrt{R})(\sqrt{T}) = (P)(M)(\sqrt{\gamma g c})(\sqrt{R}/R)(\sqrt{T}/)$
5-54

- $\left(\frac{P}{RT}\right)\left(\frac{M}{a}\right) = ((P)(M)(\sqrt{\gamma g c})(1/\sqrt{R T}) = (M)(\sqrt{\gamma g c}/RT)(P)$ 5-55

- $\left(\frac{\dot{W}}{A}\right) = \rho V = PV/RT = M \{(\sqrt{\gamma g c}/RT)(P)\}$ 5-56

- $\left(\frac{\dot{W}}{A}\right) = M \{(\sqrt{\gamma g c}/R)(P/\sqrt{T})\}$ 5-57

- $\dot{W} = (Ac)(M)\{(\sqrt{\gamma g c}/R)(P/\sqrt{T})\}$ 5-58

- And Finally : $\left(\frac{\dot{W}}{Ac}\right)((/\sqrt{T})/P) = (M)(\sqrt{\gamma g c}/R)$ 5-59

Where: The flow function is a dimensionless parameter and is defined to be the following:

- $\left(\frac{\dot{W}}{P}\right)(\sqrt{T}/Ac) = \emptyset$ 5-60

Now we can further define \emptyset by the following relationship:

- $\left\{\emptyset = \left(\frac{\dot{W}}{Ac}\right)\left(\frac{\sqrt{T}}{P}\right)\left(\frac{\sqrt{R}}{g c}\right) = (M)(\sqrt{\gamma})\right\} = (M)\left(\sqrt{\frac{\gamma g c}{R}}\right)$ 5-61

Where $M\#$ is defined to be from the previous derivation as follows:

- $M = \pm \sqrt{\frac{2}{(\gamma-1)} [P/p]^{(\gamma-1)/\gamma} - 1}$ 5-62

Now through the process of mathematical substitution & by multiplying the flow function equation throughout by $(/\sqrt{T}/P)$ yields the following:

As the flow flux was defined earlier to be the following:

- $\left(\frac{\dot{W}}{Ac}\right) = (M)\left(\sqrt{\frac{\gamma g c}{R}}\right)(P/\sqrt{T})$

Multiplying as previously stated throughout by the following parameter $\rightarrow (/ \sqrt{T_t}/P_t)$

Hence through mathematical substitutions we have the following:

- $\left(\frac{\dot{W}}{Ac}\right)((/ \sqrt{T_t})/P_t) = (M)\left(\sqrt{\frac{\gamma g c}{R}}\right)(P/\sqrt{T})(\sqrt{T_t})/P_t$ 5-63

- $\left(\frac{\dot{W}}{Ac}\right)((/ \sqrt{T_t})/P_t) = (M)\left(\sqrt{\frac{\gamma g c}{R}}\right)(P/P_t)(\sqrt{T_t})/\sqrt{T}$ 5-64

- $\left(\frac{\dot{W}}{Ac}\right)((/ \sqrt{T_t})/P_t) = (M)\left(\sqrt{\frac{\gamma g c}{R}}\right)[(P/P_t)]/(\sqrt{T})/(\sqrt{T_t})$ 5-65

Where:

- $P/P_t \rightarrow$ Static pressure / Total pressure.
- $T/T_t \rightarrow$ Static temperature / Total temperature

Now as previously defined in this dissertation; the Physics based mathematical relationships for the gas flow property ratios as a function of Mach number and specific heat ratio are the following:

- $\frac{T}{T_t} = \left\{1 + \frac{(\gamma-1)}{2} M^2\right\}^{-1}$ 5-66

- $\frac{P}{P_t} = \left\{1 + \frac{(\gamma-1)}{2} M^2\right\}^{\frac{-(\gamma)}{(\gamma-1)}}$ 5-67

Further substitution yields the following mathematical expressions: 5-68

$$\left(\frac{\dot{W}}{Ac}\right)\left(\frac{\sqrt{T_t}}{P_t}\right) = \frac{(M)\left(\sqrt{\frac{\gamma g c}{R}}\right)\left[\left(1 + \frac{(\gamma-1)}{2} M^2\right)^{\frac{-(\gamma)}{(\gamma-1)}}$$

Apply algebraic manipulations to further simplify:

Let:

- $1 + \frac{(\gamma-1)}{2} M^2 = x; \& -\frac{(\gamma)}{(\gamma-1)} = y \& -1 = n$ 5-69

Applying the laws of indices:

$$\frac{(x)^y}{\sqrt{(x)^n}} = \frac{(x)^y}{\sqrt{\frac{1}{x}}} = \frac{(x)^y}{\frac{1}{\sqrt{x}}} = \frac{(x)^y}{\frac{1}{\sqrt{x}}} = (x)^y \cdot (x)^{1/2} = (x)^{y+1/2}$$

- $(1 + \frac{(\gamma-1)}{2} M^2)^y (1 + \frac{(\gamma-1)}{2} M^2)^{1/2} = (1 + \frac{(\gamma-1)}{2} M^2)^{(\frac{-(\gamma)}{(\gamma-1)} + 1/2)}$ 5-70

Hence:

- $\left(\frac{\dot{W}}{Ac}\right) \left(\frac{\sqrt{Tt}}{Pt}\right) = (M) \left(\frac{\sqrt{\gamma g c}}{R}\right) (1 + \frac{(\gamma-1)}{2} M^2)^{(\frac{-(\gamma)}{(\gamma-1)} + 1/2)}$ 5-71

Note: $\left\{ \frac{-\gamma}{\gamma-1} + \frac{1}{2} \right\} = \frac{-2\gamma + \gamma - 1}{[(\gamma-1)2]} = \frac{-\gamma-1}{2(\gamma-1)} = \left[-\frac{(\gamma+1)}{2(\gamma-1)} \right]$ 5-72

- $\left(\frac{\dot{W}}{Ac}\right) \left(\frac{\sqrt{Tt}}{Pt}\right) = (M) \left(\frac{\sqrt{\gamma g c}}{R}\right) / [1 + 1/2(\gamma - 1)M^2]^{\left[-\frac{(\gamma+1)}{2(\gamma-1)} \right]}$ 5-73

Applying the laws of indices:

- $X^{-n} = \frac{1}{X^n}$

- Finally: $\left(\frac{\dot{W}}{Ac}\right) \left(\frac{\sqrt{Tt}}{Pt}\right) = \frac{(M) \left(\frac{\sqrt{\gamma g c}}{R}\right)}{[1 + 1/2(\gamma - 1)M^2]^{\left[\frac{(\gamma+1)}{2(\gamma-1)} \right]}}$ 5-74

Therefore, from the derived equation the flow function is as follows:

- $\phi_2 = \left(\frac{\dot{W}}{Ac}\right) \left(\frac{\sqrt{Tt}}{Pt}\right)$ 5-75

Where: Ac = Actual mechanical area of the resistance without losses, and reflects the mechanical area based on the geometrical parameters of the resistance.

Hence:

$$\bullet \quad \phi_2 = \left(\frac{\dot{W}}{A_c} \right) \left(\frac{\sqrt{T_t}}{P_t} \right) = \frac{(M) \left(\sqrt{\frac{\gamma g c}{R}} \right)}{[1 + 1/2(\gamma - 1)M^2]^{\left[\frac{(\gamma + 1)}{2(\gamma - 1)} \right]}} \quad 5-76$$

All the aforementioned derivations will now allow us to establish the process in ascertaining the required flow rate needed through the respective control volume cooling configurations, which may be either through all the respective defined control volumes or within the application of effective gas path cooling holes, porous cooling etc. mechanisms involving the emanation of low temperature fluid through the high temperature walls and into the gas path.

To further evaluate the overall control volume reflecting the gas path conditions, here we need to ascertain the associated state points gas path temperatures and pressures that will be required as boundary conditions to evaluate the sink conditions for the control volume CV(effective gas path cooling), hence at this point to evaluate the pressures and temperatures at each given state point as shown in the following figure, and it is critical that we now derive the one dimensional mean line aerodynamic physics based mathematical equations as this will lead to further defining the external temperature and pressure boundary conditions in the gas path, which is required as sink conditions for the cooling medium to emanate into, and which will consequently alter the gas path external boundary conditions hence determining a multi physics based integrated solution for the overall stage efficiency.

(5.5) 1-D: Derivation of mean-line Aerodynamics formulations

aligned to control volumes

Considering the intent of this dissertation is addressing the overall synergy or the multi-physics modeling aspects of the high-pressure turbine stage 1 analysis, including

generating the aerodynamics-based pressure and temperature conditions for the gas path. Hence, the following schematic depicts the pertinent velocity triangle including key parameters for a typical HPT Stage1 turbine. The author leverages his graduate academic background from various texts [4] to generate the overall mathematical coupling of the essential physics-based disciplines. [4][16]

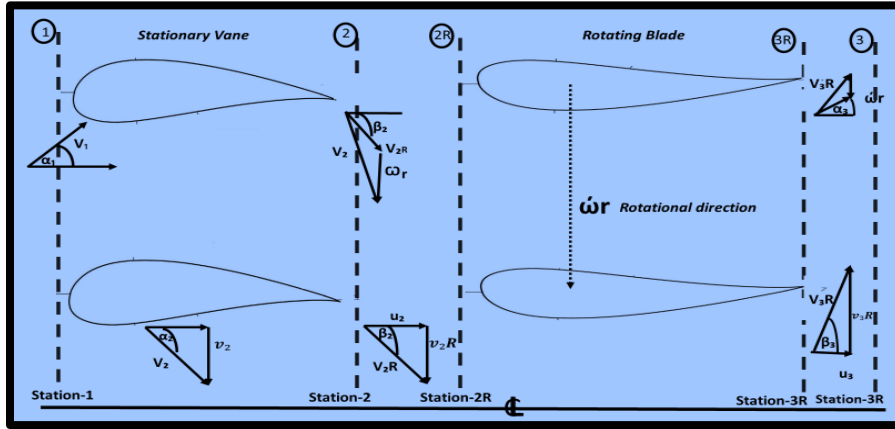


Figure 5.1 1D-Mean-Line Aerodynamics state points [4]

In reference to Figure 5.1. Control volume stage 1 nomenclature is as follows.

Station-1: Inlet of the stage1 nozzle and exit of the transition piece.

Assumptions considered: Here we don't consider the additions and subtractions of any leakage or cooling flows from both the transition to nozzle intersection plane, mouth seal region and from the leading edge of the horseshoe vortex region of the nozzle end wall bot outer and inner regions. As the overall stationary vane is characterized with one global control volume, therefore the author assumes CV_1 is a bulk average of the entire effective gas path cooling emanating into the gas path and this bulk effective gas path cooling ejection occurs at location state point (2). Note the author assumes that this is the firing temperature plane and it the temperature at station (2) that is applied towards the calculation of the blade relative temperature at station (2R).

Definition of each term [4]

- α_2 - Angle of the flow exiting from the trailing edge of the nozzle at the location station 2.
- V_2 – Absolute velocity of the flow exiting the nozzle at the stationary frame of reference.
- v_{2r} – Relative velocity of the flow entering the blade at the rotating frame of reference at the blade incidence angle
- U_2 = Axial component of the velocity of the nozzle exit
- v_2 = Tangential component of the velocity at the Nozzle exit
- β_2 = Blade incidence flow angle at inlet conditions to the blade
- α_1 = Nozzle incidence flow angle at inlet conditions to the nozzle
- T = Total/Absolute temperature
- T_{t1} = Absolute temperature at station 1
- T_1 = Static temperature at station 1 = T_{s1}
- P = Fluid pressure
- P_{t1} = Absolute/Total pressure at station- 1
- M = MACH Number

Formulations for stage Analysis:

- This section is extremely essential as is/are the following assumptions:
- The following assumptions are relative to the inlet plane of the stage 1 nozzle.
- Formulations are conducted at the mean line radius relative to the engine centerline CL.

- All formulations are in reference to the velocity vector diagrams depicted in Figure 5.1

The control volume applied toward the implementation of the formulations is specifically for the turbine hot gas path stage1, incorporating the stage 1 nozzle and the stage 1 blade with the assumptions that there is no leakage or component cooling flows diluting the hot gas path. This is only the initial assumption and subsequently in this dissertation we will introduce the component cooling flow rates in the derived multi-physics based on the physics and mathematical approach.

The other assumption is that the flow approaches the stage1 nozzle with a certain level of kinetic energy, and an inlet approach angle α_1 , and accompanied with no tangential component of the flow at the entrance to the stage 1 nozzle therefore at this plane in the gas path there are no components or parts that is imparting and angular momentum “swirl” into the fluid. The total enthalpy change across the stator is assumed to be zero as the stator does not produce any shaft work.

Note the stage 1 nozzle will by definition impart a certain amount of swirl into the gas path flow and the function of the rotating blade downstream of the rotating blade is to extract this swirl put in by the stage 1 nozzle. For a mean radius stage calculation and upstream conditions of the stage 1 nozzle known we now define the formulations required for the stage analysis.

If T_{t1} and P_{t1} are provided where T_{t1} is the turbine inlet absolute temperature defined to be at the upstream plane of the stage1 nozzle and located after the leakage plane i.e., after the transition piece -sealing location stage 1 nozzle interface (in land-based gas turbines)

The typical known parameters to be assumed are the following:

- (i) Turbine RPM (W), T_{t1} and P_{t1} (depending on combustor $[(\Delta P)/P]$)
- (ii) Radius from the engine centerline for which the evaluation is being conducted.
- (iii) Alpha (α)_{1,2}: Flow angle inlet & exiting stage 1 nozzle.

Mathematical Formulations are as follows and leveraged from the author's graduate studies reading reference: [4]

- At the stagnation point of the stage 1 nozzle the static temperature equates to the total temperature; hence $T_{s1} = T_{t1}$ based on [Stagnation velocity = 0]
- For now, for the purpose of identifying the key parameters the author chooses to neglect the effects of cooling on the gas path; hence $[T_{t2} = T_{t1}]$ as there is no work extraction by the stage 1 nozzle. Later in the dissertation the overall cooling aspects are identified and generated to establish the unified high pressure turbine formulation.

Therefore, the following formulations are as depicted below: [4]

- $T_{t1} = T_{s1}$ [i. e. Total temperature at station (1)] 5-77
- $T_{s2} = \frac{T_{t2}}{[1+1/2(\gamma-1)M_2^2]}$ i. e. Static temperature at Station (2) 5-78
- $V_2 = M_2(a)$ 5-79

Where:

- V_2 = Station (2) Velocity i.e., Absolute frame of reference at Nozzle exit
- M_2 = Station (2) Mach# i.e., At Nozzle exit
- a = Sonic Velocity & Where Sonic velocity is the following $\sqrt{\gamma g_c R T_{s2}}$

Where:

- γ = Gas property
- G_c = Gravitational acceleration
- R = Gas Constant

T_{S2} = Station (2) Static Temperature

Therefore:

- $V_2 = M_2 \left(\sqrt{\gamma g_c R \left[\frac{T_{t2}}{1 + 1/2(\gamma - 1)M_2^2} \right]} \right)$ i.e., the resultant velocity component. 5-

80

At station (2) the axial component of the velocity at the nozzle exit is:

- $U_2 = V_2 \cos \alpha_2 = \left(M_2 \sqrt{\gamma g_c R \left[\frac{T_{t2}}{1 + 1/2(\gamma - 1)M_2^2} \right]} \right) (\cos \alpha_2)$ 5-81

- $U_2 = \left(M_2 \sqrt{\gamma g_c R \left[\frac{T_{t2}}{1 + 1/2(\gamma - 1)M_2^2} \right]} \right) (\cos \alpha_2)$ - i.e., Axial resultant component. 5-82

At Station (2) the tangential component of the velocity at nozzle exit is:

- $v_2 = (V_2) \sin(\alpha_2) = \left(M_2 \sqrt{\gamma g_c R \left[\frac{T_{t2}}{1 + 1/2(\gamma - 1)M_2^2} \right]} \right) (\sin(\alpha_2))$ 5-83

- $v_2 = (M_2 \sqrt{\gamma g_c R T_{S2}}) (\sin(\alpha_2))$ i.e., This is the Tangential Resultant component of the velocity. 5-84

Note from the physics related to the high-pressure turbine the Mach# at station (2)

can also be derived by a given pressure ratio across the nozzle throat area.

$$\text{Where: Mach \#} = M_2 = \sqrt{\frac{2}{(\gamma - 1)} \left[\left(\frac{P_{t1}}{P_2} \right)^{\frac{\gamma - 1}{\gamma}} - 1 \right]} \Rightarrow \text{This is based on the Pressure Ratio}$$

dependency factor.

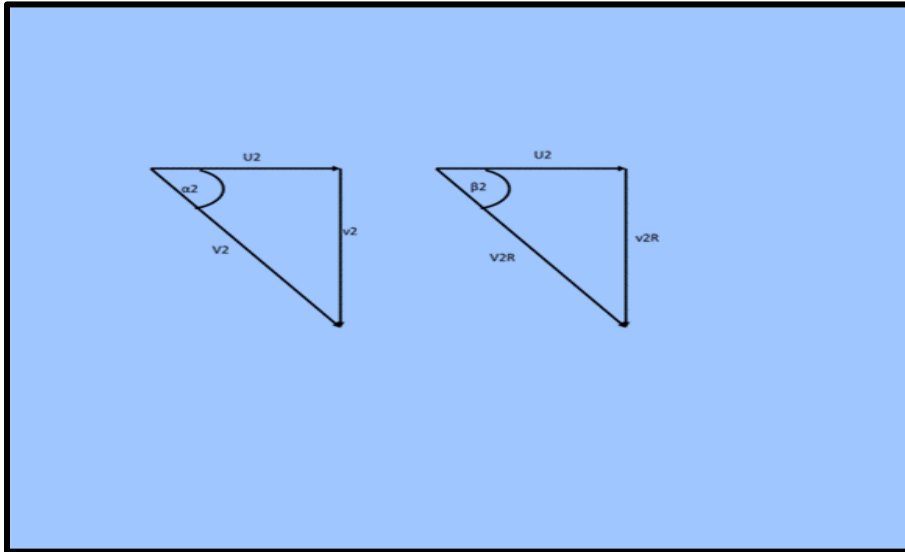


Figure 5.2 Description of the Velocity Triangle [4]

Therefore if (P_{t1}/P_2) which is the pressure ratio across the nozzle throat area is given and the gas properties are also known then the nozzle exit Mach#, at the throat can be calculated.

Note: The flow angle at the nozzle exit is not assumed to be equivalent to the bucket/blade incidence flow angle. Therefore, just as in a similar fashion there is existing a velocity triangle based on the nozzle trailing edge exit flow angle “ α_2 ” Similarly there is a velocity triangle constructed and existing based on the blade stagnation zone inlet conditions flow angle “ β_2 ”.

As of now we have derived the formulations addressing the nozzle flow exit conditions.

Now we shall derive the blade inlet flow conditions – formulations.

Later we shall see the influence of the rotating component’s inlet flow conditions-based formulations showing the influence of the flow condition parameters on the hot gas

path component heat loads. And hence we shall compute the component durability requirements accordingly.

Hence, the relative tangential velocity of the flow entering the blade rows / stage is shown to be the following:

$$\bullet \quad v_{2R} = v_2 - \omega R \quad 5-85$$

Note: as v_2 has earlier been defined as the following:

$$\bullet \quad \left\{ v_2 = \left[\left(M_2 \sqrt{\gamma g c R \left[\frac{T_{t2}}{1 + 1/2(\gamma - 1) M_2^2} \right]} \right) (\sin(\alpha_2)) \right] \right\} \quad 5-86$$

Hence:

$$\bullet \quad v_{2R} = \left[\left(M_2 \sqrt{\gamma g c R \left[\frac{T_{t2}}{1 + 1/2(\gamma - 1) M_2^2} \right]} \right) (\sin(\alpha_2)) \right] - \omega R \quad 5-87$$

Note: v_{2R} is the relative tangential velocity and is not the resultant velocity component that actually strikes the leading edge of the blade stagnation zone.

Now we need to derive the resultant velocity component that actually strikes the leading edge of the blade at the mid-span region of the blade and at the reference frame.

$$\bullet \quad V_{2R} = \sqrt{U_2^2 + v_{2R}^2} \quad 5-88$$

Where:

$$\bullet \quad U_2^2 = [V_2 \cos(\alpha_2)]^2 \quad 5-89$$

$$\bullet \quad v_{2R}^2 = (v_2 - \omega R)^2 = [(V_2 \sin(\alpha_2))^2 - \omega R]^2 \quad 5-90$$

The correspondence incidence angle aligned to the axial axis and associated with the resultant velocity component “ V_{2R} ” is termed as β which basically defines the blade entrance conditions.

At station (2):

$$\bullet \left[\beta_2 = \tan^{-1} \left(\frac{\left[\left(M_2 \sqrt{\gamma g c R \left[\frac{T_{t2}}{1+1/2(\gamma-1)M_2^2} \right]} \right) * (\sin(\alpha_2)) \right] - \omega R}{(M_2 \sqrt{\gamma g c R \left[\frac{T_{t2}}{1+1/2(\gamma-1)M_2^2} \right]}) (\cos \alpha_2)} \right) \right] \quad 5-91$$

Now we need to define / derive the Mach # at the entrance of the rotating blade at station (2R) at the rotating frame of reference.

$$\bullet M_{2R} = M_2 \left(\frac{V_{2R}}{V_2} \right) \quad 5-92$$

Where:

$$\bullet V_{2R} = \sqrt{(U_2^2 + v_2^2 R)} \quad 5-93$$

$$\bullet V_2 = M_2 (\sqrt{\gamma g c R T_{s2}}) \quad 5-94$$

Thus:

$$\bullet M_{2R} = M_2 \left(\frac{V_{2R}}{V_2} \right) \text{ This is the relative Mach\# at the entrance of the blade at the rotating frame of reference, which can also be written down as the following:}$$

$$\bullet M_{2R} = M_2 \left[\frac{\sqrt{(U_2^2 + v_2^2 R)}}{M_2 (\sqrt{\gamma g c R T_{s2}})} \right] \quad 5-95$$

$$\bullet M_{2R} = \frac{[\sqrt{(U_2^2 + v_2^2 R)}]}{(\sqrt{\gamma g c R T_{s2}})} \Rightarrow \text{This is the relative Mach\# at the entrance plane of reference of the rotating component.} \quad 5-96$$

Now we need to compute / derive the total temperature at the entrance of the rotating blade plane at station (2R).

$$T_{t2R} = \text{Static Temperature at station 2} + \frac{V_{2R}^2}{2g c p} \quad 5-97$$

This results in the following mathematical expression:

$$\bullet T_{t2R} = T_{s2} + \frac{V_{2R}^2}{2g c p} \quad 5-98$$

At this point we evaluate the flow conditions at station (3) which is defined at the rotating blade trailing edge exit plane location.

As at the exit plane the flow conditions are governed by the rotating frame of reference. Hence, at plane -3R; the author assumes that there is no stationary tangential velocity component.

- $[v_3 = 0]$ 5-99

However, at this exit plane there will be a rotational relative tangential velocity component “ v_3R ”

- $v_3 R = v_3 + \omega r$ 5-100

- $v_3 =$ exit swirl at the exit plane of the rotating component 5-101

Therefore:

- $v_3 R = \omega r + v_3$ 5-102

The absolute velocity of the flow entering the blade is V_3

- $V_3 = U_3 = U_2 \Rightarrow$ Author assumes the Axial component of the velocity at exit of the stator is the same as the velocity component at the exit of the blade.
- $U_3 =$ This is the axial component of the velocity at station (3)
- $U_2 =$ This is the axial component of the velocity at station (2)

Hence:

- $V_3 R = \sqrt{(U_3^2 - v_3^2 R)} \Rightarrow$ This is the relative velocity at the blade exit at station (3) 5-103

Now the angle the relative velocity component at the exit plane of the blade makes with the axial turbine axis is $= \beta_3$.

Where:

$$\beta_3 = \tan^{-1} \left[\frac{(\omega r + v_3)}{U_3} \right] \quad 5-104$$

As it has been assumed in this dissertation that $u_2 = u_3$ 5-105

Therefore:

- $[\beta_3 = \tan^{-1}((\omega r)/U_2)]$ 5-106

Now the total temperature at the exit of the blade at station (3) is derived;

Where: Total= Absolute

- $\left[T_{t3} = T_{t2} - \frac{\omega r}{gC_p} * \left(\left[\left(M_2 \sqrt{\gamma g C R \left[\frac{T_{t2}}{1 + 1/2(\gamma - 1)M_2^2} \right]} \right) (\sin(\alpha_2)) \right] \right) \right]$; which then becomes the following mathematical expression. 5-107

- $[T_{s3} = T_{t2} - \frac{\omega r}{gC_p} * \left(\left[\left(M_2 \sqrt{\gamma g C R \left[\frac{T_{t2}}{1 + 1/2(\gamma - 1)M_2^2} \right]} \right) (\sin(\alpha_2)) \right] \right) - (V^2_3)/2gC_p]$

This is the static temperature at station (3) 5-108

Now we derive the Mach # of the gas path at the exit of the blade at station (3).

Note the Mach# can be written down as the pressure ratio or the temperature ratio dependent.

Derivation is as follows from a Temperature Ratio perspective.

Total conditions: From the concept influenced by the steady flow energy balance; the following derivation is as follows.

Conservation of energy: In a system governed by a steady flow process (Not of a nuclear origin) The amount of energy entering the system or part of the system must be equal to the equivalent amount of energy leaving that system or part of that system.

Note the Integral form of the Energy equation is as follows [59]

$$Q - W = \iiint \frac{\partial}{\partial t}(\rho e) d(\text{vol}) + \oint \rho e \vec{V} \cdot \hat{n} dA$$

The net heat added into the control volume deducting the work accomplished by the control volume is directly proportional to the rate of change of energy based on time, within the control volume and added is the net energy that flows out of the control volume.

Hence considering the following types of energies:

- Internal Energy “U” which is in unit’s J/kg; Btu/ lb.
- Flow energy “ pv “
- Kinetic energy “ $\frac{v^2}{2g}$ “
- Potential energy “Z “which is in unit’s J/kg; (ft)(lbf)/lbm
- Heat energy “q” which is in unit’s J/kg; Btu/lb.
- Mechanical work “W” which is in unit’s J/kg; Btu/lb.

For the purpose of this dissertation, I will neglect the following for now:

- Chemical energy
- Electrical energy
- Etc.

Hence the formulation is as follows:

$$\bullet \quad U_1 + \frac{P_1 v_1}{J} + \frac{V_1^2}{2gJ} + \frac{Z_1}{J} + q = U_2 + \frac{P_2 v_2}{J} + \frac{V_2^2}{2gJ} + \frac{Z_2}{J} + W \quad 5-109$$

The equation above reflects the steady flow equation. Considering this dissertation is related to a gas turbine overall system. Hence the potential energy in the steady flow equation may be omitted.

In addition: By applying the definition of enthalpy “H”

- $[H = U + Pv]$ 5-110

Where:

- U = Internal energy of the system under consideration
- P = Pressure of the system under consideration
- V = Volume of the system under consideration

On a unit basis:

- $h = u + pv$; or $h = u + pv / J$ 5-111

Hence combining the aforementioned equations; the steady flow equation now yields:

- $h_1 + \frac{V_1^2}{2gJ} + q = h_2 + \frac{V_2^2}{2gJ} + W$ 5-112

This now reflects the basic form of the steady flow equation.

Now as the sum of the kinetic energy and the enthalpy terms are defined within the flow problems, we will now apply the following mathematical description:

- $h' = h + V^2/2gJ$ 5-113

And now we will term this parameter (h') as the total enthalpy in units J/Kg or Btu/lb.

Now we can introduce the concept of the total enthalpy (h') and align the total enthalpy h' to the thermodynamic property total temperature.

Here the total temperature is now defined as the temperature corresponding to the total enthalpy. As we know that when a gas behaves and hence adheres to the principles of the ideal gas —law;

Thus:

- $v = RT/p$

Or

- $Pv = RT$
- $(\partial u / \partial T)_p = R/p$

This in turn yields the following expression:

- $\Delta h = \int_{T_1}^{T_2} C_p \Delta T$

Now if the assumption is made to hold specific heat (C_p) as constant between the temperatures of T_1 & T_2 respectively. Then we have the following:

- $[\Delta h = c_p \Delta t = c_p (T_2 - T_1)]$

5-114

And if there is a significant variation in the magnitude of C_p then

- $\Delta h = \overline{C_p} (T_2 - T_1)$ 5-115

Where the C_p is the average value of the specific heat capacitance between T_1 & T_2 .

Now by combining the following equations:

- $h' \equiv h + V^2/2g_j$ & $h' - h = C_p (T' - T)$ 5-116

Yields

- $V^2/2g_j = (C_p (T' - T))$ 5-117

Or

- $T' - T = V^2/2gc_j C_p$ 5-118

Or

- $T' = T + V^2/2gc_j C_p$ 5-119

- Where: T' = Total temperature attained by the fluid when the fluid/gas at a constant static temperature T_s & Velocity V is brought to rest adiabatically (i.e.: No heat transfer occurring)

Now considering the following relationships:

$$\rightarrow T' = T + V^2/2gc]Cp$$

$$\rightarrow a = \sqrt{\gamma gcRTs}$$

$$\rightarrow M = V/a$$

$$\rightarrow Jc/R = \gamma/\gamma - 1$$

Yields the following:

$$\bullet \quad T'/T = 1 + \frac{1}{2} (\gamma - 1) M^2 \quad 5-120$$

-or-

$$\bullet \quad M^2[\frac{1}{2} (\gamma - 1)] + 1 = T'/T \quad 5-121$$

Where:

- T' = Total Temperature
- T = Static temperature

Therefore:

$$\rightarrow M^2[\frac{1}{2} (\gamma - 1)] = (T'/T - 1)$$

-or-

$$\rightarrow M^2 = (2 / \gamma - 1) (T'/T - 1)$$

Therefore, at station 3 the Mach number can be written as the following:

$$\bullet \quad M_3 = \sqrt{\frac{2}{(\gamma-1)} \left(\frac{Tt_3}{Tt_2 - \frac{\omega r}{gCp} * \left(\left[\left(M_2 \sqrt{\gamma g c R \left[\frac{Tt_2}{1 + 1/2 (\gamma-1) M_2^2} \right]} \right) (\sin(\alpha_2)) \right] \right) - (V_3^2)/2gCp} - 1 \right)}$$

5-122

Where:

- Tt_3 = Is the total temperature at station 3
- Ts_3 = Is the static temperature at station 3

- Therefore, $M_3 R = M_3 \frac{V_3 R}{V_3}$ 5-123

- $T_{t3} R = T_{t2} R$ 5-124

Now we generate the distributions related to fluid/gas pressure conditions.

As it is assumed that there is no change in total pressure across the nozzle the stationary component, however the static pressure changes.

- $P_{t2} = P_{t1}$ 5-125

Note: In real turbine applications $P_{t2} \neq P_{t1}$. As there will be a total pressure loss coefficient for stator as we consider mixing losses etc., however for this dissertation the author assumes that P_{t2} is approximately similar to P_{t1} .

The governing equations for the nozzle operating characteristics for isentropic flow conditions are the following:

From the entropy perspective:

$$\rightarrow P = [P_t \left(\frac{T}{T_t}\right)^{\gamma/(\gamma-1)}]$$
 5-126

-OR-

$$\rightarrow P_{2s} = P_2 \left(\frac{T_{2s}}{T_{2t}}\right)^{\gamma/(\gamma-1)}. \text{ Where } s=\text{Static} \ \& \ t=\text{Total conditions.}$$
 5-127

In the relative frame of reference:

- $P_{t2R} = P_{2s} \left(\frac{T_{t2R}}{T_{2s}}\right)^{\gamma/(\gamma-1)}$ 5-128

- $P_{t3R} = P_{2tR}$ 5-129

- $P_{t3} = P_{2t} \left(\frac{T_{t3}}{T_{t2}}\right)^{\gamma/(\gamma-1)}$ 5-130

- $P_{s3} = P_3 \left(\frac{T_{s3}}{T_{t3}}\right)^{\gamma/(\gamma-1)}$ 5-131

The aforementioned equations derived hence reflect the pertinent flow path properties for the stage 1 turbine i.e. A single stage turbine evaluation. Where state 1 is the inlet of the stage 1 nozzle and state 3 is at the exit of the blade.

The gas path properties for the upstream and downstream for both nozzle and bucket components that are related to the thermodynamic state conditions; pressures and temperatures and velocities are calculated.

Now we derive the mathematical depiction of the energy per unit mass flow exchanged between the fluid and rotor component.

To do so we derive the Euler turbomachinery mathematical based equations. This is being derived toward understanding the single stage power output.

In the science of turbomachinery determining the fundamental parameters such as the stage loading, stage reaction, and its associated impact to turbine efficiency is extremely essential.

At the last stage blade, in this single stage high pressure turbine, the absolute angle exiting the stage " α_3 " is termed the swirl angle. The swirl angle is positive if it is determined to be opposite to wheel speed direction which is also termed as backward running condition.

The importance of the swirl angle " α_3 " is pivotal to turbomachinery for two reasons:

- (a) In an axial flow gas turbine, it is difficult to perfectly evaluate or rather execute the conversion of the kinetic energy to pressure or potential energy. However, the flow KE, exiting the stage can be minimized by designing the components so that the absolute velocity of the flow to be equivalent to the axial component of the flow velocity.

In physics-based terms:[4]

- $V_3 = u_3$. Which by definition ensures that the exit swirl value = zero or [SWIRL = 0]
- (b) In addition; if the swirl angle magnitude is high (typically for a backward running condition/case) then the higher the magnitude of v_3 will be then this signifies the rationale behind the resulting higher output from the stage under consideration.
- (c) The aforementioned phenomena can be mathematically expressed by the application of the famous Euler turbine equation. This topic is beyond the scope of the dissertation, hence just the basics of turbomachinery is captured below
- (d) In a stator row the gas path fluid flow is made to accelerate while the static pressure decreases and at the exit of the stator row the tangential velocity of the fluid increases in the direction of rotation, i.e., the tangential direction.
- (e) On the other hand, the rotor component while extracting energy from the flow path decreases the magnitude of this tangential velocity in the direction of rotation; and hence while this fluid interaction is occurring there are tangential forces being extracted by the fluid onto to the rotor blades which results into a torque produced by the output shaft component.

Now that we have identified the mean line aerodynamic approach to generate the gas path external state point pressures and temperatures, we proceed toward further identifying the necessary parameters at Station (2) i.e., exit region of the stage (1) nozzle and where the following physics based mathematical expression holds:

- $P_{2s} = P_{2t} \left(\frac{T_{2s}}{T_{2t}} \right)^{\frac{\gamma}{\gamma-1}}$ 5-132

- Now we know the entrance or stagnation pressure for the stage (1)Nozzle = P_{t1} . As across the stationary component the total pressure is maintained as per previous assumptions, hence $P_{2t} = P_{1t}$
- Now we assume that the control volume of the fluid flow emanating out into the gas path is located somewhere between $P_{1t} = P_{2s}$ 5-133
closer to the location of the trailing edge of the nozzle
- At this point from the previous aerodynamic mean line analysis, we have evaluated the static pressure at the trailing edge plane or aka region 2.
- However, we don't know the actual static pressure distribution from region 1-2 of the stage 1 nozzle as one dimensional aerodynamics assessment is assumed and not a two or three dimensional evaluation, The reason behind the aforementioned rationale is that the scope of this dissertation is based solely on a one-dimensional aerodynamic mean line flow path analysis; hence we don't have the actual geometrical configuration of the airfoil profile evaluated; thus we don't have the velocity distribution as a function of the distance or length of the airfoil, or rather the Mach number distribution from region 1-2 as a function of the traversing length or the normalized parameter x/l .
- As determining the actual airfoil curvature and associated geometry is beyond the scope of this dissertation hence it will be assumed that the orifice or effective gas path cooling hole/row control volume discharges its corresponding mass flow rate into the Gas path at the exit trailing edge region between the trail edge of the stage 1 nozzle and the leading edge of the stage 1 blade. This region will be slightly

upstream of the Firing plane; hence recovery effects will be introduced. This region will be defined as P_{1a} .

- Therefore: P_{t1} = Entrance region of the stage 1 nozzle & P_{s2} is the static pressure at the exit plane i.e., at the region-2 of the stage1 nozzle firing plane.
- Hence for calculations purposes based on average conditions:

$$P_{1a} = \sim \left\{ \frac{P_{t1} + P_{s2}}{2} \right\} \quad 5-134$$

- Thus: The pressure ratio applied toward determining the associated mass flow rate of CV- effective gas path cooling row/hole is the following:
 - (i) The supply pressure into the effective gas path cooling row/hole = P_{excv3}
 - (ii) The gas path pressure $\rightarrow P_{1a}$; Hence this gives the following:
 - [Pressure ratio = P_{excv3} / P_{1a}]
 - (iii) Across the hole emanating the cooling medium “effective gas path cooling hole” the corresponding pressure ratio is the following:
 - [Pressure ratio = P_{excv3} / P_{1a}]. This assumes there is no pressure losses incurred within CV_2 while then fluid discharges from CV_3 to CV_2 .

Hence the corresponding Mach number expression across the throat area of the resistance; is the following:

$$M_{fh} = \pm \sqrt{\frac{2}{(\gamma-1)} \left(\frac{P_{excv3}}{P_{1a}} \right)^{(\gamma-1/\gamma)} - 1} \quad 5-135$$

Hence at this point we have derived the expression of the Mach# (M-fh) across the effective gas path cooling hole, based on the average pressure conditions at the gas path location. Therefore: Further substitution of the M-fh# into the flow function parameter yields:

$$\dot{W}_{fh} = \left\{ \frac{(M\#_{fh}) \sqrt{\frac{\gamma g_c}{R}}}{[1 + \frac{1}{2}(\gamma - 1)(M\#_{fh})^2]^{\frac{(\gamma + 1)}{2(\gamma - 1)}}} \right\} \left(\frac{(A_c P_t)}{\sqrt{T_t}} \right) \quad 5-136$$

Where: leveraging from the earlier derived control volume based nomenclature/terminology we now have the following:

- $\dot{W}_{fh} \rightarrow$ Flow rate across the effective gas path cooling hole
- $M\#_{fh} \rightarrow$ Mach number of the flow stream emanating out of the effective gas path cooling hole
- $\gamma \rightarrow$ Gamma is the specific heat ratio
- $A_c \rightarrow$ Actual mechanical area of effective gas path cooling hole (Ideal condition)
- $P_{tcv3} \rightarrow$ Supply “total” pressure (P_{excv3}) at the entrance of the effective gas path cooling hole
- $T_{tcv3} \rightarrow$ Supply temperature (T_{excv3}) at the entrance of the effective gas path cooling hole

Note: It is assumed in this dissertation that at the entrance of the effective gas path cooling hole there is going to be a boundary layer separation hence a vena-contracta is formed which will reduce the diameter of the effective gas path cooling hole and this resulting area is what the flow actually emanates from i.e., a reduced cross-sectional flow area which is perpendicular to the flow stream vector.

Hence in order to capture the vena contracta phenomenon the actual mechanical area is multiplied by a loss or discharge coefficient “Cd”

$$\text{Hence: } [A_c = (C_d) \cdot (A_c)]$$

Where: $C_d \rightarrow$ This value is obtained from experimental data.

Therefore, the Mass flowrate expression in Eq 5-136 can now be rewritten down as the following as shown below.

$$\dot{W}_{fh} = \left\{ \frac{(M\#_{fh}) \sqrt{\frac{\gamma g_c}{R}}}{[1 + 1/2(\gamma - 1)(M\#_{fh})^2]^{1/2}} \right\} \left(\frac{(C_d(A_c).P_{ex_3})}{\sqrt{T_{mexcv_3}}} \right) \quad 5-137$$

The above equation couples the external gas path pressure ascertained from the velocity vector diagrams, the effective gas path cooling hole flow conditions and the associated effective gas path cooling hole geometry as well as the effective gas path cooling hole entrance or supply conditions based on the effective gas path cooling hole upstream control volume analysis.

Prior to evaluating CV_1 , we need to evaluate the conditions at the exit section of the effective gas path cooling hole.

The corresponding flow through the effective gas path cooling hole will absorb heat into the fluid medium from its surrounding walls, as the environment around the walls surrounding the fluid is not under adiabatic conditions. Thus, the flow exit temperature emanating out of the effective gas path cooling hole is indeed an extremely critical parameter as the flow emanating out the cooling hole on reaching the gas path dilutes the hot gas path temperature and hence negatively impacting the performance in terms of the turbine efficiency due to mixing and hence depreciates the temperature of the hot gas path, and hence subsequently influences the decrease of the firing temperature.

In order to evaluate the effective gas path cooling [5] associated mass flow rate's exit temperature exiting out of the effective gas path cooling hole; the following methodology based on the physics of enthalpy mixing is applied.

Physics based mathematical analysis is as follows:

Referring to the control volume of the effective gas path cooling hole:

The listed items below depict the critical parameters applied in the proposed methodology and is as defined as follows:

(i) Component under consideration- Bulk cooling effectiveness:

$$\eta_{\text{bulk}} = \frac{\left(\left[\frac{T_t}{1 + \frac{(\gamma-1)M^2}{2}} \right] + \left[1 + \frac{(\gamma\gamma RM^2)}{2C_p} \right] \right) - T_{\text{bmetal}}}{\left(\left[\frac{T_t}{1 + \frac{(\gamma-1)M^2}{2}} \right] + \left[1 + \frac{(\gamma\gamma RM^2)}{2C_p} \right] \right) - T_{\text{coolant,in}}} \quad 5-138$$

(ii) Coolant medium corresponding effectiveness:

$$\eta_{\text{film}} = \frac{\left(\left[\frac{T_t}{1 + \frac{(\gamma-1)M^2}{2}} \right] + \left[1 + \frac{(\gamma\gamma RM^2)}{2C_p} \right] \right) - \text{EGPT}}{\left(\left[\frac{T_t}{1 + \frac{(\gamma-1)M^2}{2}} \right] + \left[1 + \frac{(\gamma\gamma RM^2)}{2C_p} \right] \right) - \text{EGPT,out}} \quad 5-139$$

(iii) Component heat load parameter:

$$\alpha = \frac{\dot{M}_{\text{in}} C_p}{\left[\left(\frac{K_g}{X} \right) (0.0296) (\text{Pr}^{1/3}) \left[\sqrt{\frac{\gamma g C}{RT_g}} \right] (P1_a) \left\{ \frac{M}{[1 + \frac{(\gamma-1)M^2}{2}]^{\gamma+1/2(\gamma-1)}} \right\} (X/\mu) \right] A_{\text{avg}}} \quad 5-140$$

(iv) Total conductance (Based on Fourier law):

$$UA = \left\{ \frac{1}{\left(\left[\left(\frac{K_g}{X} \right) (0.0296) (\text{Pr}^{1/3}) \left[\sqrt{\frac{\gamma g C}{RT_g}} \right] (P1_a) \left\{ \frac{M}{[1 + \frac{(\gamma-1)M^2}{2}]^{\gamma+1/2(\gamma-1)}} \right\} \left(\frac{X}{\mu} \right) \right] A_g \right] \right\}} \right\} + \left(\frac{\Delta x}{k} \right) r1 + \left(\frac{\Delta x}{k} \right) r2 + \left[\frac{1}{h_{c,Ac}} \right] \quad 5-141$$

(v) Energy equation

$$Q - W = \iiint \frac{\partial}{\partial t} (\rho e) d(\text{vol}) + \oint \mathbf{e} p \vec{V} \cdot \hat{n} dA$$

$$Q(\text{heat load}) = \dot{W} C_p \Delta T \quad 5-142$$

Where: $\Delta T = (\Delta T - \text{LMTD})$

(Vi) Now mathematically we express the LMTD; aka The Log Mean temperature difference as follows: The author leverages from his graduate studies from reference [10]

$$\bullet \quad \{ \Delta T_{\text{LMTD}} = [(\Delta T_2 - \Delta T_1) / (\ln (\Delta T_2 / \Delta T_1))] \} \quad 5-143$$

Note: In the energy equation: $\Delta T = \text{LMTD}$; aka The Log Mean temperature difference; ΔT_{LMTD}

In the preceding section the author derived the mathematical expression for the flow emanating out of the film hole. Now it is essential to also compute the temperature of the associated flow emanating out of the film hole, however, to do so we need to better understand the sources of the heat loads into the control volume, and hence as one of the sources besides the gas path temperature is the gas path heat transfer coefficient. Prior to determining the temperature of the associated flow emanating out of the film hole, the external heat transfer coefficient physics is established in the following section.

Hence, Note the Energy equation (Overall Heat flux): -Eq 5-142, is a function of the boundary layer reflecting the Hot Gas Path environment, hence it is critical to now establish the fundamental physics based mathematical equations reflection the external gas path boundary conditions, and hence to do so the following are the engineering-based assumptions and associated derivations:

In summary, the objective at this point of the dissertation is to mathematically derive an expression coupling the film cooling temperature to the film hole exit (mass flow rate) coolant temperature aligned to an assumed boundary layer based film cooling

effectiveness. Hence to do so the following section will first and foremost focus on the external gas path heat transfer boundary conditions derivations in order to compute the external boundary conditions and hence the overall heat load into the component.

(5.6) External environment: Hot Gas Path parameter derivation aligned to control volumes

Gas Path Boundary Layer environment -One Dimensional Assessment-Derivation of boundary conditions: The author is leveraging from literature research [8] [10] [54], while applying the mathematical equations to conduct the derivations aligned to the control volume under consideration.

Derivation of predicting heat flux to the component from the source i.e., the hot gas path is based on essentially comprehending the boundary layer development over the external surface of the component in question and under consideration. The thorough understanding of the flow transition from laminar to turbulence, understanding the potential flow velocity distribution and in addition it is also necessary and pivotal to comprehend the temperature profile (i.e., pattern factor) of the emitted gas stream exiting the heat source.

This section of the dissertation is devoted to theoretically deriving the external heat transfer formulations impacting the component and applicable to the flat and curved surfaces and begin with the brief understanding of the boundary layer phenomenon.

From the general stress system in a deformable body and considering the authors previous academic experiences in the derivations of the equations of motion for a compressible fluid. The author notes the process of deriving the stress tensor the flow field velocity is defined to be the following:

$w = iu + jv + kw$; where u, v, w are the orthogonal components and hence these three components, the pressure “ p ” and the density “ ρ ” are all conceived as functions of the cartesian coordinates x, y, z and also including the time “ t ”.

For mathematical simplicity purposes, assuming that that surface force per unit volume can be calculated from the equations denoting the force on the boundary per unit volume, and the nine quantities forming the stress tensor the then substituting into the equations of motion which is the following:

$$\rho \frac{Dw}{Dt} = F + P$$

Where:

$$F = iX + jY + kZ \quad \text{Body Force}$$

$$P = iP_x + jP_y + kP_z \quad \text{Surface force}$$

Hence subsequent to mathematical evaluations, we arrive at the system of three equations containing the six stresses as follows,

$\sigma_x, \sigma_y, \sigma_z, \tau_{xy}, \tau_{xz}, \tau_{yz}$ and we denote the following three equations as the Navier Stokes equations of motion.[59]

$$\rho \frac{Du}{Dt} = X + \left\{ \frac{\partial}{\partial x} \left[-\frac{2}{3} \mu \text{div } w + 2\mu \frac{\partial u}{\partial x} \right] - \frac{\partial p}{\partial x} + \frac{\partial}{\partial y} \left[\mu \left(\frac{\partial u}{\partial y} + \frac{\partial v}{\partial x} \right) \right] + \frac{\partial}{\partial z} \left[\mu \left(\frac{\partial u}{\partial z} + \frac{\partial w}{\partial x} \right) \right] \right\}$$

$$\rho \frac{Dv}{Dt} = Y + \left\{ \frac{\partial}{\partial x} \left[\mu \left(\frac{\partial u}{\partial y} + \frac{\partial v}{\partial x} \right) \right] - \frac{\partial p}{\partial y} + \frac{\partial}{\partial y} \left[-\frac{2}{3} \mu \text{div } w + 2\mu \frac{\partial v}{\partial y} \right] + \frac{\partial}{\partial z} \left[\mu \left(\frac{\partial w}{\partial y} + \frac{\partial v}{\partial z} \right) \right] \right\}$$

$$\rho \frac{Dw}{Dt} = Z + \left\{ \frac{\partial}{\partial x} \left[\mu \left(\frac{\partial u}{\partial z} + \frac{\partial w}{\partial x} \right) \right] - \frac{\partial p}{\partial z} + \frac{\partial}{\partial y} \left[\mu \left(\frac{\partial v}{\partial z} + \frac{\partial w}{\partial y} \right) \right] + \frac{\partial}{\partial z} \left[-\frac{2}{3} \mu \text{div } w + 2\mu \frac{\partial w}{\partial z} \right] \right\}$$

For the purpose of this dissertation the author will now proceed towards focusing on the convection boundary layer.

The following discussion [10] will be focused mainly on the convection boundary layer. This topic describes the required energy that is transferred between the solid surface and the fluid medium that traverses over the solid surface, in this the control volume under consideration.

The selected region depicting the surface of the control volume is assumed to be held at a constant temperature, where the T_s (surface temperature) is not equivalent to the gas path fluid temperature T_∞ . It is also assumed that the transfer of the energy as aforementioned is due to the overall bulk motion of the fluid particles from a macroscopic level.

Assuming the local flux influences the region selected for the control volume we have the following mathematical expression.

$q'' = h(T_s - T_\infty)$ Where h is the local convection coefficient. As the flow conditions are not constant hence the h and q'' will change in magnitude in the lateral direction, from one control volume regions to another.

The rate of heat transfer is mathematically describes as to be the following

$$q = \int_{A_s} q'' dA_s$$

$$q = \int_{A_s} h(T_s - T_\infty) dA_s$$

$$q = (T_s - T_\infty) \int_{A_s} h dA_s$$

Now we introduce the concept of the boundary layer velocity profile, where the axial component of the fluid “ u ” varies in the vertical direction from the surface to the free stream and basically reaches the free stream velocity of u_∞ , where ∞ is denoted to signify the free stream conditions of the overall bulk flow conditions.

These condition that are related to the velocity boundary layer profile of the fluid flow under consideration has two regions that is identified as the (a) a very thin layer of the boundary layer within which the velocity gradients and the corresponding shear stresses are large in magnitude and (b) a region identified on the periphery of the boundary layer within which the velocity gradients and the associated shear stresses are minimal hence of no contribution. As the fluid traverses in the axial direction, the corresponding profile of the boundary layer enlarges as the boundary layer thickness grows larger as a function of the axial distance from its original point.

In addition, it is also known that the velocity boundary layer thickness as mentioned previously, can be depicted mathematically as the following $[\delta = 0.37x(\text{Re}_x)^{-1/5}]$ [10] and based on the authors derivations and mathematical substitutions it can also be written as the following.

$$\delta = 0.37x \left[\left\{ \frac{\gamma g}{R[Tt_2[1 + 1/2(\gamma - 1) * M_2^2]]} (P1_a) \frac{M}{[1 + \frac{\gamma - 1}{2} (M)^2]^{\gamma + 1/2(\gamma - 1)}} \right\} (X/\mu) \right]^{-1/5}$$

Also noting that there is an inherent synergy of the surface shear stress τ and associated frictional influences, which is the fundamental basis of determining the friction coefficient.

Noting the modified Reynolds number or the Chilton-Colburn analogies as depicted below,

- $\frac{Cf}{2} = (\text{St})(\text{Pr})^{2/3} = jH$. Where $0.6 < \text{Pr\#} < 60$ [10] 5-144

And referring to turbulent flow conditions that are practically influenced by the Reynolds number up to approximately 10^7 .

It is well known from literature that the local friction coefficient is correlated by the expression show below:

- $C_{f,x} = (0.0592)(Re)_x^{-1/5}$. Where $Re_x \leq 10^7$ [10] 5-145

Our next step is to identify a dimensionless parameter that involves bot the Reynolds number and Prandtl number respectively.

We start off with the comprehension of the fundamental physics-based formulations of Newtons law of cooling:

The heat transfer rate equation is of the form of the following:

- $q'' = h(T_s - T_\infty)$ This is basically known as the Newtons Law of cooling. [10] 5-146

Where:

- q'' Is defined as the convective heat flux
- T_s Is defined as the body surface temperature
- T_∞ Is defined as the fluid temperature
- h Is defined as the convection heat transfer coefficient

Now at this point we shall identify the key aspects of the thermal boundary layer:

Synonymous to the velocity boundary layer development of a fluid flowing a flat or curved surface, a consequential thermal boundary also develops as a result of the temperature difference between the fluid stream and the surface wall that the fluid under consideration is flowing over.

An example of the aforementioned phenomenon is one of an isothermal flat plate. At the advent of the flow occurring at the front or the leading edge of the flat plate where the fluid particles are not in direct contact with the plate; the corresponding temperature

profile within the fluid domain in the radial direction “y” is uniform. Where $T(y) = T(\infty)$. Refer to Figure 5.3

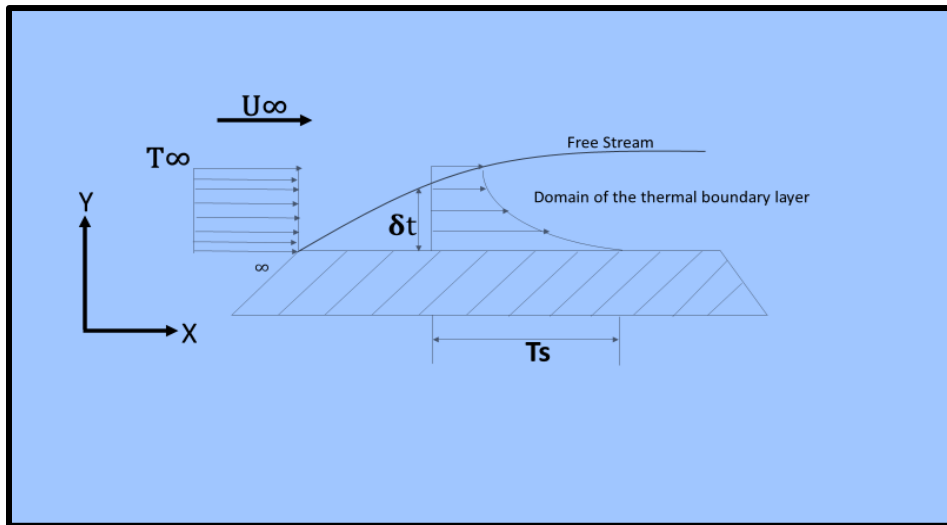


Figure 5.3 Flat Plate Boundary Layer example

As the fluid comes into contact with the surface region of the plate the fluid particles near the plate become thermally equilibrated at the plate’s temperature. In this equilibrating process the fluid particles experience an energy transfer within the fluid particles residing in the adjacent layers and hence resulting in a temperature differential within the fluid domain.

This domain of the fluid experiencing the temperature gradient is defined and known as the thermal boundary layer.

The corresponding thickness of this generated thermal boundary layer is denoted by δ_t . With the fluid stream traveling away from the leading edge and unto the surface of the flat plate the influence of the heat transfer mechanisms or energy exchange within the adjacent layers of the within the overall boundary layer, further penetrates the free stream hence resulting in the further growth of the thermal boundary layer.

To determine the convection heat transfer coefficient the local heat flux is derived by applying the Fourier's law of heat conduction to the fluid at the leading-edge region where the vertical height or growth of the boundary layer $y=0$

The mathematical expression as per literature is the following:

- $Q''_{\text{surface}} = - (K_{\text{fluid}}) (\partial t / \partial y)|_{y=0}$ [10] 5-147

It should be noted that at the plate surface the actual surface of the plate hinders and hence stops the adjoining fluid stream from moving hence there is no fluid movement and therefore the process of energy transfer is actually attained by the mechanism of conduction.

In order to define the convective heat transfer coefficient; we need to combine the following two fundamental equations as follows:[18]

- (i) $q'' = h (T_s - T_{\infty})$ 5-148

- (ii) $q'' = (k_f) (\partial t / \partial y)|_{y=0}$ 5-149

Therefore:

- $h = \frac{q''}{(T_s - \{[\frac{T_t}{1 + \frac{(Y-1)M^2}{2}}] + [1 + \frac{(r\gamma RM^2)}{2C_p}]\})}$ 5-150

- Hence by mathematical substitution yields:

- $h = \frac{k_f * (\partial t / \partial y)|_{y=0}}{(T_s - \{[\frac{T_t}{1 + \frac{(Y-1)M^2}{2}}] + [1 + \frac{(r\gamma RM^2)}{2C_p}]\})}$ 5-151

Note:

- T_s = Defined as the plate wall surface temperature
- T_{∞} = Defined as the fluid stream temperature

Where: $(T_s - T_{\infty})$ = Constant and is totally independent of the lateral (x) direction.

However, δt which is defined as the thermal boundary layer increases with the flow traversing in the lateral direction (x). This is due to the fact that as the fluid traverses over the plate the associated fluid particles contacting the plate surface are achieving thermal equilibrium. This results in the following phenomenon that is the temperature gradient developed in the fluid decreases in the lateral direction(x) hence resulting in the magnitude of the corresponding heat transfer coefficient diminishing in the lateral direction(x).

The aforementioned derivations and associated learnings based on leveraging of the fundamental equations from literature, are conducted by the author in order to support the derivations of both the flat plate turbulent boundary layer and also the cylindrical geometry turbulent boundary layer external gas path boundary conditions, which basically strongly affect the turbine high pressure region components external heat loads.

Theoretical based Prediction of the heat loads or the heat flux to the component:

The following section is devoted to deriving the external high-pressure turbine external gas path turbulent boundary layer heat transfer coefficients for the leading edge and also the corresponding pressure and suction sides of the airfoil, and this is conducted by having the flat plate and cylinder in cross flow mathematical equations be applied.

The author is leveraging from literature research while associating the mathematical equations to conduct the derivations aligned to the control volume under consideration.

On deriving the external gas path convective coefficient and also assuming during this derivation the associated resistances the heat flux vector and corresponding heat loads are determined by also coupling the turbine thermodynamic state properties that was derived earlier in this dissertation.

This section will now introduce the approach and process the author utilizes to depict the multi-physics integration that occurs within the high-pressure regions of the control volume the author has chosen.

We shall commence by deriving the flat plate turbulent boundary layer local Nusselt number and subsequently the corresponding heat transfer coefficient.

The author starts off by defining the Reynolds Analogy. And, as the author has studied and researched the book by Schlichting “For boundary flow fields” [8] the author based on leveraging from literature that there exists a unique relationship between heat transfer and skin friction which in its simplest form was discovered by O. Reynolds. It is for this reason that this Physics based relationship is known as the Reynolds Analogy; which in mathematical terms is shown to be

- $\left[\frac{C_f}{2} = St \equiv St_m \right] [10]$ 5-152

This equation is known as the Reynolds analogy and relates to the key engineering parameters of the velocity, thermal and concentration boundary layers.

Thus, leveraging from the theory of the study of turbulent flow physics; empirical data obtained from experiments, it is known that for turbulent flows for Reynolds number up to approximately 10^7 ; that the local friction coefficient is depicted to be mathematically

- $C_{f,x} = (0.0592)(Re_x)^{-1/5}$; Where $Re_x \leq 10^7$ [10] 5-153

- $Nu_x = (0.0296)(Re_x)^{-1/5} (Re_x)(Pr) / (Pr^{2/3})$ [10] 5-154

- $Nu_x = (0.0296)(Re_x)^{-4/5} (Pr^{1/3})$ 5-155

Or in terms of convective “H”

Note:

- $h = (K_g)(Nu)/D_h$ 5-156

or

- $h = (K_g) * (Nu)/L *$ 5-157

Where:

- L^* is defined as the characteristic length.
- X = Defined to be the Flow traversing distance along the surface – ft. from the stagnation (L/e) of the plate.
- Re_x = Defined to be the Reynolds number as a function of the traversing length “x” distance
- Pr = Prandtl number

Hence:

- $Re \# = [(\rho) * (V_g) * (X)/(\mu)]$ 5-159

Where:

- ρ = Defined as the gas density Kg/m^3
- V_g = Defined as the gas velocity component in the x, direction; m/sec; ft/sec
- (μ) is defined as the fluid viscosity, $(N * Sec)/m^2$; lb./Ft * sec
- Pr is defined as the Prandtl number = $K\mu C_p/k_{gas}$ 5-160

Where:

- K = dimensional constant; 3600 sec/Hr.
- C_p = Specific heat at constant pressure; $J/(kg * K)$; Btu /lb. Degree R
- K_{gas} = Gas conductivity; $Btu/HrFt^2 \circ F$ – or – $Btu/HrFt^2 \circ R$ 5-161

5-162

Now also note that the modified Reynolds number or the Chilton-Colburn, analogies mathematically can be expressed as:

- $\frac{C_f}{2} = (St)(Pr)^{2/3} \equiv J_h; \quad 0.6 < Pr < 60 \quad [10] \quad 5-163$
- $\frac{C_f}{2} = (Stm)(Sc)^{2/3} \equiv J_m; \quad 0.6 < Sc < 3000 \quad [10]$

Where J_h & J_m are the Colburn j factors for heat and mass transfer:

Using the following equations:

- $C_{f,x} = (0.0592)(Re_x)^{-1/5}$
- $C_f = 2(St)(Pr^{2/3})$
- $C_f = 2(Stm)(Sc^{2/3})$
- $Nu_x = (St)(Re_x)(Pr)$

Yields:

- $Nu_x = \frac{C_f}{2} \left(\frac{1}{Pr} \right)^{2/3} (Re_x)(Pr)$
- $Nu_x = [1/2 (0.0592)(Re_x)^{-1/5} \left(\frac{1}{Pr} \right)^{2/3}] (Re_x)(Pr) \quad 5-164$

At this point we arrive at the core of deriving the external gas path heat transfer coefficient. As a function of external flow path conditions including flow path velocity and pressure.

The following are the associated assumptions:

- Ideal gas path conditions (Perfect gas)
- Applying the following compressible flow and heat transfer equations.

As stated earlier:

- $Re \# = [(\rho)(Vg)(X)/(\mu)]$

And from leveraging from the continuity equation:

- $\dot{W} = (\rho g)(Ug)(A)$

Or As (\dot{W}/A) is the flow flux.

Thus:

- $(\dot{W}/A) = (\rho g)(Ug)$

Hence:

- $Re_x = (\dot{W}/A)(X/\mu)$

From the compressible flow equation; the flow flux is defined to be as the following.

Reference authors derivation previous section.

$$\phi_2 = \left(\frac{\dot{W}}{Ac} \right) \left(\frac{\sqrt{\left\{ \left[\frac{T_t}{1 + \frac{(\gamma-1)M^2}{2}} \right] + \left[1 + \frac{(\gamma RM^2)}{2C_p} \right] \right\}}}{P_t} \right) \sqrt{\frac{R}{gc}} = \frac{(M)(\sqrt{\gamma})}{[1 + 1/2(\gamma-1)M^2]^{\left[\frac{(\gamma+1)}{2(\gamma-1)} \right]}}$$

From which now we can show through mathematical manipulation:

- $\frac{\dot{W}}{Ac} = \left\{ \frac{\sqrt{\frac{\gamma}{gR}}}{\sqrt{\left\{ \left[\frac{T_t}{1 + \frac{(\gamma-1)M^2}{2}} \right] + \left[1 + \frac{(\gamma RM^2)}{2C_p} \right] \right\}}} (P_t) \right\} \frac{(M)}{[1 + 1/2(\gamma-1)M^2]^{\left[\frac{(\gamma+1)}{2(\gamma-1)} \right]}}$

Where:

- $Ac = (Cd)(Am)$

Hence now we show the mathematical expression of the Reynolds number for the external surface:

- $Re_x = \left\{ \frac{\sqrt{\frac{\gamma g}{R[T_t[1 + 1/2(\gamma-1)M_2^2]]}}}{(P1_a)} \frac{M}{[1 + \frac{\gamma-1}{2}(M)^2]^{\gamma+1/2(\gamma-1)}} \right\} (X/\mu) \quad 5-165$

Note as the geometry varies for suction and pressure sides of the airfoil due to curvature effects, aero profile, roughness etc. and hence the Mach number of the gas path

varies as well between the pressure and suction side due to the aerodynamic loading of the airfoil, however for this dissertation, the author assumes an average or bulk Reynolds number from the stagnation side to the trailing edge for the pressure and suction sides of the component; that can apply towards the assessment the external heat transfer. Hence for computations purposes the author assumes a bulk average Re_x to be applicable for both pressure and suction sides of the component under consideration.

Now in terms of the heat transfer coefficient the mathematical expression [17] is as follows:

- $h_g = (K_g) \left(\frac{Nu_x}{X} \right)$

Where:

- $X =$ Characteristic length

Hence:

- $h_g = \frac{K_g}{X} * (0.0296)(Pr^{1/3})(Re_x^{4/5})$

Hence with mathematical substitution [17] we see the following:

- $h_g = \left(\frac{K_g}{X} \right) (0.0296)(Pr^{1/3}) \left[\sqrt{\frac{\gamma g c}{R [T_t [1 + 1/2(\gamma - 1) M_2^2]]}} \right] (P1_a) \left\{ \frac{M}{[1 + (\frac{\gamma - 1}{2}) M^2]^{\gamma + 1/2(\gamma - 1)}} \right\}$
 (X / μ) 5-166

The aforementioned mathematical expression reflects and applied for the non-curved surface i.e., flat surface of the high-pressure turbine airfoil. I have leveraged the literature and derived through mathematical evaluations the first order approximation for the zero-pressure gradient.

Where:

- $K_g =$ The flow or gas path fluid conductivity

- Pr = The flow or gas path fluid Prandtl
- γ_g = Specific heat ratio of the external flow or gas path at constant pressure and volume
- g_c = Constant gravitational acceleration = $32.17 \text{ (lbm} - \text{ft)}/(\text{lbf} - \text{sec}^2)$
- R = gas constant; $\frac{\text{ft-lb}}{\text{lb-deg R}}$
- M = Mach number
- μ = viscosity $(\text{N} * \text{Sec})/\text{m}^2$; $\text{lb.}/\text{ft} - \text{sec}$
- T_g = Flow or gas path temperature

Now we shall focus our attention to the leading edge of the airfoil and from the literature review the author leverages the cylinder in cross flow heat transfer correlation applicability and associated details.

For the heat transfer coefficient “ h_g ” at the leading-edge region of the airfoil is the following formulation. [17]

Leading edge:

- $h_g = a [(1.14)(Kg/D) [(\rho_g)(u_g)(D/\mu)]^{1/2}(Pr)^{0.4}] (1 - |\varphi/90|)^3$
- $[-80\text{deg} < \varphi < 80\text{deg}]$

Where:

- a = Augmentation factor
- D = The airfoil nose diameter at the leading edge; m, ft
- $u_{g\infty}$ = This is the flow path gas velocity approaching the stagnation region of the airfoil leading edge; m/sec; ft/sec

- ϕ = This is the angular distance from the leading-edge stagnation point; degrees.

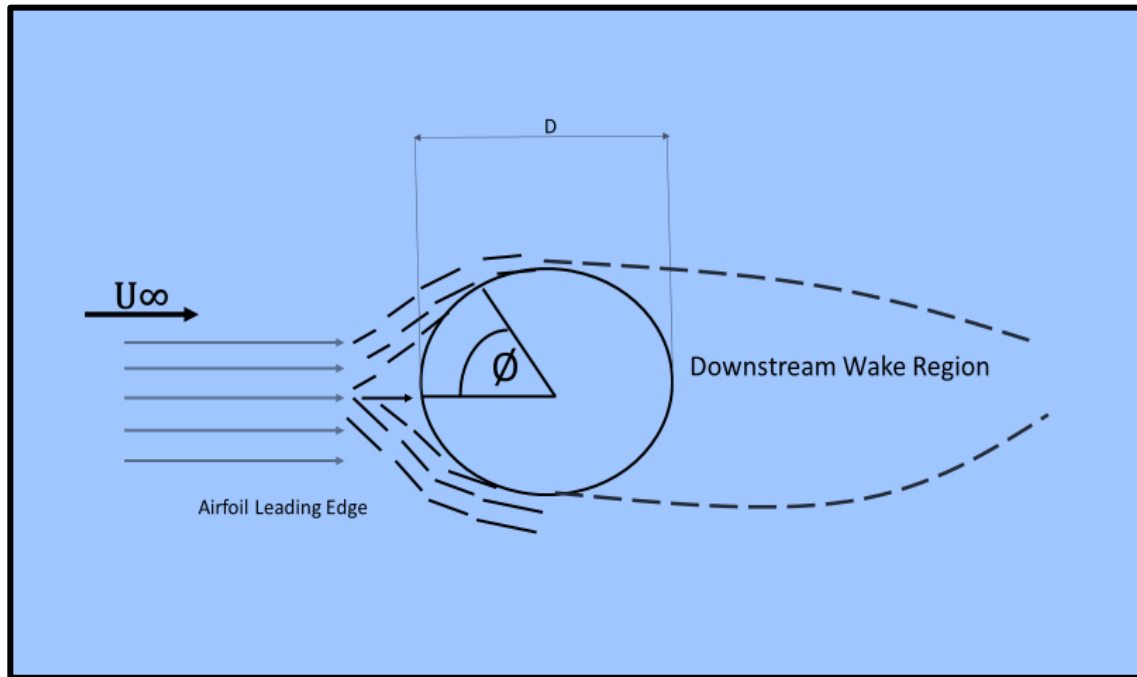


Figure 5.4 Cylinder in cross flow boundary layer example

Airfoil leading edge:

- a = Augmentation factor used to adjust the coefficient in order to account for the highly turbulent mainstream flow approaching the leading edge of the airfoil section.
- At this point we now have the external factors directly related to the heat load into the airfoil component.
- The leading-edge correlation leveraged from the literature can now be further evaluated by mathematical substitution by applying the flow function equation as the author of this dissertation has tried to conduct to his best ability as conducted previously in a similar manner as done for the flat plate region.
- The reason behind the mathematical substitution that the author of this dissertation has conducted is because he is trying to integrate the gas path flow

conditions physics into the aforementioned leading-edge curved surface literature-based correlation.

In this section we shall conduct the substitution and convert the leading-edge correlation to include the stage pressure parameter.[17]

As derived earlier: $Re_x = \left\{ \sqrt{\frac{\gamma g}{R[Tt_2[1+1/2(\gamma-1)*M_2^2]]}} (Pt) \frac{M}{[1+\frac{\gamma-1}{2}(M)^2]^{\gamma+1/2(\gamma-1)}} \right\} (X/\mu)$

Now substituting the above equation in terms of gas path we get the following mathematical expression:

$$hg\left(\frac{L}{e}\right) = a [(1.14) \left(\frac{Kg}{D}\right) \left\{ \sqrt{\frac{\gamma g}{R[Tt_2[1+1/2(\gamma-1)*M_2^2]]}} (Pt) \frac{M}{[1+\frac{\gamma-1}{2}(M)^2]^{\gamma+1/2(\gamma-1)}} (X/\mu) \right\}^{0.5} [(Pr)^{0.4} (1 - |\varphi/90|^3)]$$

With the aforementioned physics based mathematical analysis the gas path external conditions of the airfoil turbine component have been synergistically coupled.

In summary: The flat plate and cylinder in cross flow external heat transfer regions [17] have been respectively identified as the following:

- $hg = \left(\frac{Kg}{X}\right) (0.0296) (Pr^{1/3}) \left[\sqrt{\frac{\gamma g_c}{R[Tt_2[1+1/2(\gamma-1)*M_2^2]]}} \right] (P1_a) \left\{ \frac{M}{[1+(\frac{\gamma-1}{2})M^2]^{\gamma+1/2(\gamma-1)}} \right\} (X/\mu)$ 5-167

- $hg\left(\frac{L}{e}\right) = a [(1.14) \left(\frac{Kg}{D}\right) \left\{ \sqrt{\frac{\gamma g}{R[Tt_2[1+1/2(\gamma-1)*M_2^2]]}} (Pt) \frac{M}{[1+\frac{\gamma-1}{2}(M)^2]^{\gamma+1/2(\gamma-1)}} (X/\mu) \right\}^{0.5} [(Pr)^{0.4} (1 - |\varphi/90|^3)]$ 5-168

Now that we have established the physics based mathematical formulations for the external gas path heat transfer coefficients that is a predominant parameter in solving for the heat source or heat loads into the control volume under consideration and as the

earlier section was devoted specifically toward generating the physics-based formulations for the film hole Mach number and associated flowrate. Note both the flat plate and leading-edge regions are a function of the gas path pressure and temperature conditions.

Now the next step is to now to compute the temperature of the associated flow emanating out of the film hole based on the heat load generated from the gas path conditions; and to also evaluate the physics-based formulations pertaining to the cooling side of the airfoil component; with the prime objective of assessing the durability of the component under consideration in terms of the resistances 's thermal conditions and the associated corresponding substrate's health or life for the control volume under consideration.

(5.7) Internal environment: Component cooling parameter derivation aligned to control

Generating the physics-based formulations to compute the temperature of the associated flow emanating out of the film hole

Hence as mentioned earlier; the key objective is to mathematically derive an expression coupling the component cooling fluid emanating out of the perforations and into the gas path, aka coolant exit temperature, to the film cooling exit mass flowrate coolant temperature, accompanied with an assumed boundary layer-based condition overall cooling effectiveness.

The focus of the following section is now to couple the following key parameters and solve for the fluid exit temperature emanating out of the cooling hole.

Key parameters are the following:

- (i) Total conductance of the cooled substrate "metal wall"

- (ii) Cooling hole film cooling effectiveness
- (iii) Heat gained in the fluid medium being applied for the film temperature
- (iv) Mass flow rate applied toward film cooling
- (v) Pressure ratio across the cooling hole configuration

Physics based Mathematical Analysis: Commencing with the Log Mean

temperature difference previously derived and applying to the film cooling hole control volume;

$$\Delta T_{lm} = \left\{ \frac{[(Ths_{FH} - TFH_{out}) - (Ths_{FH} - TFH_{in})]}{\ln [(Ths_{FH} - TFH_{out}) / (Ths_{FH} - TFH_{in})]} \right\} \quad 5-169$$

Where:

Ths_{FH} = Temperature of the inner cooled side location of the film cooling hole, which is assumed to be based on the heat transfer conduction and convection computations executed in control volume CV_3 and the film hole inner surface temperature is hence assumed to be the average temperature of the substrate, and it this average temperature that is assumed throughout the entire length of the inner surface of the film hole. This assumption the author has made as the control volume surface area for CV_2 is much less compared to the surface area for CV_3 , hence it is CV_3 surface area that dominates the overall differential in temperature across each of the resistances.

- TFH_{out} = Exit temperature of the fluid exiting the film hole which is a function of the heat pick up along the entire length of the cooling hole.
- TFH_{in} = Inlet fluid temperature supplied into the film hole. This can also be referred to as the following: $\{T_{mexc3} = T_{exc3} = T_{incv2}\}$

Hence:

- $\dot{W}_{fh} C_p (T_{FHout} - T_{FHin}) =$

$$[(H_{avg}) (A_s)]_{fh} \left\{ \frac{[(T_{hsFH} - T_{FHout}) - (T_{hsFH} - T_{FHin})]}{\ln [(T_{hsFH} - T_{FHout}) / (T_{hsFH} - T_{FHin})]} \right\} \quad 5-170$$

Therefore:

The film hole exit temperature (based on the film hole geometric configuration) is solved for yielding the following transcendental mathematical expression which is solved via iteration.

- $T_{FHout} = \frac{\left[\frac{H_{AsFH}(T_{FHin})}{\dot{m}_{fh}} \right] + [\dot{W}_{FH}(C_p)(T_{FHin})]}{[(H_{AsFH}/\dot{m}_{fh} + \dot{W}_{FH} \cdot C_p)]}$

5-171

Note: $(T_{FHin} = T_{mexcv_3})$

Note: T_{FHout} is not the Film temperature but the temperature of the fluid stream exiting out of the film cooling configuration, based on the heat pickup from the external loading conditions.

Now we re-introduce the "EGPT" external gas path temperature cooling effectiveness mathematical expression, which is based on the authors mathematical substitution into the commonly applied effectiveness formulation.

- $\eta_{film} = \frac{\left(\left[\frac{T_t}{\left(1 + \frac{(\gamma-1)M^2}{2} \right)} \right] + \left[1 + \frac{(r\gamma RM^2)}{2C_p} \right] \right)_{avg-EGPT}}{\left(\left[\frac{T_t}{\left(1 + \frac{(\gamma-1)M^2}{2} \right)} \right] + \left[1 + \frac{(r\gamma RM^2)}{2C_p} \right] \right) - T_{FH,out}}$

5-172

Or

$$\bullet \quad \eta_{\text{film}} = \frac{\left(\left[\frac{T_t}{1 + \frac{(\gamma-1)M^2}{2}} \right] + \left[1 + \frac{(\gamma RM^2)}{2C_p} \right] \right)_{\text{avg}} - \text{EGPT}}{\left(\left[\frac{T_t}{1 + \frac{(\gamma-1)M^2}{2}} \right] + \left[1 + \frac{(\gamma RM^2)}{2C_p} \right] \right)_{\text{avg}} - \frac{\left[\frac{H_{\text{AsFH}}(T_{\text{FHin}})}{\dot{m}_{\text{fh}}} \right] + [\dot{W}_{\text{FH}}(C_p)(T_{\text{FHin}})]}{[(H_{\text{AsFH}}/\dot{m}_{\text{fh}} + \dot{W}_{\text{FH}} \cdot C_p)]}} \quad 5-173$$

Where EGPT= Effective Gas Path Temperature

From here we now have the following:

$$\bullet \quad T_{\text{FHout}} = \left[\left[\frac{T_t}{1 + \frac{(\gamma-1)M^2}{2}} \right] + \left[1 + \frac{(\gamma RM^2)}{2C_p} \right] \right]_{\text{avg}} - \left(\left[\frac{T_t}{1 + \frac{(\gamma-1)M^2}{2}} \right] + \left[1 + \frac{M^2(\gamma RM^2)}{2C_p} \right] \right)_{\text{avg}} - \text{EGPT} / \eta_{\text{film}} \quad 5-173A$$

$$\bullet \quad \left\{ \frac{\left[\frac{H_{\text{AsFH}}(T_{\text{FHin}})}{\dot{m}_{\text{fh}}} \right] + [\dot{W}_{\text{FH}}(C_p)(T_{\text{FHin}})]}{[(H_{\text{AsFH}}/\dot{m}_{\text{fh}} + \dot{W}_{\text{FH}} \cdot C_p)]} = \left(\left[\frac{T_t}{1 + \frac{(\gamma-1)M^2}{2}} \right] + \left[1 + \frac{(\gamma RM^2)}{2C_p} \right] \right)_{\text{avg}} - \left(\left[\frac{T_t}{1 + \frac{(\gamma-1)M^2}{2}} \right] + \left[1 + \frac{(\gamma RM^2)}{2C_p} \right] \right)_{\text{avg}} - \text{EGPT} / \eta_{\text{film}} \right\} \quad 5-173B$$

Now we proceed in solving for the Effective gas path Temperature “EGPT”

Hence:

$$\bullet \quad \left[\frac{\left(\left[\frac{T_t}{1 + \frac{(\gamma-1)M^2}{2}} \right] + \left[1 + \frac{(\gamma RM^2)}{2C_p} \right] \right)_{\text{avg}} - \text{EGPT}}{\eta_{\text{film}}} \right] = \left(\left[\frac{T_t}{1 + \frac{(\gamma-1)M^2}{2}} \right] + \left[1 + \frac{(\gamma RM^2)}{2C_p} \right] \right)_{\text{avg}} - \left\{ \frac{\left[\frac{H_{\text{AsFH}}(T_{\text{FHin}})}{\dot{m}_{\text{fh}}} \right] + [\dot{W}_{\text{FH}}(C_p)(T_{\text{FHin}})]}{[(H_{\text{AsFH}}/\dot{m}_{\text{fh}} + \dot{W}_{\text{FH}} \cdot C_p)]} \right\}$$

$$\bullet \quad \left(\left(\left[\frac{T_t}{1 + \frac{(\gamma-1)M^2}{2}} \right] + \left[1 + \frac{(\gamma RM^2)}{2C_p} \right] \right)_{\text{avg}} - \text{EGPT} \right) = \eta_{\text{film}} \left\{ \left(\left[\frac{T_t}{1 + \frac{(\gamma-1)M^2}{2}} \right] + \left[1 + \frac{(\gamma RM^2)}{2C_p} \right] \right)_{\text{avg}} - \left\{ \frac{\left[\frac{H_{\text{AsFH}}(T_{\text{FHin}})}{\dot{m}_{\text{fh}}} \right] + [\dot{W}_{\text{FH}}(C_p)(T_{\text{FHin}})]}{[(H_{\text{AsFH}}/\dot{m}_{\text{fh}} + \dot{W}_{\text{FH}} \cdot C_p)]} \right\} \right\} \quad 5-174$$

Further mathematical assessment yields:

$$\begin{aligned}
& \bullet \left(\frac{1}{\eta_{\text{film}}} \right) \left\{ \left[\frac{T_t}{1 + \frac{(\gamma-1)M^2}{2}} \right] + \left[1 + \frac{M^2(r\gamma RM^2)}{2C_p} \right] \right\}, \text{avg} - \frac{\text{EGPT}}{\eta_{\text{film}}} = \left\{ \left[\frac{T_t}{1 + \frac{(\gamma-1)M^2}{2}} \right] + \left[1 + \right. \right. \\
& \left. \left. \frac{M^2(r\gamma RM^2)}{2C_p} \right] \right\}, \text{avg} - \left\{ \frac{\left[\frac{\text{HAsFH}(\text{TFHin})}{\dot{m}_{\text{fh}}} \right] + [\dot{W}_{\text{FH}}(C_p)(\text{TFHin})]}{[(\text{HAsFH}/\dot{m}_{\text{fh}} + \dot{W}_{\text{FH}} * C_p)]} \right\}
\end{aligned} \tag{5-175}$$

Finally, we have a mathematical expression depicting the overall coupling of the effective gas path Temperature (EGPT) with the associated factors:

$$\begin{aligned}
& \bullet \text{EGPT} = \frac{\left(\left\{ \left[\frac{T_t}{1 + \frac{(\gamma-1)M^2}{2}} \right] + \left[1 + \frac{(r\gamma RM^2)}{2C_p} \right] \right\}, \text{avg} - \text{EGPT} \right)}{\left(\left\{ \left[\frac{T_t}{1 + \frac{(\gamma-1)M^2}{2}} \right] + \left[1 + \frac{(r\gamma RM^2)}{2C_p} \right] \right\}, \text{avg} - \text{TFHout} \right)} \left\{ \left\{ \left[\frac{T_t}{1 + \frac{(\gamma-1)M^2}{2}} \right] + \left[1 + \right. \right. \right. \\
& \left. \left. \left. \frac{(r\gamma RM^2)}{2C_p} \right] \right\}, \text{avg} \left[\frac{1}{\left(\left\{ \left[\frac{T_t}{1 + \frac{(\gamma-1)M^2}{2}} \right] + \left[1 + \frac{(r\gamma RM^2)}{2C_p} \right] \right\}, \text{avg} - \text{EGPT} \right)} - 1 \right] + \right. \\
& \left. \left\{ \frac{\left[\frac{\text{HAsFH}(\text{TFHin})}{\dot{m}_{\text{fh}}} \right] + [\dot{W}_{\text{FH}}(C_p)(\text{TFHin})]}{[(\text{HAsFH}/\dot{m}_{\text{fh}} + \dot{W}_{\text{FH}} * C_p)]} \right\} \right\}
\end{aligned} \tag{5-176}$$

Where: EGPT = effective gas path temperature.

At this stage the author of this dissertation has derived and generated through rigorous physics based mathematical rationale derivations, a coupled process aligned to the overall multi-physics approach & also coupled the effective gas path temperature to the external gas path conditions, internal cooling hole fluid dynamics and associated heat flux conditions across the metal wall and substrate in which the cooling mechanism geometry imbedded.

Derived control volume mathematical assessment:

To obtain the effective gas path temperature at the exit of the cooling mechanisms geometry, in the form of the exit fluid temperature emanating out of the control volume (3) the following physics based mathematical formulation is used and along with the following substitutions are applied and thus yields:

$$\bullet \quad \text{EGPT} = \eta_{\text{film}} \left\{ \left[\frac{T_t}{1 + \frac{(\gamma-1)M^2}{2}} \right] + \left[1 + \frac{(r\gamma RM^2)}{2C_p} \right] \right\}, \text{avg} \left[\frac{1}{\eta_{\text{film}}} - 1 \right] + \left\{ \frac{\left[\frac{\text{HAsFH}(\text{TFHin})}{\dot{m}_{\text{fh}}} \right] + [\dot{W}_{\text{FH}}(C_p)(\text{TFHin})]}{[(\text{HAsFH}/\dot{m}_{\text{fh}} + \dot{W}_{\text{FH}} * C_p)]} \right\} \quad 5-177$$

And the corresponding coolant temperature emanating out of the cooling mechanism as earlier derived and applied to the control volume under consideration is the following:

$$\text{TFHout} = \left\{ \frac{\left[\frac{\text{HAsFH}(\text{TFHin})}{\ln[(\text{ThsFH} - \text{TFHout})/(\text{ThsFH} - \text{TFHin})]} \right] + [\dot{W}_{\text{FH}}(C_p)(\text{TFHin})]}{[(\text{HAsFH}/\ln[(\text{ThsFH} - \text{TFHout})/(\text{ThsFH} - \text{TFHin})] + \dot{W}_{\text{FH}} * C_p)]} \right\} \quad 5-178$$

Hence: The effective gas path temperature can also be written down as the following

$$\text{EGPT} = \eta_{\text{film}} \left\{ \left[\frac{T_t}{1 + \frac{(\gamma-1)M^2}{2}} \right] + \left[1 + \frac{(r\gamma RM^2)}{2C_p} \right] \right\}, \text{avg} \left(\frac{1}{\eta_{\text{film}}} - 1 \right) + \left\{ \frac{\left[\frac{\text{HAsFH}(\text{TFHin})}{\ln[(\text{ThsFH} - \text{TFHout})/(\text{ThsFH} - \text{TFHin})]} \right] + [\dot{W}_{\text{FH}}(C_p)(\text{TFHin})]}{[(\text{HAsFH}/\ln[(\text{ThsFH} - \text{TFHout})/(\text{ThsFH} - \text{TFHin})] + \dot{W}_{\text{FH}} * C_p)]} \right\} \quad 5-179$$

Based on the preceding physics-based derivations, we now proceed toward evaluating control volume CV₁; which is the control volume in the gas path located at the cooling hole geometry exit conditions of the cooling row of holes.

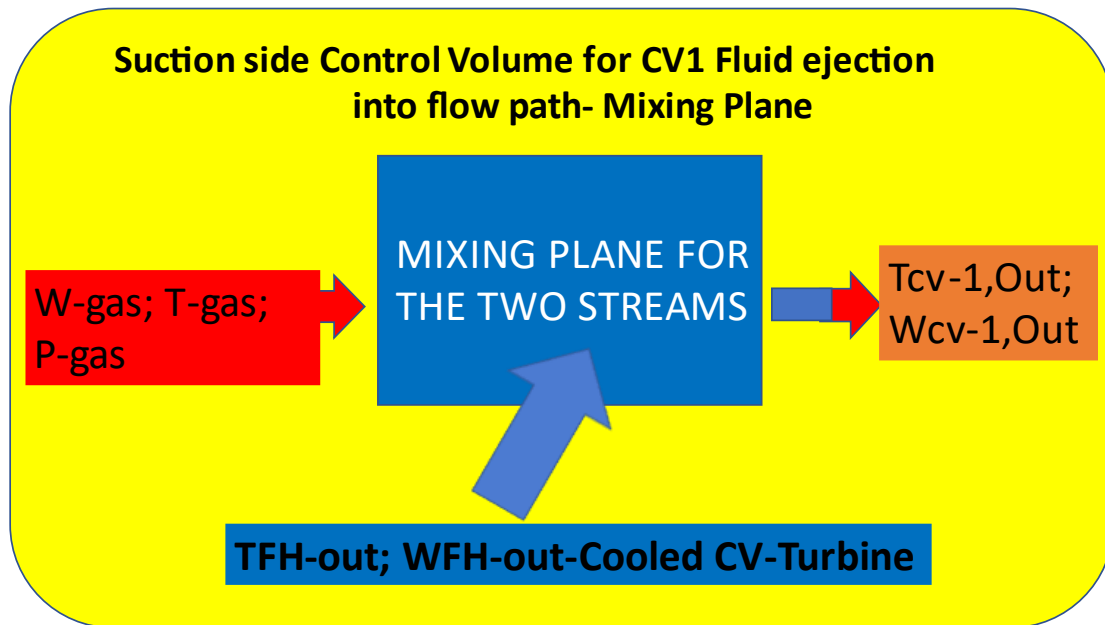


Figure 5.5 Airfoil Suction side Control volume; Mixing Plane

Where:

- (i) $\dot{W}_g \rightarrow$ External flow path mass flow rate
- (ii) $T_{\text{gas-avg}} \rightarrow$ External flow path gas path temperature
- (iii) $TFH_{\text{out}} \rightarrow$ Cooling hole exit fluid medium temperature
- (iv) $T_{\text{cv1, out}} \rightarrow$ Mixed cup temperature of the free stream at the exit of the control volume CV_1
- (v) $\dot{W}_{\text{cv1, out}} \rightarrow$ Total mixed accumulated flow rate exiting out of control volume CV_1

Now we need to derive the flow rate of the external gas path that is allowed to pass through the stage 1 nozzle throat area.

From the previously referenced and derived one dimensional compressible flow equation from which based on mathematical evaluation we achieve the following physics based mathematical formulation

$$\bullet \dot{W}, N1At = \left\{ \frac{M, NAt \sqrt{\frac{\gamma g c}{R}}}{\left[1 + \frac{\gamma - 1}{2} M, NAt^2 \right]^{\frac{\gamma + 1}{2(\gamma - 1)}}} \right\} (AN, 1At \left(\frac{P_t}{\sqrt{T_t}} \right)) \quad 5-180$$

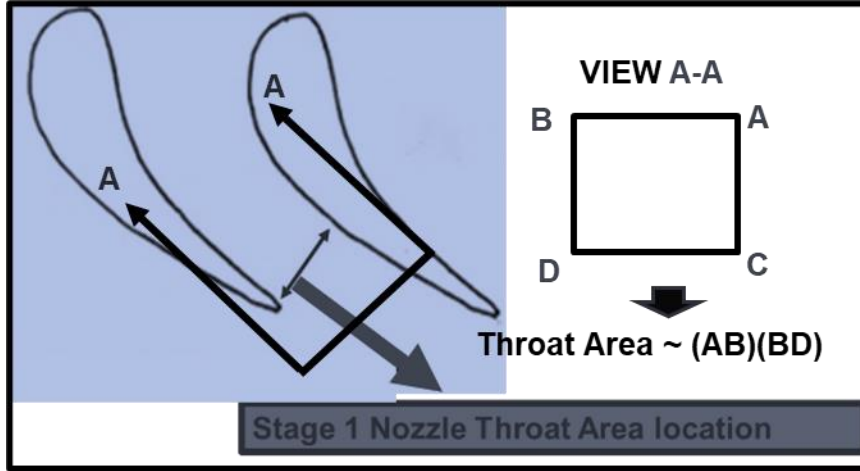


Figure 5.6 Stage 1 Nozzle Throat area assumptions

From the earlier aerodynamics mean line & thermodynamics gas path assessment we know that the cycle parameters such as the pressure, temperature at each state point or station.

Where:

- $AN1At$ = Nozzle throat area \equiv Area (ABCD)
- $M, N1At$ = Mach number @ throat of nozzle
- $HN1t$ = Nozzle height @ trailing edge $\sim BD$:

From a mass balance perspective the following mathematical expressions contribute towards the assessment of the control volume exit temperature.

$$\bullet \dot{W}, N1At + \dot{W}, FHout = \dot{W}, CV1out$$

&

$$(\dot{W}, N1At)(Cp, avg)(T_{gas, avg}) + (\dot{W}, FHout)(Cp, avg)(TFHout) =$$

$$(\dot{W}, CV1out)(Cp, avg)(TCV1, out)$$

5-181

Solving for control volume exit temperature (T-CV1, out); we get the following mathematical formulation:

$$T, CV1, out = \{(\dot{W}, N1At)(Cp, avg) \left(\left[\frac{Tt}{\left(1 + \frac{(\gamma-1)M^2}{2}\right)} \right] + \left[1 + \frac{(\gamma RM^2)}{2Cp} \right] \right), avg \} \\ (\dot{W}, FHout)(Cp, avg) \left(\left(\frac{\left[\frac{HAsFH(TFHin)}{\ln [(ThsFH - TFHout)/ (ThsFH - TFHin)]} \right] + [\dot{W}FH(Cp)(TFHin)]}{\left[(HAsFH/\ln [(ThsFH - TFHout)/ (ThsFH - TFHin)] + \dot{W}FH * Cp) \right]} \right) \right) / \\ (Cp, avg)(\dot{W}, N1At + \dot{W}, FHout) \quad 5-182$$

Where: T-CV1, out; is the total, absolute temperature discharged out of CV₁, which can be converted into mass fractions to solve for the Stage 1 nozzle Firing temperature at absolute temperature conditions.

Note: As it was recognized earlier in this dissertation that the total temperature magnitude at the stagnation location of the stage 1 nozzle is constant across the flow path of the entire component. As the flow is initially assumed to be adiabatic i.e., no mixing with the emanated flowrate related to the component cooling fluid medium; however with the cooling holes ejection into the gas path the associated mixing of the emanated cooling medium with the hot gas path decreases the total temperature of the hot gas path fluid temperature at the location of the coolant medium ejection and hence influences the downstream hot gas path fluid temperature. This decrease in hot gas path fluid temperature impacts the firing temperature plane and hence also the turbine rotor component inlet temperature.

From a relative perspective:

Hence the mixed temperature is defined as previously derived: 5-183

$$\begin{aligned}
T - CV1, out = & \left\{ \left(\frac{M, Nat \sqrt{\frac{\gamma g c}{R}}}{\left[1 + \frac{\gamma-1}{2} * M, Nat^2 \right]^{\frac{\gamma+1}{2(\gamma-1)}}} \right) (AN, 1At \left(\frac{Pt}{\sqrt{Tt}} \right)) (Cp, avg) \left(\left[\frac{Tt}{\left(1 + \frac{(\gamma-1)M^2}{2} \right)} \right] + \right. \right. \\
& \left. \left[1 + \frac{(r\gamma RM^2)}{2Cp} \right] \right\}, avg) + \\
& \left(\left(\frac{(M\#fh) \sqrt{\frac{\gamma g c}{R}}}{\left[1 + \frac{1}{2(\gamma-1)(M\#fh)^2} \right]^{\frac{(\gamma+1)}{2(\gamma-1)}}} \right) \left(\frac{(Cd(Ac).Pex^3)}{\sqrt{Tmexc v^3}} \right) (Cp, avg)(TFHout) \right) / \\
& (Cp, avg) \left(\left(\frac{M, Nat \sqrt{\frac{\gamma g c}{R}}}{\left[1 + \frac{\gamma-1}{2} * M, Nat^2 \right]^{\frac{\gamma+1}{2(\gamma-1)}}} \right) (AN, 1At \left(\frac{Pt}{\sqrt{Tt}} \right)) + \left\{ \frac{(M\#fh) \sqrt{\frac{\gamma g c}{R}}}{\left[1 + \frac{1}{2(\gamma-1)(M\#fh)^2} \right]^{\frac{(\gamma+1)}{2(\gamma-1)}}} \right\} \left(\frac{(Cd(Ac).Pex^3)}{\sqrt{Tmexc v^3}} \right) \right)
\end{aligned}$$

Where:

T-CV1, out ➔ Total; Absolute temperature at the mixing plane.

Note: When there is no emanation of the coolant medium discharge into the gas path, then in the above physics based mathematical equation we can substitute $\dot{W}, FHout = 0$, and hence by conducting so, we obtain the physics based mathematical expression:
 $T - CV1, out = T_{gas}$, which is referred to as the total “Firing” temperature at the exit plane of the stage 1 nozzle.

Hence, with the coolant discharging into the hot gas path all parameters downstream of the mixing plane and also at the mixing plane get affected and thus impacting the overall thermodynamic cycle and finally influencing the thermodynamic condition of the high-pressure turbine’s stage efficiency.

Detailed explanation of the parameters in the above preceding derived equation is as follows:

- $\dot{W}, N1A_{t, out} \Rightarrow$ This is the flowrate exiting the throat area of the static stage-1 component. The velocity vectors should be perpendicular to the plane ABDC. Dependent on the Pressure Ratio (PR) across the throat region, and the mean-line aerodynamic pressure.
- $T_{gas} \Rightarrow$ High pressure turbine hot gas path external gas path fluid temperature in the absolute frame of reference as the static component does not extract any work out of the fluid and with coolant ejection decreases in total temperature due to enthalpy mixing.
- $\dot{W}, FH_{out} \Rightarrow$ This is the coolant ejection flowrate that is mixed with the High-pressure turbine hot gas path external gas path fluid temperature.
- $TFH_{out} \Rightarrow$ This is the exit coolant medium discharge temperature.

CHAPTER 6:

THE UNIFIED MULTI-PHYSICS HPT FORMULATION – A MULTIPLE RESPONSE SURFACE FORMULATION

Finally, the author mathematically re-arranges the High-pressure turbine stage (1) efficiency mathematical expression to eventually depict the overall coupled multi-physics approach by incorporating the following interactive physics-based disciplines, thereby yielding A Unified Hot Gas Path Theory “UHGPT”

- (i) One dimensional mean-line aerodynamics
- (ii) Thermodynamics
- (iii) High-pressure turbine Component cooling assumptions
- (iv) High-pressure turbine hot gas path external temperature
- (v) High-pressure turbine component geometry & corresponding conduction and convection paths.

The Unified Multi-Physics HPT formulation: At this point of the dissertation the author has derived mathematically the parameter “ $T-CV_1$, out” and this parameter is the most essential parameter that plays an influential role in ascertaining the firing temperature plane and hence also the turbine rotor component inlet temperature, which directly impacts the high-pressure turbine stage efficiency which in accordance to the laws of thermodynamics is based on the temperature differential “Delta-T” across the high-pressure turbine static component.

Now we can go ahead and substitute the mathematical expressions of each parameter included in the parameter “ $T-CV_1$, out” formulation. This is conducted in order to depict the process of how the “ $T-CV_1$, out” expression has been mathematically derived by applying a coupled multi-physics approach for the entire range of the high-pressure turbine stage section.

Assuming that the mixing plane consolidates the overall high-pressure turbine stage static section, bulk average-based conditions, then the “ $T-CV_1$, out” associated temperature is the total mixed-cup temperature which further influences the firing temperature of the turbine.

The enthalpy temperature is assumed to be located at the inlet plane of the turbine rotor, and it is this temperature that is associated to produce work. Hence the higher this firing temperature’s magnitude is the more optimum is the turbine efficiency which leads to an overall higher Gas Turbine thermodynamic cycle efficiency.

Thus, the author’s effort lies in the synergy or rather the multi-physics coupling aspects of the overall higher Gas Turbine thermodynamic cycle efficiency, while simultaneously assessing the associated durability of the hot gas path components.

The author also further assumes in this dissertation that there is no leakage affects and hence leakages are assumed to be a negligible influence on the magnitude of the static component exit temperature, and thereby the following physics based mathematical expression holds:

(6.1) Mathematical formulations depicting overall discipline synergy for

Response surface-1 stage thermal efficiency

“T-CV₁, out” is the total temperature at the firing plane. However note that “T-CV₁, out” is expressed as total temperature hence the actual hot gas path temperature at the firing plane is influenced by the fluid dynamics recovery effects hence the temperature at the firing plane should be the recovery temperature which is substituted in the equation for “T-CV₁, out” and thereby “T-CV₁, out” is now converted to T-Static and the recovery temperature is defined to be as follows:

$$\bullet \quad T_{rec} = \left\{ \left[\frac{T_t}{\left(1 + \frac{(\gamma-1)M^2}{2} \right)} \right] + \left[1 + \frac{(\gamma R M^2)}{2 C_p} \right] \right\} \quad 6-0$$

Nomenclature:

- $T_{rec} \Rightarrow$ Gas path fluid medium recovery temperature based on Prandtl number recovery factor.
- $r \Rightarrow$ Recovery factor
- $C_p \Rightarrow$ Specific heat at constant temperature
- $M \Rightarrow$ Mach number at the location of interest i.e., firing plane
- $\gamma \Rightarrow$ Gamma, specific heat ratio
- $R \Rightarrow$ Gas constant
- $T_t \Rightarrow$ Total temperature at firing plane prior to any mixing with leakage flow or any other parasitic flows.

Hence:

T, CV_{1, out} =

$$\begin{aligned}
 & \left(\left\{ \frac{M, NAt \sqrt{\frac{\gamma g c}{R}}}{\left[1 + \frac{\gamma-1}{2} * M, NAt^2 \right]^{\frac{\gamma+1}{2(\gamma-1)}}} \right\} (AN, 1At \left(\frac{Pt}{\sqrt{Tt}} \right)) (Cp, avg) (Trecavg) + \right. \\
 & \left. \left(\left\{ \frac{(M\#fh) \sqrt{\frac{\gamma g c}{R}}}{\left[1 + 1/2(\gamma-1)(M\#fh)^2 \right]^{\frac{(\gamma+1)}{2(\gamma-1)}}} \right\} \left(\frac{(Cd(Ac).Pex_3)}{\sqrt{Tmexcv_3}} \right) (Cp, avg) (TFHout) / \right. \\
 & (Cp, avg) \left(\left\{ \frac{M, NAt \sqrt{\frac{\gamma g c}{R}}}{\left[1 + \frac{\gamma-1}{2} * M, NAt^2 \right]^{\frac{\gamma+1}{2(\gamma-1)}}} \right\} (AN, 1At \left(\frac{Pt}{\sqrt{Tt}} \right)) + \right. \\
 & \left. \left\{ \frac{(M\#fh) \sqrt{\frac{\gamma g c}{R}}}{\left[1 + 1/2(\gamma-1)(M\#fh)^2 \right]^{\frac{(\gamma+1)}{2(\gamma-1)}}} \right\} \left(\frac{(Cd(Ac).Pex_3)}{\sqrt{Tmexcv_3}} \right) \right) \quad 6-1
 \end{aligned}$$

Now we embark on establishing the Unified Gas Turbine “HPT” theory.

As:

$$\bullet \quad \dot{W}, N1At = \left(\left\{ \frac{M, NAt \sqrt{\frac{\gamma g c}{R}}}{\left[1 + \frac{\gamma-1}{2} * M, NAt^2 \right]^{\frac{\gamma+1}{2(\gamma-1)}}} \right\} (AN, 1At \left(\frac{Pt}{\sqrt{Tt}} \right)) \right) \quad 6-2$$

$$\bullet \quad Trec = \left\{ \left[\frac{Tt}{1 + \frac{(\gamma-1)M^2}{2}} \right] + \left[1 + \frac{(r\gamma RM^2)}{2Cp} \right] \right\} \quad 6-3$$

$$\bullet \quad \dot{W}FH, out = \left(\left\{ \frac{(M\#fh) \sqrt{\frac{\gamma g c}{R}}}{\left[1 + 1/2(\gamma-1)(M\#fh)^2 \right]^{\frac{(\gamma+1)}{2(\gamma-1)}}} \right\} \left(\frac{(Cd(Ac).Pex_3)}{\sqrt{Tmexcv_3}} \right) \right) \quad 6-4$$

$$\bullet \quad TFHout = \left\{ \frac{\left[\frac{HAsFH(TFHin)}{\ln [(ThsFH - TFHout) / (ThsFH - TFHin)]} \right] + [\dot{W}FH(Cp)(TFHin)]}{\left[\frac{HAsFH}{\ln [(ThsFH - TFHout) / (ThsFH - TFHin)]} + \dot{W}FH * Cp \right]} \right\} \quad 6-5$$

- HAsFH= This parameter is the through cooling hole internal heat transfer coefficient based upon the internal hole geometry surface area and aligned to the Dittus-Boelter heat transfer Nusselt number for smooth ducts.

6-5A

For simplicity purposes for further physics based mathematical derivations/formulations;

Let:

$$\alpha = (\dot{W}, N1At)(Cp) \left(\left[\frac{T_t}{1 + \frac{(\gamma-1)M^2}{2}} \right] + \left[1 + \frac{M^2(r\gamma RM^2)}{2Cp} \right] \right) \quad 6-6$$

$$\Omega = (\dot{W}_{FH, out}) (Cp) \left\{ \frac{\left[\frac{HAsFH(TFHin)}{\ln [(ThsFH - TFHout) / (ThsFH - TFHin)] + \dot{W}_{FH} * Cp} \right] + [\dot{W}_{FH}(Cp)(TFHin)]}{[(HAsFH / \ln [(ThsFH - TFHout) / (ThsFH - TFHin)] + \dot{W}_{FH} * Cp)] + \dot{W}_{FH} * Cp} \right\}$$

6-7

$$\Delta = (Cp) \left\{ \dot{W}, N1At + \left(\frac{(M\#fh) \sqrt{\frac{\gamma g C}{R}}}{[1 + 1/2(\gamma-1)(M\#fh)^2] \left[\frac{(\gamma+1)}{2(\gamma-1)} \right]} \right) \left(\frac{(Cd(Ac).Pex_3)}{\sqrt{Tmexc_{v3}}} \right) \right\} \quad 6-8$$

& Thus:

$$\bullet \quad T - CV1, out = (\alpha + \Omega) / \Delta \quad 6-9$$

Now from the thermodynamics of the cycle, point of view: For a given combustor exit temperature and assuming negligible transition mouth seal circumferential leakage, the combustor exit temperature = T_t , defined at the location of the inlet plane of the high-pressure turbine static component, i.e., stage 1 nozzle. Hence, if no coolant is mixed with the external gas path stream then the fundamental physics dictates that the following mathematical expression is true.

$$\bullet \quad [T_{t2} = T_{t1}] \quad 6-10$$

However, if any coolant medium mixes with the external gas path stream then the fundamental physics dictates that the following mathematical expression is true.

$$\bullet \quad [T_{t2} < T_{t1}] \Rightarrow \text{This is due to the mixing and eventual dilution of the external hot gas path stream.}$$

&

- $T_{t_2} = T_{CV1, out} = (\alpha + \Omega) / \Delta$ 6-11

& Now let

- $(\alpha + \Omega) / \Delta = T\Theta_2$ 6-12

Therefore:

- $T\Theta_2$ = Total temperature at station (2), AK.A Enthalpy extraction Temperature at station 2.

Based on the formulations resulting from the velocity triangle assessments earlier derived; the temperature $T\Theta_2$ will now influence all subsequent station parameters evaluations.

Hence, from the preceding section on the derivations for the HPT Stage, adiabatic efficiency point of view; we now have the following:

As depicted in the earlier sections, the author here forth applies the above equation for Turbine efficiency η_t , by taking into account the cooled turbine physics implementation.

Where: From the Figure 3.1

- T_{t_1} = Given combustor exit temperature 6-13

- $T_{t_3} = T_{t_2} - \omega r(v_2 + v_3) / gcp$ 6-14

- $T_{t_2} = T\Theta_2$ = Total temperature at station (2), AK.A Enthalpy Extraction at station 2.

- $T_{t_3} = T\Theta_2 - \omega r(v_2 + v_3) / gcp$ 6-15

Where:

- ω = Turbine RPM

- r = Radis from engine centerline
- ωr = Given input parameters
- v_2 = Tangential component of the velocity at the Nozzle exit
- v_3 = Tangential component of the velocity at the blade exit
- α_2 = Given stationary component exit angle

$$v_2 = (M_2\#) (\sqrt{\gamma g c R T_{s_2}}) (\sin \alpha_2) \quad 6-16$$

Hence:

$$T_{t_3} = \{T\theta_2 - \omega r / g C_p [(M_2\#) (\sqrt{\gamma g c R T_{s_2}}) (\sin \alpha_2)]\}$$

Where:

$$T_{s_2} = \frac{T\theta_2}{1 + \frac{\gamma - 1}{2} M_2^2} \quad 6-17$$

$$T_{t_3} = \{T\theta_2 - \omega r / g C_p [(M_2\#) (\sqrt{\gamma g c R}) (\frac{T\theta_2}{1 + \frac{\gamma - 1}{2} M_2^2}) (\sin \alpha_2)]\} \quad 6-18$$

From an overall synergistically coupled formulation we can now depict the High-Pressure Turbine High-Pressure section, Thermal efficiency based on the following mathematical expression:

In reference to the derived Unified High Pressure Turbine formulation and process, accompanied with cooling streams, the Actual work and ideal work included into the High-Pressure Turbine Thermal efficiency formulation is as follows:

$$\text{As } \eta_{\text{thermal}} = \frac{\text{Work Actual}}{\text{Work Ideal}}$$

Hence: Once again Referring to Equation 3-25 derived earlier and shown below; and superimposing the thermodynamic state points in Figure 5.1 hence referring to the actual control volume of this dissertation with the derived key parameters aligned to the control volume, yields the following equation:

$\eta_t - \text{thermal} =$

$$\frac{\{Cp_{gt}[Tt_1 - \{(\alpha + \Omega)/\Delta - \omega r/gCp[(M_2\#)(\sqrt{\gamma}gc/R)(\frac{(\alpha + \Omega)/\Delta}{1 + \frac{\gamma-1}{2}M_2^2})(\sin\alpha_2)\}]\} + Cp_c[T\theta_2 - Tt_1(Pt_3/Pt_1)^{\frac{\gamma-1}{\gamma}}]\}}{Cp_{gt}Tt_1[1 - (Pt_3/Pt_1)^{\frac{\gamma-1}{\gamma}}] + \{Cp_c(T\theta_2)[1 - (\frac{P_2t(\frac{Tt_3}{Tt_2})^{\gamma/(\gamma-1)}}{Pt_1})^{\frac{\gamma-1}{\gamma}}]\}} \quad 6-19$$

However the above equation is still subtly devoid of the overall influence of the mass fractions of the two mixing streams; and hence now the author will include the necessary mass fractions of the two mixing streams (i.e. gas path flow and coolant fluid medium) as stated earlier in section 3, we now, from a physics based mathematical variable definition, have the following work related terms reflecting the two mixing streams mass fractions, coupled to the selected control volume interface temperatures, external gas path and coolant side heat transfer, cooling geometry domain, and work extraction terms based on the influence of the two streams.

Where Work Actual is derived as the following equation:

$$W_{\text{actual}} = \{1 - [(cpr)(Re, \text{gas})^{-\frac{1}{5}} / (Re, \text{cool})^{-\frac{1}{5}}] \left(\left[\frac{Tt}{1 + \frac{(\gamma-1)M^2}{2}} \right] + \left[1 + \frac{(r\gamma RM^2)}{2Cp} \right] \right), \text{avg} -$$

$$T, \text{hotm}) / (T, \text{coolm} - 1/2(TCDT +$$

$$\frac{(HAsFH)(TFHin)/\dot{m}fh + \left(\frac{(M, fh) \left(\sqrt{\frac{\gamma gc}{R}} \right) \left[\frac{(Cd.Ac)(Pexcv3)}{\sqrt{Texcv3}} \right]}{\left(\frac{1}{2(\gamma-1)M^{\#}fh^2} \right)} \right) (\bar{Cp})(TFHin)}{(HAsFH)/\dot{m}fh + \left(\frac{(M, fh) \left(\sqrt{\frac{\gamma gc}{R}} \right) \left[\frac{(Cd.Ac)(Pexcv3)}{\sqrt{Texcv3}} \right]}{\left(\frac{1}{2(\gamma-1)M^{\#}fh^2} \right)} \right) (\bar{Cp})} \right) [(cpg)(Tt_1 - (T\theta_2 -$$

$$\omega r/gCp[(M_2\#)(\sqrt{\gamma}gc/R)(\frac{T\theta^2}{1 + \frac{\gamma-1}{2}M^2})(\sin\alpha_2)] + \{[(cpc)(cpr)(Re, \text{gas})^{-\frac{1}{5}}/$$

$$Re\#cool^{-\frac{1}{5}}] \left(\left[\frac{Tt}{1 + \frac{(\gamma-1)M^2}{2}} \right] + \left[1 + \frac{(r\gamma RM^2)}{2Cp} \right] \right), \text{avg} - T, \text{hotm}) / (T, \text{coolm} - 1/2(TCDT +$$

$$\frac{(HAsFH)(TFHin))/\dot{m}fh + \left(\frac{(M, fh) \left(\sqrt{\frac{\gamma g C}{R}} \right) \left[\frac{(Cd.Ac)(Pexcv3)}{\sqrt{Texcv3}} \right]}{\left(\frac{1}{2(\gamma-1)M^{\#}fh^2} \right)} \right) (\overline{Cp})(TFHin)}{(HAsFH)/\dot{m}fh + \frac{(M, fh) \left(\sqrt{\frac{\gamma g C}{R}} \right) \left[\frac{(Cd.Ac)(Pexcv3)}{\sqrt{Texcv3}} \right]}{\left(\frac{1}{2(\gamma-1)M^{\#}fh^2} \right)} (\overline{Cp})} \left[\left(\frac{\alpha + \Omega}{\Delta} \right) - (T\theta_2 - \right.$$

$$\left. \omega r/gCp[(M_2\#) (\sqrt{\gamma g C/R}) \left(\frac{T\theta_2}{1 + \frac{\gamma-1}{2} M_2^2} \right) (\sin \alpha_2)) \right] \quad 6-20$$

And the Where Work Ideal is derived as the following equation:

$$W_{ideal} = \{ [1 - (cpr)(Re, gas)^{-\frac{1}{5}} / (Re, cool)^{-\frac{1}{5}}] \left(\left[\frac{T_t}{1 + \frac{(\gamma-1)M^2}{2}} \right] + \left[1 + \frac{(r\gamma RM^2)}{2Cp} \right] \right) \}, avg -$$

$$T, hotm) / (T, coolm - 1/2(TCDT +$$

$$\frac{(HAsFH)(TFHin))/\dot{m}fh + \left(\frac{(M, fh) \left(\sqrt{\frac{\gamma g C}{R}} \right) \left[\frac{(Cd.Ac)(Pexcv3)}{\sqrt{Texcv3}} \right]}{\left(\frac{1}{2(\gamma-1)M^{\#}fh^2} \right)} \right) (\overline{Cp})(TFHin)}{(HAsFH)/\dot{m}fh + \frac{(M, fh) \left(\sqrt{\frac{\gamma g C}{R}} \right) \left[\frac{(Cd.Ac)(Pexcv3)}{\sqrt{Texcv3}} \right]}{\left(\frac{1}{2(\gamma-1)M^{\#}fh^2} \right)} (\overline{Cp})} \left[(cpg)(Tt_1) + \right.$$

$$\left. [(cpr)(Re, gas)^{-\frac{1}{5}} / (Re\#cool)^{-\frac{1}{5}}] \left(\left[\frac{T_t}{1 + \frac{(\gamma-1)M^2}{2}} \right] + \left[1 + \frac{(r\gamma RM^2)}{2Cp} \right] \right) \right\}, avg - T, hotm) /$$

$$(T, coolm - 1/2(TCDT +$$

$$\frac{(HAsFH)(TFHin))/\dot{m}fh + \left(\frac{(M, fh) \left(\sqrt{\frac{\gamma g C}{R}} \right) \left[\frac{(Cd.Ac)(Pexcv3)}{\sqrt{Texcv3}} \right]}{\left(\frac{1}{2(\gamma-1)M^{\#}fh^2} \right)} \right) (\overline{Cp})(TFHin)}{(HAsFH)/\dot{m}fh + \frac{(M, fh) \left(\sqrt{\frac{\gamma g C}{R}} \right) \left[\frac{(Cd.Ac)(Pexcv3)}{\sqrt{Texcv3}} \right]}{\left(\frac{1}{2(\gamma-1)M^{\#}fh^2} \right)} (\overline{Cp})} \left[(cpc) \left[\frac{(\alpha + \Omega)}{\Delta} \right] [1 - (1 - \right.$$

$$(\prod t)^{\gamma-1/\gamma}) \} \quad 6-21$$

At this point equations 6-19A & 6-20 derived above; include the two mixing streams and also included is the overall synergistic factors involving the Thermal efficiency “η,thermal”, such as the Work Actual & Work Ideal for the High-Pressure turbine is now

coupled with the associated disciplines involving the pertinent sciences of Thermodynamics “cycle parameters” ; one dimensional mean line Aerodynamics , Turbine external gas path heat transfer, Turbine component cooling internal heat transfer and associated fluid dynamics, and finally the overall durability of the component, i.e. the control volume interface temperatures respectively.

Now we also make the underlying assumption that the $PT_2 = PT_1$; even though due to the coolant fluid emanating out into the external hot gas path will disrupt the flow field and hence alter the external gas path boundary layer, Total Pressure conditions etc. However, for this dissertation I the author shall assume that this is negligible hence $PT_2 = PT_1$; & PT_1 is a given input condition.

Therefore:

$$\bullet \quad Pt_3 = Pt_2 \left(\frac{T_{t3}}{T_{t2}} \right)^{\frac{\gamma}{\gamma-1}} \quad 6-22$$

Hence if $PT_2 = PT_1$, then by direct substitution we have the following mathematical expression:

$$\bullet \quad Pt_3 = Pt_1 \left(\frac{T_{t3}}{T_{t2}} \right)^{\frac{\gamma}{\gamma-1}}$$

$$\bullet \quad \Pi_t = \left(\frac{Pt_3}{Pt_1} \right)^{\frac{\gamma}{\gamma-1}} \text{ Turbine Pressure ratio} \quad 6-23$$

Where:

- $Pt_1 \Rightarrow$ Is a thermodynamic property defined to be at inlet plane of the Stage (1) Nozzle, which is also defined as the combustor exit plane of the transition piece or the combustor liner exit plane location.

In conclusion the Author Sanjay Chopra has mathematically derived a unique physics based coupled formulation based on the Work actual and the Work ideal and applied the

resulting formulations toward the computation for the Unified High Pressure Turbine efficiency and as mentioned previously this process couples the basic fundamental physics involving the thermodynamics, gas path state point locations, one dimensional aerodynamics, component interface resistance geometries and associated resistances temperatures , external and internal fluid and heat transfer physics and ultimately being aligned to the overall stage efficiency parameter and also the durability of the part under consideration.

The UNIFIED HIGH PRESSURE TURBINE EQUATION (UHPT) Is as follows:

In summary, leveraging from the equations depicting the actual work and ideal work, including mixing of the two streams with the associated mass fractions (gas & coolant streams); and along with mathematical simplification, the following Unified High Pressure Turbine efficiency is derived based on the thermodynamic state points depicted in Figure 5.1:

Response surface (1) Unified High Pressure Turbine (UHPT) Transfer Equation (1)

$\eta_{t, \text{HPT}} =$

$$\left(\frac{\left(\frac{M_{\text{NAt}} \sqrt{\frac{\gamma g_c}{R}}}{\left[1 + \frac{\gamma-1}{2} M_{\text{NAt}}^2 \right]^{\frac{\gamma+1}{2(\gamma-1)}}} \right) \left(AN_{1\text{At}} \left(\frac{P_t}{\sqrt{T_t}} \right) \right)}{\dot{W}_{\text{FH,out}}} \right) \left(c_p c \left(\frac{(\alpha + \Omega)}{\Delta} \right) \left[c_p c \left(\frac{\left(\frac{M_{\text{NAt}} \sqrt{\frac{\gamma g_c}{R}}}{\left[1 + \frac{\gamma-1}{2} M_{\text{NAt}}^2 \right]^{\frac{\gamma+1}{2(\gamma-1)}}} \right) \left(AN_{1\text{At}} \left(\frac{P_t}{\sqrt{T_t}} \right) \right)}{\dot{W}_{\text{FH,out}}} \right) \right. \right. \right. \\ \left. \left. \left. + \left(1 - \left(\frac{\dot{W}_{\text{N1At}}}{\dot{W}_{\text{FH,out}}} \right) C_{pg} \right) + \left[1 - \left(\frac{\dot{W}_{\text{N1At}}}{\dot{W}_{\text{FH,out}}} \right) (C_{pg})(T_{t1}) \right] \right] \right) /$$

$$\begin{aligned}
& \left\{ \left(1 - \frac{\left(\left(\frac{M, NAt \sqrt{\frac{\gamma g c}{R}}}{\left[1 + \frac{\gamma - 1}{2} * M, NAt^2 \right]^{\frac{\gamma + 1}{2(\gamma - 1)}}} \right) (AN, 1At(\frac{Pt}{\sqrt{Tt}})) \right)}{\dot{W}FH, out} \right) (Cpg)(Tt_1) \right. \\
& + \left. \frac{\left(\left(\frac{M, NAt \sqrt{\frac{\gamma g c}{R}}}{\left[1 + \frac{\gamma - 1}{2} * M, NAt^2 \right]^{\frac{\gamma + 1}{2(\gamma - 1)}}} \right) (AN, 1At(\frac{Pt}{\sqrt{Tt}})) \right)}{\dot{W}FH, out} \right) \left((cpc) \left(\frac{(\alpha + \Omega)}{\Delta} \right) \right) \\
& \left[1 - \left(\frac{P_2 t \left(\frac{Tt_3}{Tt_2} \right)^{\gamma/(\gamma - 1)}}{Pt_1} \right)^{\frac{\gamma - 1}{\gamma}} \right] \}
\end{aligned} \tag{6-24}$$

(6.2) Response Surface-2: Aligning unified HPT formulation to the Stress Field

In this chapter the author introduces a multiple response surface approach by Coupling of the UHPT mathematical expression to the overall structural integrity or the durability of the component under consideration via a rigorous mathematical evaluation.

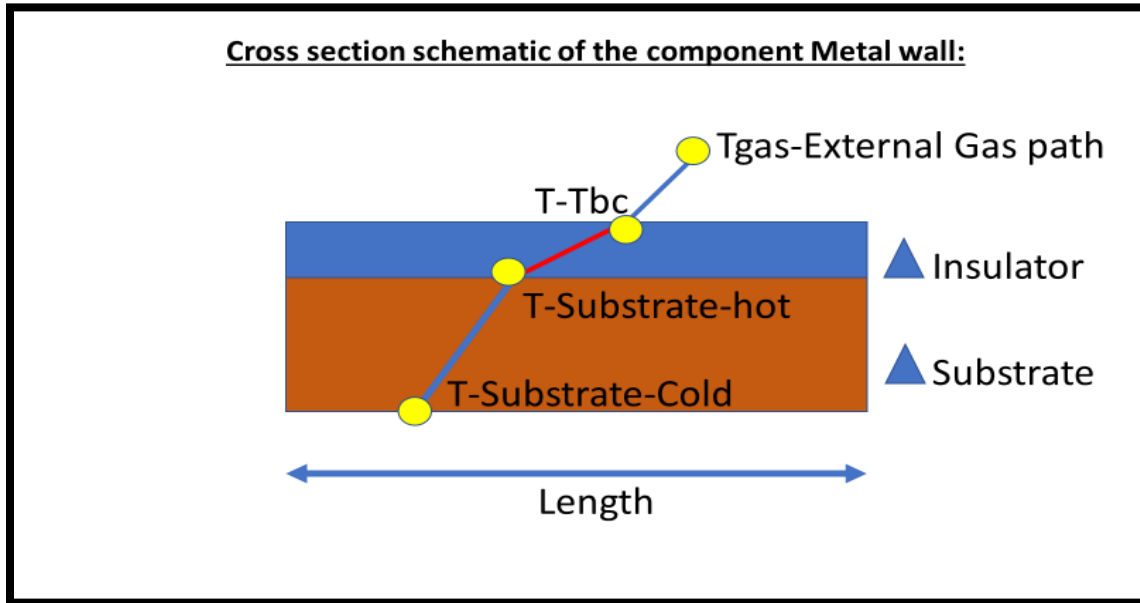


Figure 6.1 Cross section assumed for Substrate undergoing thermal stress

For the purpose of this dissertation simplification of the following statements will be introduced: For a stationary part with zero rotation the overall parameters influencing the durability of the part is assumed as the following: Please note there are other failure mechanisms as well however for this dissertation only the following will be evaluated. In this dissertation only the stationary part will be assessed and coupled to the overall UHPT equation.

- **Thermal Stress**
- **Temperature differentials**

In this dissertation the author will be evaluating as aforementioned the one-dimensional thermal stress induced across the metal due to being subjected by both the external conditions and internal conditions as well.

To better understand the physics of the overall stress field coupled with the corresponding strain and temperature parameters, the author derives the stress equations

of equilibrium, coupled to the net axial strains and finally the associated temperature effects.[24],[25],[26],[27]

Derivation of the stress equations of equilibrium:

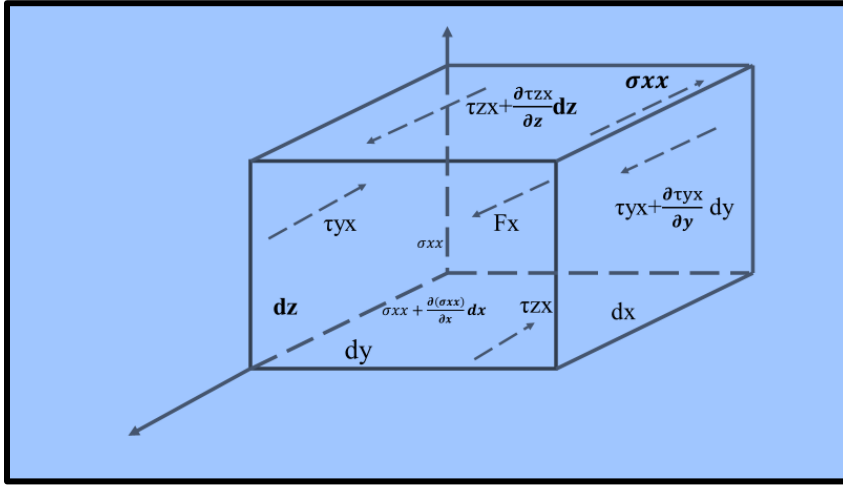


Figure 6.2 Overall Stress Field description

Figure 6.2 above represents a localized minute element extracted from the body of a control volume depicting the stresses imposed in the axial or the X-Direction.

Within a body subjected to body and surface loads or forces, resulting stresses of various magnitudes and associated vector directions are developed and hence produced throughout the given body under consideration. However, the Physics indicates that the distribution of the stresses should be acting in such a manner so that the overall equilibrium or balance is maintained throughout.

Referring to the Figure 6.2; only the associated body forces and the corresponding stress components are included in the X-direction; however, in a similar fashion component do exist and also act similarly in the Y & Z direction as well. These stresses illustrated are assumed to be averaged values at each face of the element. [25B]

Mathematical implementation: (Reference to figure 6.2), Here the author leverages from his graduate studies from reference [24]

- $\sum F_x = 0$; Summation of the forces acting in the axial or X – direction.
- $\left\{ \left[\sigma_{xx} + \frac{\partial(\sigma_{xx})}{\partial x} dx - \sigma_{xx} \right] dydz + \left[\tau_{yx} + \frac{\partial\tau_{yx}}{\partial y} dy - \tau_{yx} \right] dx dz + \left[\tau_{zx} + \frac{\partial\tau_{zx}}{\partial z} dz - \tau_{zx} \right] dx dy + F_x dx dy dz = 0 \right\}$ 6-25

Where:

- $\sigma_{xx} \Rightarrow$ Normal Stress
- $\tau_{xy} \Rightarrow$ Shear Stress
- $\partial\tau_{yx}/\partial y \Rightarrow$ Rate of change of the stress w.r.t. "x"
- $[\partial\tau_{yx}/\partial y]dx \Rightarrow$ Amount of change of the stress w.r.t. "x" over a distance of dx.

Now taking the above equation and dividing through dx dy dz yields the following mathematical expression:

- $\{ [\partial(\sigma_{xx})/\partial x - \partial\tau_{yx}/\partial y + \partial\tau_{zx}/\partial z] + F_x = 0 \} \Rightarrow$ In the X – Direction only.

6-26A

By conducting the aforementioned mathematical assessment on the y & z faces in a similar fashion as mathematically conducted earlier the following equations result aligned to the Y & Z directions. Hence the equations of equilibrium for all three faces are the following: [24],[25],[26], [27]

$$(i) \quad \frac{\partial(\sigma_{xx})}{\partial x} - \frac{\partial\tau_{yx}}{\partial y} + \frac{\partial\tau_{zx}}{\partial z} + F_x = 0 \quad 6-26B$$

$$(ii) \quad \frac{\partial(\sigma_{yy})}{\partial y} - \frac{\partial\tau_{xy}}{\partial x} + \frac{\partial\tau_{zy}}{\partial z} + F_y = 0 \quad 6-27$$

$$(iii) \quad \frac{\partial(\sigma_{zz})}{\partial z} - \frac{\partial\tau_{xz}}{\partial x} + \frac{\partial\tau_{yz}}{\partial y} + F_z = 0 \quad 6-28$$

The above matrix depicts the system of equations which are also known as the stress equations of equilibrium where F_x , F_y & F_z are termed as body forces in units of (lb/in-cube); or N/m-cube), in the X, Y & Z directions respectively. [24],[25],[26], [27]

Now that the author through his academic experience has developed the well-known stress equations of equilibrium, and as the equations aforementioned are devoid of the inherent strains in the material. The author will now evaluate the specific strains in the material. To do so we need to comprehend the specific properties of the material.

The initial assumption for this dissertation is that the material acts like an isotropic material, which is the fundamental material characteristics and basically this means that the material properties are uniform in all directions, and that Hooke's law governs the material which signifies that the inherent behavior of the material is linearly elastic.

The aforementioned assumptions are now used [24] by the author of this dissertation, to develop the synergistic aspects or the coupling between the stress and strain within the material body.

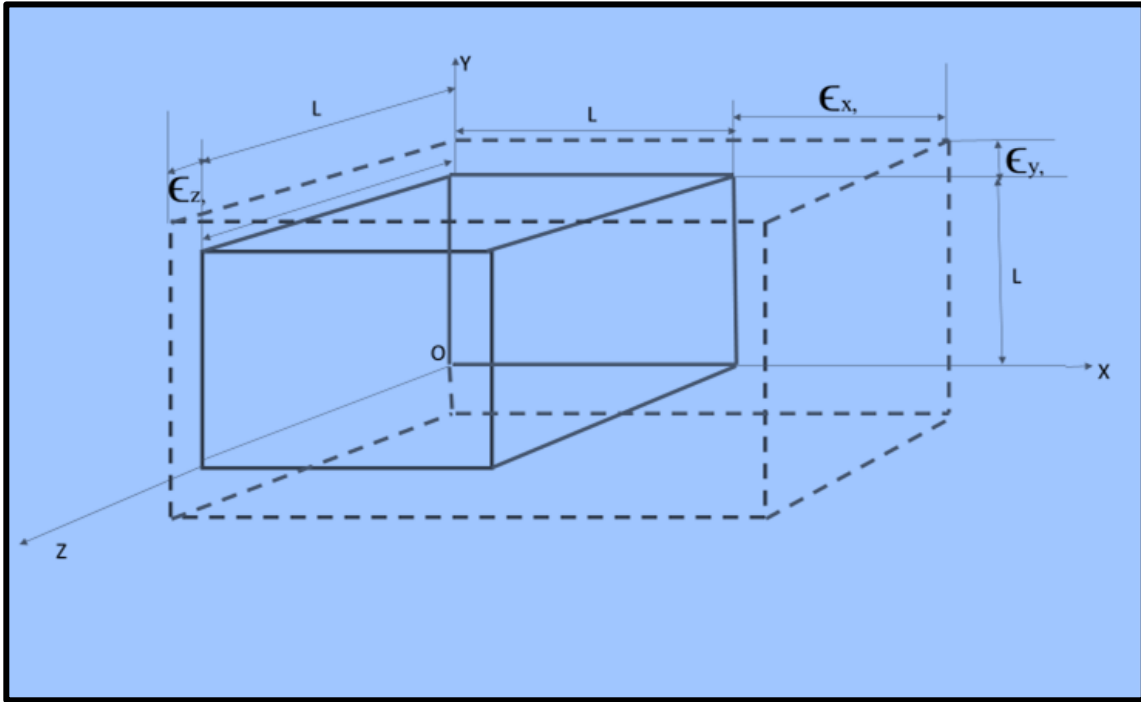


Figure 6.3 Depiction of Normal Strains

In the above figure we depict the normal strains ϵ_x , ϵ_y , ϵ_z , acting upon the infinitesimal small cube with equivalent edge dimensions of unit length. In the figure above all three strains depicted are in the positive direction hence the elongation of the material specimen is assumed.

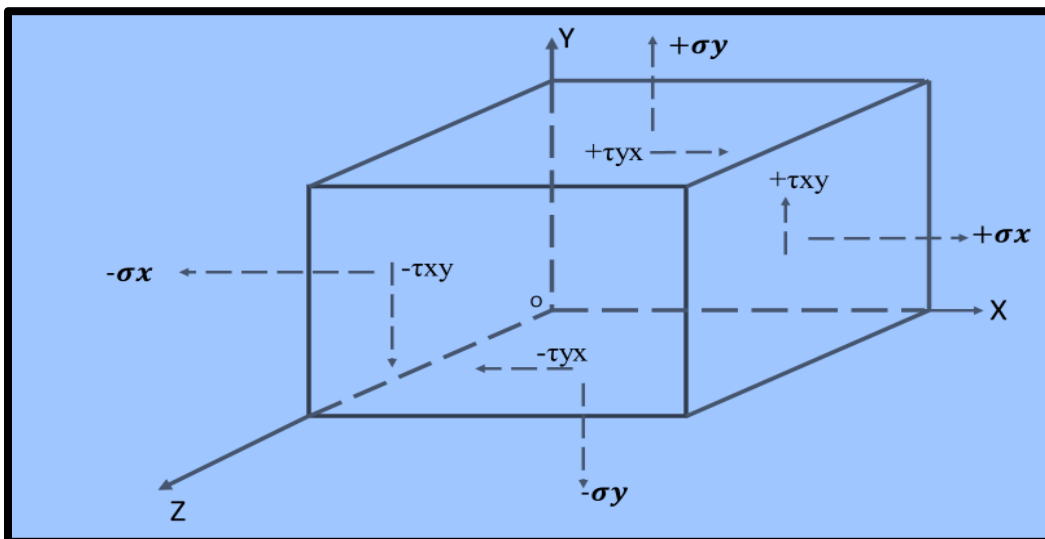


Figure 6.4 Element in plane stress

The above figure depicts the element in plane stress. In plane stress only the x,y faces of the element in the above figure are subjected to stresses and these stresses act parallel to the co-ordinate x,y axis. For example, the stresses σ_x , acts on the X-Face of the element and if +ve then the stress is in tension, and if -ve then in compression.

The shear stress shown in the element above; has or is denoted by two subscripts. [24], [25], [26], [27].

For example: τ_{xy} , where the first subscript x denotes the face on which the stress is acting upon and the second subscript y denotes the direction of the stress on that face.

In order to introduce strains and have the strains be depicted in terms of the corresponding stress we start by superimposing the impact or the effect of the individual stresses.

That is the stress σ_x will be resulting in a strain ϵ_x & Stress σ_y will result in a strain ϵ_y .

Now we introduce the generalized Hooke's law:

Note the stresses in the x-direction (σ_x & $-\sigma_x$) causes a positive strain for the $+\sigma_x = +\epsilon_x$

Therefore: $[\epsilon_x = \sigma_x/E] \Rightarrow$ As Stress/Strain= Modulus of elasticity, as long as it is within the elastic limit.

Thus: Now each of the induced positive stresses in the y & z direction results in a negative strain in the X-direction and this phenomenon is due the poison's effect.

$$(i) \quad \text{Stress } \sigma_x \text{ results in } \epsilon_x = \sigma_x/E \quad 6-29$$

$$(ii) \quad \text{Stress } \sigma_y \text{ results in } \epsilon_x' = -\nu\sigma_y/E \quad 6-30$$

$$(iii) \quad \text{Stress } \sigma_z \text{ results in } \epsilon_x'' = -\nu\sigma_z/E \quad 6-31$$

Hence this results in the following physics based mathematical expressions:

[24],[25],[26], [27]

$$\bullet \quad \epsilon_x = \sigma_x/E - \nu\sigma_y/E - \nu\sigma_z/E \quad 6-32$$

Similarly:

$$\bullet \quad \epsilon_y = \sigma_y/E - \nu\sigma_x/E - \nu\sigma_z/E \quad 6-33$$

&

$$\bullet \quad \epsilon_z = \sigma_z/E - \nu\sigma_y/E - \nu\sigma_z/E - \nu\sigma_x/E \quad 6-34$$

Note: The net axial strains in three dimensional co-ordinate system only assumed for isotropic materials in the elastic range.

Note: In the above Figure 6.4; the shear stress τ_{xy} , results in zero normal strain in the x-direction.

Now that we have derived the net axial normal strains when the stresses are identified; the author of this dissertation will now introduce the relationship of The ***Heat Vector (B)*** to the ***Stress field***.

Introducing thermal stresses and strains:

If a body is allowed to expand or contract without any constraints at its free edges, hence resulting in no stress fields induced in the body under consideration. However, if the associated displacements and corresponding deformations is prevented then the resulting condition will induce stresses in the body, and this is known as thermal stresses and associated strains are called thermal strains.

In reference to the net axial strains Matrix: By applying the plane stress theoretical considerations in the XY Plane it signifies that σ_z , τ_{yz} & τ_{zx} are zero hence the corresponding stress-strain relationship becomes the following:

- $\epsilon_x = \frac{\sigma_x}{E} - \frac{\nu \sigma_y}{E} = \frac{1}{E(\sigma_x - \nu \sigma_y)}$ 6-35

- $\epsilon_y = \frac{\sigma_y}{E} - \frac{\nu \sigma_x}{E} = \frac{1}{E(\sigma_y - \nu \sigma_x)}$ 6-36

The theory of elasticity [33] depicts that if associated support conditions do not resist thermal induced influenced expansions or contractions and assuming that the material of the body is isotropic then the thermal field can be assumed as either constant or linear function hence the normal strains are the following:

- $\epsilon_x = \alpha x(\beta);$ 6-37

- $\epsilon_y = \alpha y(\beta);$ 6-38

Now as previously defined:

- $\epsilon_x = \frac{1}{E}(\sigma_x - \nu \sigma_y)$

- $\epsilon_y = \frac{1}{E}(\sigma_y - \nu \sigma_x)$

We superimpose the normal strains due to the overall heat vector effects in the above equations and these yields:

- $\epsilon_x = \frac{1}{E}(\sigma_x - \nu \sigma_y) + \alpha(\beta)$ 6-39

- $\epsilon_y = \frac{1}{E}(\sigma_y - \nu \sigma_x) + \alpha(\beta)$ 6-40

To further reduce towards simplifying the aforementioned equations the mathematical expressions derived above translate to the following formulations based on the figure Figure 6.4

Assume in the lateral (X) direction the wall is prevented from extending or elongating in the x-direction, hence this constraint yields the following mathematical expression:

- $\epsilon_x = \frac{\sigma_x}{E} - \frac{\nu \sigma_y}{E} + \alpha \beta$ 6-41

Where in the equation above:

- β = Is defined to be the “Heat Vector” or the gradient across the solid structure under consideration. 6-42

$$\bullet \quad \beta = \left\{ \left[\left(\left\{ \left[\frac{T_t}{\left(1 + \frac{(\gamma-1)M^2}{2}\right)} \right] + \left[1 + \frac{(r\gamma RM^2)}{2C_p} \right] \right\} - \frac{(hc) \left\{ \frac{(T_{c_2 cv_3 ex} - T_{c_1 cvin_3})}{\ln \left[\frac{-T_{c_2 cv_3 ex} + T_h}{-T_{c_1 cvin_3} + T_h} \right]} \right\}}{H_g} \right) - \left(\frac{(hc) \left\{ \frac{(T_{c_2 cv_3 ex} - T_{c_1 cvin_3})}{\ln \left[\frac{-T_{c_2 cv_3 ex} + T_h}{-T_{c_1 cvin_3} + T_h} \right]} \right\}}{\frac{\Delta x}{KR_1}} \right) \right] - \left[\left(\left\{ \left[\frac{T_t}{\left(1 + \frac{(\gamma-1)M^2}{2}\right)} \right] + \left[1 + \frac{(r\gamma RM^2)}{2C_p} \right] \right\} - \frac{(hc) \left\{ \frac{(T_{c_2 cv_3 ex} - T_{c_1 cvin_3})}{\ln \left[\frac{-T_{c_2 cv_3 ex} + T_h}{-T_{c_1 cvin_3} + T_h} \right]} \right\}}{H_g} \right) - \left(\frac{(hc) \left\{ \frac{(T_{c_2 cv_3 ex} - T_{c_1 cvin_3})}{\ln \left[\frac{-T_{c_2 cv_3 ex} + T_h}{-T_{c_1 cvin_3} + T_h} \right]} \right\}}{\frac{\Delta x}{KR_1}} \right) - \left(\frac{(hc) \left\{ \frac{(T_{c_2 cv_3 ex} - T_{c_1 cvin_3})}{\ln \left[\frac{-T_{c_2 cv_3 ex} + T_h}{-T_{c_1 cvin_3} + T_h} \right]} \right\}}{\frac{\Delta x}{KR_2}} \right) \right] \right\}$$

The author references the example of the rectangular solid structure with an imposed state of plane stress from Figure 6.1.

The author also assumes that the heat vector ξ be a function of the dimension Y, and independent of the dimensions X & Z.

Now from the previously derived equations for the conditions of equilibrium we assume these conditions of equilibrium are addressed only if we assume that $\sigma_y = \tau_{xy} = 0$ and it is also assumed that σ_x now only depends upon Y.

Now the author makes the assumption based on his academic studies, that compatibility aspects are satisfied and that the one-dimensional thermal loading induced structure can be depicted by the following physics based differential equation:

$$\begin{aligned}
& \bullet \frac{d^2}{dy^2} \left(\sigma x + E \alpha \left\{ \left[\left(\left[\frac{T_t}{\left(1 + \frac{(\gamma-1)M^2}{2} \right)} \right] + \left[1 + \frac{(\gamma RM^2)}{2C_p} \right] \right\} - \frac{(hc) \left\{ \frac{(T_{c2}cv3ex - T_{c1}cvin3)}{\ln \left[\frac{-T_{c2}cv3ex + Th}{-T_{c1}cvin3 + Th} \right]} \right\}}{Hg} \right) - \right. \\
& \left. \left(\frac{(hc) \left\{ \frac{(T_{c2}cv3ex - T_{c1}cvin3)}{\ln \left[\frac{-T_{c2}cv3ex + Th}{-T_{c1}cvin3 + Th} \right]} \right\}}{\frac{\Delta x}{KR1}} \right) \right] - \left[\left(\left[\frac{T_t}{\left(1 + \frac{(\gamma-1)M^2}{2} \right)} \right] + \left[1 + \frac{(\gamma RM^2)}{2C_p} \right] \right\} - \right. \\
& \left. \frac{(hc) \left\{ \frac{(T_{c2}cv3ex - T_{c1}cvin3)}{\ln \left[\frac{-T_{c2}cv3ex + Th}{-T_{c1}cvin3 + Th} \right]} \right\}}{Hg} \right) - \left(\frac{(hc) \left\{ \frac{(T_{c2}cv3ex - T_{c1}cvin3)}{\ln \left[\frac{-T_{c2}cv3ex + Th}{-T_{c1}cvin3 + Th} \right]} \right\}}{\frac{\Delta x}{KR1}} \right) - \right. \\
& \left. \left(\frac{(hc) \left\{ \frac{(T_{c2}cv3ex - T_{c1}cvin3)}{\ln \left[\frac{-T_{c2}cv3ex + Th}{-T_{c1}cvin3 + Th} \right]} \right\}}{\frac{\Delta x}{KR2}} \right) \right] \right\} = 0
\end{aligned} \tag{6-43}$$

Note the above differential equation, based on the authors academic studies that he has referenced is the Airy stress function and also based on the compatibility concept, which basically means that a relationship must exist amongst the strains if the concept of compatibility is to exist, i.e. If a material does not break, then there will be no cracks induced hence no cracks will appear and the displacement field is continuous.

Solving the above differential equation yields the following:

$$\bullet \quad \frac{d^2}{dy^2}(\sigma_X) + \frac{d^2}{dy^2}(E\alpha\left\{\left[\left(\left\{\left[\frac{Tt}{\left(1+\frac{(\gamma-1)M^2}{2}\right)}\right]\right\} + \left[1 + \frac{(r\gamma RM^2)}{2Cp}\right]\right\} - \right. \right. \\ \left. \left. \frac{(hc)\left\{\frac{(Tc_2cv3ex - Tc_1cvin3)}{\ln\left[\frac{-Tc_2cv3ex + Th}{-Tc_1cvin3 + Th}\right]}\right\}}{Hg} - \left(\frac{(hc)\left\{\frac{(Tc_2cv3ex - Tc_1cvin3)}{\ln\left[\frac{-Tc_2cv3ex + Th}{-Tc_1cvin3 + Th}\right]}\right\}}{\frac{\Delta x}{KR1}}\right)\right] - \left[\left(\left\{\left[\frac{Tt}{\left(1+\frac{(\gamma-1)M^2}{2}\right)}\right]\right\} + \left[1 + \frac{(r\gamma RM^2)}{2Cp}\right]\right\} - \frac{(hc)\left\{\frac{(Tc_2cv3ex - Tc_1cvin3)}{\ln\left[\frac{-Tc_2cv3ex + Th}{-Tc_1cvin3 + Th}\right]}\right\}}{Hg} - \left(\frac{(hc)\left\{\frac{(Tc_2cv3ex - Tc_1cvin3)}{\ln\left[\frac{-Tc_2cv3ex + Th}{-Tc_1cvin3 + Th}\right]}\right\}}{\frac{\Delta x}{KR1}}\right) - \right. \right. \\ \left. \left. \left(\frac{(hc)\left\{\frac{(Tc_2cv3ex - Tc_1cvin3)}{\ln\left[\frac{-Tc_2cv3ex + Th}{-Tc_1cvin3 + Th}\right]}\right\}}{\frac{\Delta x}{KR2}}\right)\right\}\right\} = 0$$

$$\bullet \quad \frac{d^2}{dy^2} (\sigma_X) = - \frac{d^2}{dy^2} (E\alpha \left\{ \left[\left(\left[\frac{Tt}{\left(1 + \frac{(\gamma-1)M^2}{2} \right)} \right] + \left[1 + \frac{(\gamma RM^2)}{2Cp} \right] \right) \right\} - \right. \\ \left. \frac{(hc) \left\{ \frac{(Tc_2cv3ex - Tc_1cvin3)}{\ln \left[\frac{-Tc_2cv3ex + Th}{-Tc_1cvin3 + Th} \right]} \right\}}{Hg} - \left(\frac{(hc) \left\{ \frac{(Tc_2cv3ex - Tc_1cvin3)}{\ln \left[\frac{-Tc_2cv3ex + Th}{-Tc_1cvin3 + Th} \right]} \right\}}{\frac{\Delta x}{KR1}} \right) \right] - \left[\left(\left[\frac{Tt}{\left(1 + \frac{(\gamma-1)M^2}{2} \right)} \right] + \left[1 + \right. \right. \right.$$

$$\begin{aligned}
& \left. \left. \left. \left. \frac{(r\gamma RM^2)}{2Cp} \right] \right\} - \frac{(hc) \left\{ \frac{(Tc_2cv3ex - Tc_1cvin3)}{\ln \left[\frac{-Tc_2cv3ex + Th}{-Tc_1cvin3 + Th} \right]} \right\}}{Hg} \right) - \left(\frac{(hc) \left\{ \frac{(Tc_2cv3ex - Tc_1cvin3)}{\ln \left[\frac{-Tc_2cv3ex + Th}{-Tc_1cvin3 + Th} \right]} \right\}}{\frac{\Delta x}{KR1}} \right) - \\
& \left(\frac{(hc) \left\{ \frac{(Tc_2cv3ex - Tc_1cvin3)}{\ln \left[\frac{-Tc_2cv3ex + Th}{-Tc_1cvin3 + Th} \right]} \right\}}{\frac{\Delta x}{KR2}} \right) \Bigg] \Bigg\}
\end{aligned} \tag{6-45}$$

Integrating the above differential equation both sides

$$\begin{aligned}
\bullet \quad \int \frac{d^2}{dy^2}(\sigma x) &= \int \frac{d^2}{dy^2} \left(E\alpha \left\{ \left[\left(\left[\frac{Tt}{\left(1 + \frac{(\gamma-1)M^2}{2} \right)} \right] + \left[1 + \frac{(r\gamma RM^2)}{2Cp} \right] \right\} - \right. \right. \\
& \left. \left. \frac{(hc) \left\{ \frac{(Tc_2cv3ex - Tc_1cvin3)}{\ln \left[\frac{-Tc_2cv3ex + Th}{-Tc_1cvin3 + Th} \right]} \right\}}{Hg} \right) - \left(\frac{(hc) \left\{ \frac{(Tc_2cv3ex - Tc_1cvin3)}{\ln \left[\frac{-Tc_2cv3ex + Th}{-Tc_1cvin3 + Th} \right]} \right\}}{\frac{\Delta x}{KR1}} \right) \right] - \left[\left(\left[\frac{Tt}{\left(1 + \frac{(\gamma-1)M^2}{2} \right)} \right] + \left[1 + \right. \right. \right. \\
& \left. \left. \frac{(r\gamma RM^2)}{2Cp} \right] \right\} - \frac{(hc) \left\{ \frac{(Tc_2cv3ex - Tc_1cvin3)}{\ln \left[\frac{-Tc_2cv3ex + Th}{-Tc_1cvin3 + Th} \right]} \right\}}{Hg} \right) - \left(\frac{(hc) \left\{ \frac{(Tc_2cv3ex - Tc_1cvin3)}{\ln \left[\frac{-Tc_2cv3ex + Th}{-Tc_1cvin3 + Th} \right]} \right\}}{\frac{\Delta x}{KR1}} \right) - \\
& \left. \left. \left(\frac{(hc) \left\{ \frac{(Tc_2cv3ex - Tc_1cvin3)}{\ln \left[\frac{-Tc_2cv3ex + Th}{-Tc_1cvin3 + Th} \right]} \right\}}{\frac{\Delta x}{KR2}} \right) \right] \right\} \Bigg\}
\end{aligned} \tag{6-46}$$

$$\begin{aligned}
\bullet \quad \frac{d}{dy}(\sigma x) = & - \left(E\alpha \left\{ \left[\left(\left[\frac{T_t}{\left(1 + \frac{(\gamma-1)M^2}{2}\right)} \right] + \left[1 + \frac{(r\gamma RM^2)}{2C_p} \right] \right\} - \frac{(hc) \left\{ \frac{(T_{c2}cv3ex - T_{c1}cvin3)}{\ln \left[\frac{-T_{c2}cv3ex + Th}{-T_{c1}cvin3 + Th} \right]} \right\}}{Hg} \right) - \right. \\
& \left(\frac{(hc) \left\{ \frac{(T_{c2}cv3ex - T_{c1}cvin3)}{\ln \left[\frac{-T_{c2}cv3ex + Th}{-T_{c1}cvin3 + Th} \right]} \right\}}{\frac{\Delta x}{KR1}} \right) \left. \right] - \left[\left(\left[\frac{T_t}{\left(1 + \frac{(\gamma-1)M^2}{2}\right)} \right] + \left[1 + \frac{(r\gamma RM^2)}{2C_p} \right] \right\} - \right. \\
& \left. \frac{(hc) \left\{ \frac{(T_{c2}cv3ex - T_{c1}cvin3)}{\ln \left[\frac{-T_{c2}cv3ex + Th}{-T_{c1}cvin3 + Th} \right]} \right\}}{Hg} \right) - \left(\frac{(hc) \left\{ \frac{(T_{c2}cv3ex - T_{c1}cvin3)}{\ln \left[\frac{-T_{c2}cv3ex + Th}{-T_{c1}cvin3 + Th} \right]} \right\}}{\frac{\Delta x}{KR1}} \right) - \\
& \left. \left(\frac{(hc) \left\{ \frac{(T_{c2}cv3ex - T_{c1}cvin3)}{\ln \left[\frac{-T_{c2}cv3ex + Th}{-T_{c1}cvin3 + Th} \right]} \right\}}{\frac{\Delta x}{KR2}} \right) \right\} \right\} \frac{d}{dy} + C1
\end{aligned}$$

6-47

Integrating again yields:

$$\begin{aligned}
\bullet \quad \int \frac{d}{dy}(\sigma x) = & - \left(E\alpha \left\{ \left[\left(\left[\frac{T_t}{\left(1 + \frac{(\gamma-1)M^2}{2}\right)} \right] + \left[1 + \frac{(r\gamma RM^2)}{2C_p} \right] \right\} - \right. \right. \\
& \left. \frac{(hc) \left\{ \frac{(T_{c2}cv3ex - T_{c1}cvin3)}{\ln \left[\frac{-T_{c2}cv3ex + Th}{-T_{c1}cvin3 + Th} \right]} \right\}}{Hg} \right) - \left(\frac{(hc) \left\{ \frac{(T_{c2}cv3ex - T_{c1}cvin3)}{\ln \left[\frac{-T_{c2}cv3ex + Th}{-T_{c1}cvin3 + Th} \right]} \right\}}{\frac{\Delta x}{KR1}} \right) \right] - \left[\left(\left[\frac{T_t}{\left(1 + \frac{(\gamma-1)M^2}{2}\right)} \right] + \left[1 + \right. \right. \right.
\end{aligned}$$

$$\begin{aligned}
& \left. \frac{(r\gamma RM^2)}{2C_p} \right\} - \frac{(hc)\left\{\frac{(T_{c2}cv3ex - T_{c1}cvin3)}{\ln \left[\frac{-T_{c2}cv3ex + Th}{-T_{c1}cvin3 + Th}\right]}\right\}}{Hg} - \left(\frac{\frac{(hc)\left\{\frac{(T_{c2}cv3ex - T_{c1}cvin3)}{\ln \left[\frac{-T_{c2}cv3ex + Th}{-T_{c1}cvin3 + Th}\right]}\right\}}{\frac{\Delta x}{KR1}}}{KR1} \right) - \\
& \left(\frac{(hc)\left\{\frac{(T_{c2}cv3ex - T_{c1}cvin3)}{\ln \left[\frac{-T_{c2}cv3ex + Th}{-T_{c1}cvin3 + Th}\right]}\right\}}{\frac{\Delta x}{KR2}} \right) \left. \right\} \int \frac{d}{dy} + \int C1
\end{aligned} \tag{6-48}$$

$$\begin{aligned}
\bullet \quad \sigma_{thx} = E\alpha \left\{ \left[\left(\left[\frac{T_t}{\left(1 + \frac{(\gamma-1)M^2}{2}\right)} \right] + \left[1 + \frac{(r\gamma RM^2)}{2C_p} \right] \right) - \frac{(hc)\left\{\frac{(T_{c2}cv3ex - T_{c1}cvin3)}{\ln \left[\frac{-T_{c2}cv3ex + Th}{-T_{c1}cvin3 + Th}\right]}\right\}}{Hg} \right] - \right. \\
\left. \left(\frac{(hc)\left\{\frac{(T_{c2}cv3ex - T_{c1}cvin3)}{\ln \left[\frac{-T_{c2}cv3ex + Th}{-T_{c1}cvin3 + Th}\right]}\right\}}{\frac{\Delta x}{KR1}} \right) \right] - \left[\left(\left[\frac{T_t}{\left(1 + \frac{(\gamma-1)M^2}{2}\right)} \right] + \left[1 + \frac{(r\gamma RM^2)}{2C_p} \right] \right) - \right. \\
\left. \frac{(hc)\left\{\frac{(T_{c2}cv3ex - T_{c1}cvin3)}{\ln \left[\frac{-T_{c2}cv3ex + Th}{-T_{c1}cvin3 + Th}\right]}\right\}}{Hg} \right) - \left(\frac{(hc)\left\{\frac{(T_{c2}cv3ex - T_{c1}cvin3)}{\ln \left[\frac{-T_{c2}cv3ex + Th}{-T_{c1}cvin3 + Th}\right]}\right\}}{\frac{\Delta x}{KR1}} \right) - \right. \\
\left. \left(\frac{(hc)\left\{\frac{(T_{c2}cv3ex - T_{c1}cvin3)}{\ln \left[\frac{-T_{c2}cv3ex + Th}{-T_{c1}cvin3 + Th}\right]}\right\}}{\frac{\Delta x}{KR2}} \right) \right] \right\} + C1y + C2y
\end{aligned} \tag{6-49}$$

Where C1 & C2 are the constants of integration. Now we leveraged the previously mentioned assumptions, and that is if the ends of the rectangular structure in the X-Direction are constrained that is it is prevented from elongating i.e., hence not allowed to

deform then the constants of integration C1 & C2 in the following mathematical

equation; $[\sigma_x = -E\alpha \beta + C_1y + C_2]$ becomes $C_1=0$ & $C_2=0$

The response surface (2) or the transfer function reflecting the physical state of the durability of the structure under consideration is the following:

Response surface (2) now becomes the following:

6-50

$$\sigma_{thx} = E\alpha \left\{ \left[\left(\left[\frac{T_t}{\left(1 + \frac{(\gamma-1)M^2}{2}\right)} \right] + \left[1 + \frac{(r\gamma RM^2)}{2C_p} \right] \right) - \frac{(hc) \left\{ \frac{(T_{c2}cv3ex - T_{c1}cvin3)}{\ln \left[\frac{-T_{c2}cv3ex + Th}{-T_{c1}cvin3 + Th} \right]} \right\}}{Hg} \right] - \left(\frac{(hc) \left\{ \frac{(T_{c2}cv3ex - T_{c1}cvin3)}{\ln \left[\frac{-T_{c2}cv3ex + Th}{-T_{c1}cvin3 + Th} \right]} \right\}}{\frac{\Delta x}{KR1}} \right) \right] - \left[\left(\left[\frac{T_t}{\left(1 + \frac{(\gamma-1)M^2}{2}\right)} \right] + \left[1 + \frac{(r\gamma RM^2)}{2C_p} \right] \right) - \frac{(hc) \left\{ \frac{(T_{c2}cv3ex - T_{c1}cvin3)}{\ln \left[\frac{-T_{c2}cv3ex + Th}{-T_{c1}cvin3 + Th} \right]} \right\}}{Hg} \right] - \left(\frac{(hc) \left\{ \frac{(T_{c2}cv3ex - T_{c1}cvin3)}{\ln \left[\frac{-T_{c2}cv3ex + Th}{-T_{c1}cvin3 + Th} \right]} \right\}}{\frac{\Delta x}{KR1}} \right) - \left(\frac{(hc) \left\{ \frac{(T_{c2}cv3ex - T_{c1}cvin3)}{\ln \left[\frac{-T_{c2}cv3ex + Th}{-T_{c1}cvin3 + Th} \right]} \right\}}{\frac{\Delta x}{KR2}} \right) \right] \right\}$$

The above transfer equation integrates the structures material properties, heat loads and associated hat fluxes along with the thermodynamic state points of the turbine stage.

(6.3) Final derived Unified Multi-Physics HPT Equations explanation and application

The two derived transfer functions depicting the overall synergy of the multi-physics coupled solution involving the fundamental disciplines of, aerodynamics, external and internal heat transfer, thermodynamic state points and also the coolant paths, are the following UHPT Transfer functions 1 & 2

Response surface (1) Unified High-Pressure Turbine (UHPT) Transfer Equation

(1):

$\eta_{\text{b HPT}} =$

$$\left\{ \left(\frac{\left(\frac{M, NAt \sqrt{\frac{\gamma g c}{R}}}{\left[1 + \frac{\gamma - 1}{2} * M, NAt^2 \right]^{\frac{\gamma + 1}{2(\gamma - 1)}}} \right) (AN, 1At(\frac{Pt}{\sqrt{Tt}}))}{\dot{W}_{FH, out}} \right) (cpc) \left(\frac{(\alpha + \Omega)}{\Delta} \right) \right.$$

$$\left. [cpc \left(\frac{\left(\frac{M, NAt \sqrt{\frac{\gamma g c}{R}}}{\left[1 + \frac{\gamma - 1}{2} * M, NAt^2 \right]^{\frac{\gamma + 1}{2(\gamma - 1)}}} \right) (AN, 1At(\frac{Pt}{\sqrt{Tt}}))}{\dot{W}_{FH, out}} \right) + \right.$$

$$\left. \left(1 - \left(\frac{\dot{W}, N1At}{\dot{W}_{FH, out}} \right) C_{pg} \right] + \left[1 - \left(\frac{\dot{W}, N1At}{\dot{W}_{FH, out}} \right) (C_{pg})(T_{t1}) \right] \right\} /$$

$$\left\{ \left(1 - \frac{\left(\frac{\left(\frac{M, NAt \sqrt{\frac{\gamma g c}{R}}}{\left[1 + \frac{\gamma - 1}{2} * M, NAt^2 \right]^{\frac{\gamma + 1}{2(\gamma - 1)}}} \right) (AN, 1At(\frac{Pt}{\sqrt{Tt}}))}{\dot{W}_{FH, out}} \right) \right) (C_{pg})(T_{t1}) + \right.$$

$$\left(\frac{\left(\left\{ \frac{M, NAt \sqrt{\frac{\gamma G C}{R}}}{\left[1 + \frac{\gamma - 1}{2} * M, NAt^2 \right]^{\frac{\gamma + 1}{2(\gamma - 1)}}} \right\} (AN, 1At(\frac{Pt}{\sqrt{Tt}})) \right)}{\dot{W}FH, out} \right)$$

$$\left((cpc) \left(\frac{(\alpha + \Omega)}{\Delta} \right) \left[1 - \left(\frac{P_2 t \left(\frac{Tt_3}{Tt_2} \right)^{\gamma/(\gamma - 1)}}{Pt_1} \right)^{\frac{\gamma - 1}{\gamma}} \right] \right\} \quad 6-51$$

Response surface (2) Durability Unified High-Pressure Turbine (UHPT)

Transfer Equation (2):

$$\begin{aligned} \sigma_{thx} = E\alpha \left\{ \left[\left(\left\{ \left[\frac{Tt}{\left(1 + \frac{(\gamma - 1)M^2}{2} \right)} \right] + \left[1 + \frac{(r\gamma RM^2)}{2Cp} \right] \right\} - \frac{(hc) \left\{ \frac{(Tcv3ex - Tcvin3)}{\ln \left[\frac{-Tcv3ex + Th}{-Tcvin3 + Th} \right]} \right\}}{Hg} \right) - \right. \right. \\ \left. \left(\frac{(hc) \left\{ \frac{(Tcv3ex - Tcvin3)}{\ln \left[\frac{-Tcv3ex + Th}{-Tcvin3 + Th} \right]} \right\}}{\frac{\Delta x}{KR1}} \right) \right] - \left[\left(\left\{ \left[\frac{Tt}{\left(1 + \frac{(\gamma - 1)M^2}{2} \right)} \right] + \left[1 + \frac{(r\gamma RM^2)}{2Cp} \right] \right\} - \frac{(hc) \left\{ \frac{(Tcv3ex - Tcvin3)}{\ln \left[\frac{-Tcv3ex + Th}{-Tcvin3 + Th} \right]} \right\}}{Hg} \right) - \right. \\ \left. \left(\frac{(hc) \left\{ \frac{(Tcv3ex - Tcvin3)}{\ln \left[\frac{-Tcv3ex + Th}{-Tcvin3 + Th} \right]} \right\}}{\frac{\Delta x}{KR1}} \right) - \left(\frac{(hc) \left\{ \frac{(Tcv3ex - Tcvin3)}{\ln \left[\frac{-Tcv3ex + Th}{-Tcvin3 + Th} \right]} \right\}}{\frac{\Delta x}{KR2}} \right) \right] \right\} \quad 6-52 \end{aligned}$$

Note the independent variables imbedded in UHPT Response surface Transfer equation (2), are ascertained by solving UHPT Response surface Transfer equation (1), as the corresponding heat loads are obtained by solving Response surface Transfer equation (1).

CHAPTER 7:

VALIDATION OF THE ANALYTICAL BASED UNIFIED HIGH-PRESSURE TURBINE COMPARED TO LITERATURE RESEARCH

(7.1) Gas Turbine Overall Thermal Efficiency (UHPT Process Vs. GT World Simple Cycle Specifications Efficiency data. [51]

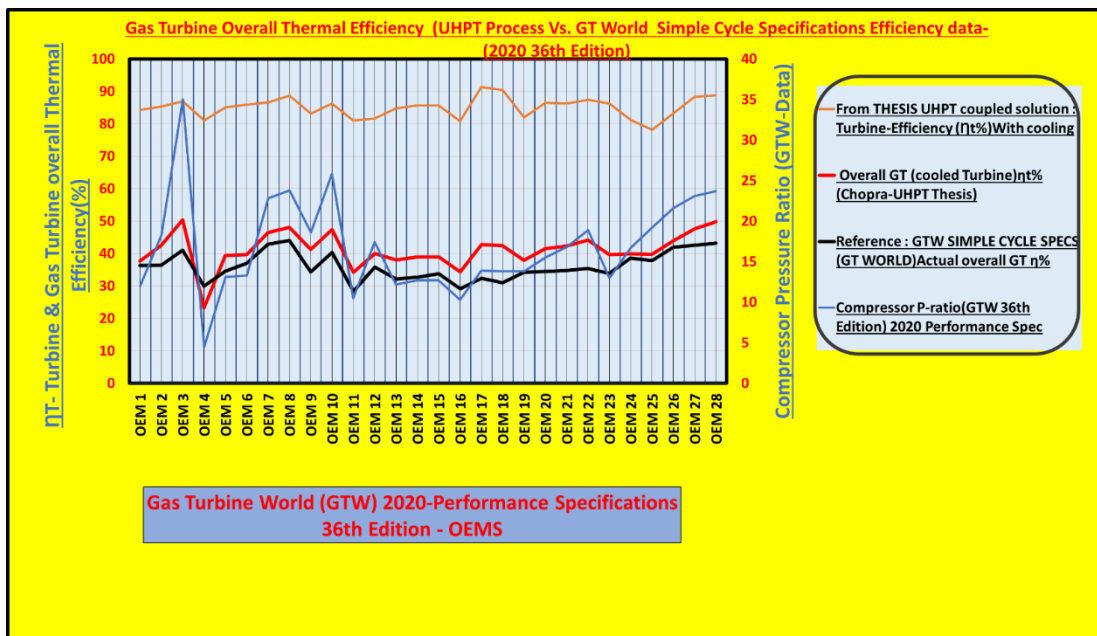


Figure 7.1 Gas Turbine Overall Thermal Efficiency (UHPT Process Vs. GT World) Simple Cycle Specifications Efficiency data- (2020 36th Edition)-Literature Search

**(7.2) Gas Turbine Trends - Comparing GTW Compressor Ratio Data Vs. UHPT
process High Pressure Turbine Temperature Characteristics**

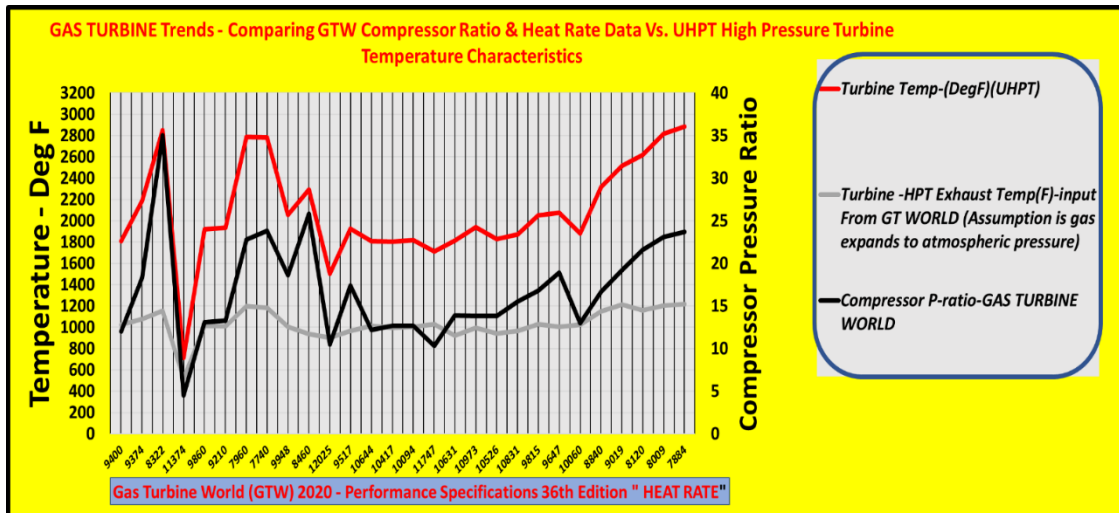


Figure 7.2 Gas Turbine Overall Thermal Efficiency (UHPT Process Vs. GT World)
Simple Cycle Turbine Temperature Characteristics- aligned to Engine Heat Rate
Specifications Efficiency data- (2020 36th Edition) Literature Search

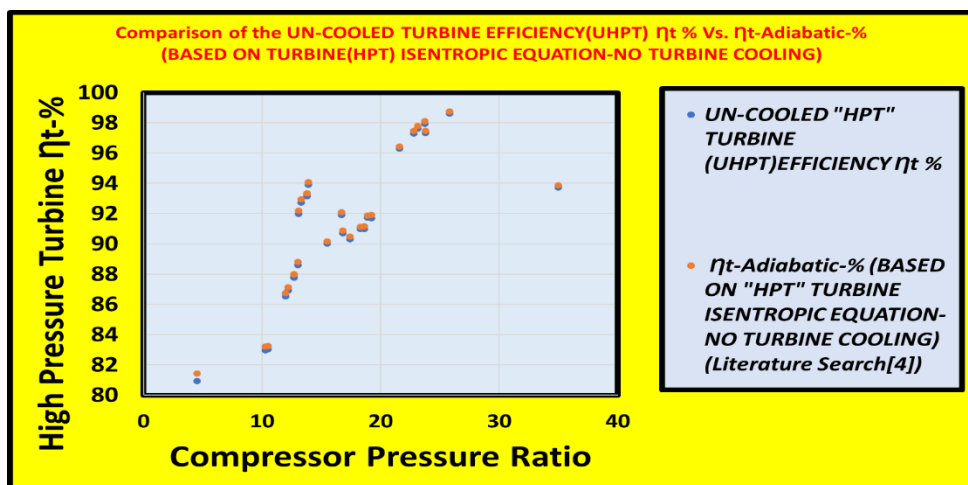
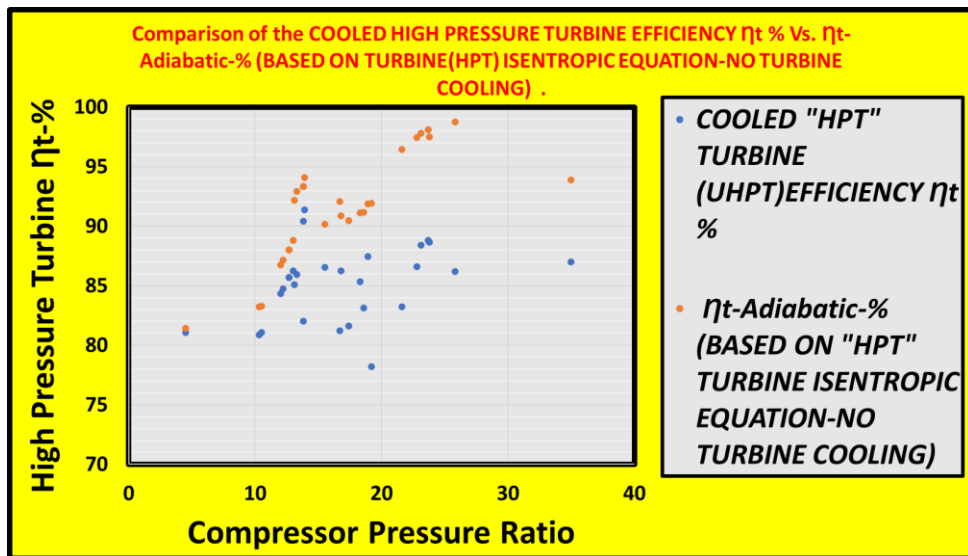


Figure 7.3 Comparison of the Cooled Turbine Efficiency (UHPT Formulation) Vs. The Turbine Isentropic Formulation without Cooling & also Comparison of the UHPT (No Cooling) Vs. Turbine Isentropic Formulation without Cooling

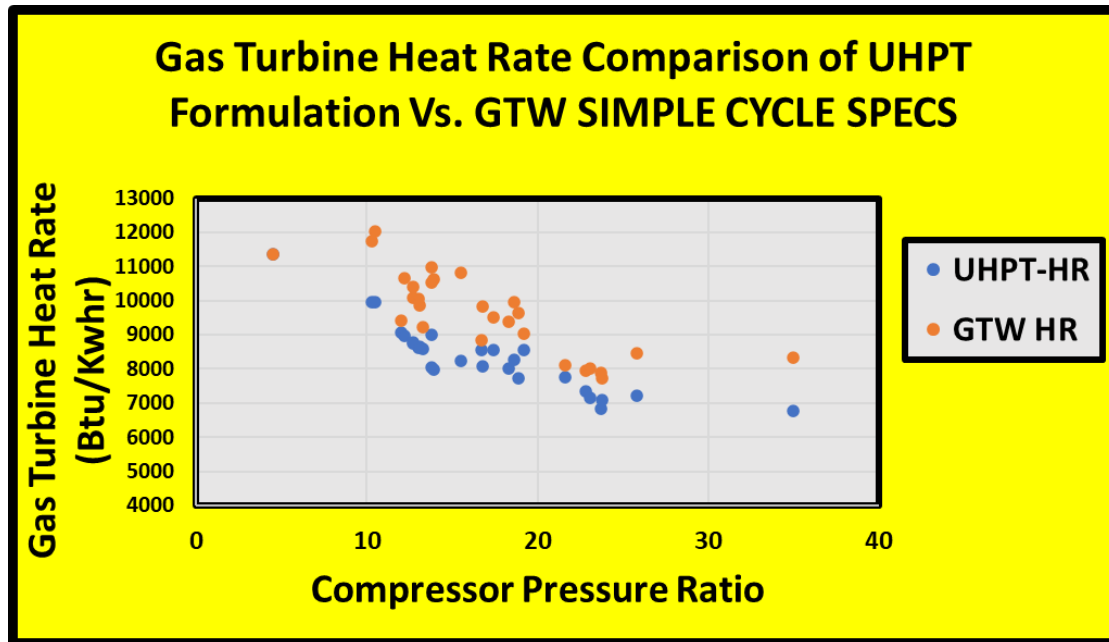


Figure 7.4 Comparison of Gas Turbine Heat Rate based on the UHPT Formulation Vs. GTW Simple Cycle Specifications- Literature Search

CHAPTER 8:

HIGH PRESSURE TURBINE; UHPT PROCESS SENSITIVITY OF THE KEY PARAMETERS ASSESSMENT

(8.1) Sensitivity of Temperature to Cooled Turbine Stage Efficiency η_t , for
various Compressor Pressure Ratio and Gas Turbine Exhaust Temperature ranges

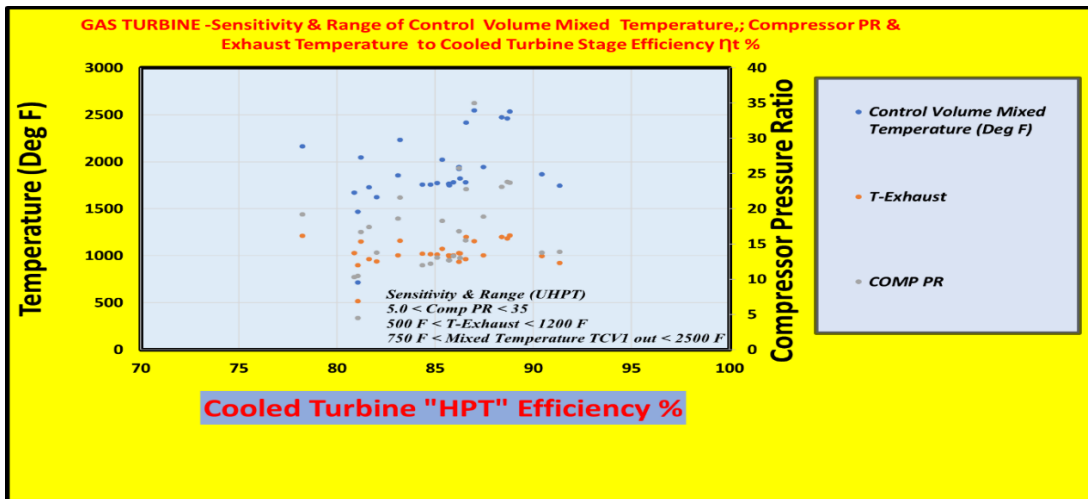


Figure 8.1 Gas turbine – Sensitivity of Control Volume Mixed Temperature, to cooled turbine stage efficiency for range of Compressor Pressure Ratio & Turbine Exhaust Temperature

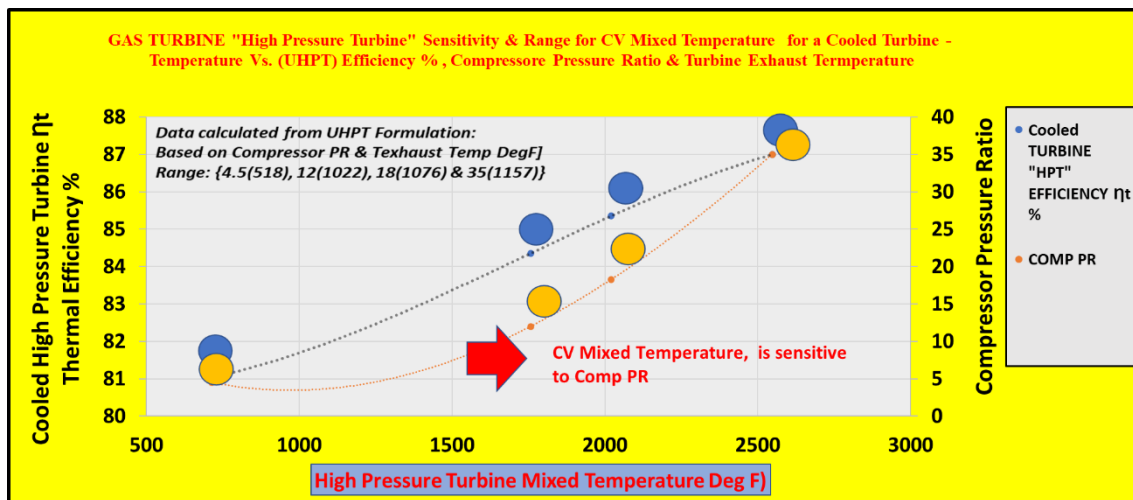


Figure 8.2 Gas turbine – Sensitivity of Mixed temperature TCV1 out, to cooled turbine stage efficiency for range of Compressor Pressure Ratio & Turbine Exhaust Temperatures- A detailed view

CHAPTER 9:

CONCLUSIONS AND REMARKS

Owing to the importance of addressing fuel cost, plant availability and increases in RAM(Reliability , Availability & Maintainability) and most of all addressing environmental concerns such as reduction of carbon footprint, collectively have prompted a paradigm shift in constantly challenging the status quo on turbine heat rate and the associated longevity of the Hot Gas Path components, hence the author through rigorous physics based research of the overall high pressure turbine has addressed in this dissertation, the overall synergistic physics based coupling of the mathematical formulations by considering and leveraging the effects of the various technical principles that govern the fundamentals of Thermodynamics, Mean Line Aero, Compressible fluid flow, external & Internal gas path HT , stress/strain and integrating from a systems approach.

To meet the ever-increasing demand for power generation; expeditious preliminary engine assessment, part evaluation and dispositioning of turbine component integrity while simultaneously sustaining optimal engine heat rate are required to be predicted from a preliminary perspective. This is leads to executing appropriate business decisions towards maintaining the longevity of the components considering optimum quality, design for manufacturing, time to market and competitive cost.... As an approximately 1% improvement in engine Efficiency can save ~ \$20 million In FUEL over the life of a typical Gas-fired 400-500 MW CC-power plant....

The author has coupled the various physics-based disciplines pertaining to the high-pressure gas turbine to generate a unified consolidated equation that can be leveraged towards predicting from a preliminary approach, a first cut, GT High Pressure Turbine efficiency, which feeds into the overall Gas Turbine thermal efficiency and in conjunction the author has also generated a mathematical formulation addressing from a preliminary one dimensional basis the component durability by introducing cooling only to the stationary component and hence the author has leveraged his academic learnings of the laws of thermodynamics, conservation of mass & energy, rate equation and continuum mechanics and aligned it to a defined control volume approach.

The author has also depicted an overall comparison of the computed Gas Turbine efficiency and compared the findings to the open literature [51]. This is extremely essential as the primary purpose of the turbine is to convert the enthalpy (energy) of the external gas path flow into shaft power to also drive the compressor, Today's most optimum and robust turbines have turbine efficiencies driven to be higher than approximately 90+%, and this is being done to ensure the OEM's remain competitive in the market and also simultaneously address carbon footprint and fuel savings. To ensure meeting the durability of the components the prerequisites to maintain component durability is against the needs to meet overall Gas Turbine engine cycle performance. Hence, ensuring the coupling or rather the integration from a systems perspective of the various disciplines is of the utmost importance.

The Unified High-Pressure Formulation based process as per aforementioned derivations of the major key parameters synergistically coupled based on the overall high pressure turbine Physics, can be applied towards a preliminary "first cut" evaluation based

on having knowledge of all aspects of the related high-pressure turbine required parameters. However, for the overall validation efforts, as the open literature[51] information leveraged from the Gas Turbine World 2020 performance specifications, is devoid of the high pressure turbine component based geometric information, such as component dimensions, internal and external specification of the actual loading conditions, e.g., actual three dimensional aerodynamic profile, Zweifel number, intermediate pressure and temperature variations, external gas path heat transfer coefficient, internal coolant path heat transfer coefficient based on turbulence promoters, cooling geometry, component mechanical constraints, overall mass flow distributions and variations etc. Hence, the author had to rely on the limited information provided in the aforementioned references and thus the conclusions or rather the scientific findings resulting from the Unified High Pressure Turbine formulation to the open literature[51] information, is holistically based on the authors bulk parameter based engineering assumptions leveraged from years of academic research and hence applied to the overall thermal resistances, heat load parameter[44], cooling effectiveness[44], cooling efficiencies gas path conditions, bulk based internal and external flow physics, overall assumptions on bulk mass fractions, and associated bulk losses, mechanical bearing losses[15], polytropic efficiencies[15], compressor adiabatic efficiencies[15], Discharge pressures and temperatures, bulk based specific heat ratio's, bulk Reynold number fractions between the gas path and coolant, etc. and by doing so the results of the validation is within approximately +/- (5% - 15%) of the overall Gas Turbine frame thermal " η_t " efficiency[51].

(9.1) Uncertainty band & Range of Parameters

Range of pertinent “bulk” based parameter assumptions are approximately the following:

- (i) $0.2 < \text{Cooling effectiveness} < 0.8$ [44]
- (ii) $0.2 < \text{Heat Load Parameter} < 2.5$ [44]
- (iii) $6000 < \text{Heat Rate (Btu/Kw-H)} < 12000$ [51]
- (iv) $0.85 < \text{Turbine } \eta_p \text{ (small stage eta-polytropic)} < 0.98$ [15]
- (v) $4.5 < \text{Compressor Pressure Ratio} < 35$ [51]
- (vi) $500 \text{ degF} < \text{Turbine-Exhaust} < 1220$ [51]
- (vii) $0.8 < \text{Compressor Adiabatic Efficiency} < 0.96$ [15]
- (viii) $700 \text{ F} < \text{Compressor Discharge Temperature} < 1000 \text{ F}$ [51]
- (ix) $60 \text{ PSIA} < \text{Compressor Discharge Pressure} < 500 \text{ PSIA}$ [51]
- (x) $0.82 < \text{Compressor Polytropic Efficiency} < 0.95$ [15]
- (xi) $0.90 < \text{Overall Comp \& Turbine (Bearing losses, friction etc.)} < 0.98$ [15]
- (xii) $1 < \text{Turbine Expansion Ratio} < 3.5$ [15]
- (xiii) $3000 < \text{RPM } (\omega) < 12000$ [51]

REFERENCES

- [1] Newby, R.A., Archer, D.H., Bannister, R.L. (1995), “Conversion of an advanced natural gas-fueled combustion turbine to coal based fuel applications” ASME 95-GT-162.
- [2] Southhall L., McQuiggan G., (1995), “New 200 MW Class 501G Combustion Turbine” ASME Paper 95-GT-215.
- [3] Editor, Sawyer John W., (1972), “Sawyer’s gas turbine engineering handbook”, second edition; Gas Turbine publications, inc.
- [4] Mattingly, Jack. D. (1996), “Elements of Gas Turbine propulsion” McGraw Hill Serues in Aeronautical and Aerospace Engineering, International editions 1996.
- [5] Chowdhury, Nafiz H.K., Zirakzadeh, Hootan, Han, Je-Chin, (2017) “A predictive Model for preliminary Gas turbine blade cooling Analysis”, (ASME; Journal of turbomachinery, VOL 139/091010-1).
- [6] Han, Je-Chin, Dutta, Sandip, and Ekkad, Srinath, (2000), “Gas Turbine Heat Transfer and cooling Technology” Second edition; CRC Press).
- [7] Zucrow, Maurie J., Joe., Hoffman D., (1976) “Gas Dynamics” Volume 1, John Wiley & Sons, Inc.
- [8] Schlichting Dr. Hermann, (1979) “Boundary Layer Theory” 7th Edition; McGraw Hill.

- [9] Moran, Michael J., Shapiro, Howard N., (1988), “Fundamentals of Engineering Thermodynamics” Second edition, John Wiley & Sons, Inc.
- [10] Incropera, Frank P. & DeWitt, David P., (1981),” Fundamentals of Heat and Mass Transfer”, Fourth Edition, John Wiley & Sons, Inc.
- [11] Cengel, Yunus. A & Boles, Michael A, (2006), “Thermodynamics-An engineering Approach”, Fifth edition, McGraw Hill
- [12] Wilson, David Gordon & Korakianitis, Theodosios, (1998), “The design of high Efficiency turbomachinery and gas turbines” Second edition; Prentice Hall)
- [13] Horlock, J.H., (1996) “Axial flow turbines (Fluid mechanics & thermodynamics)” BUTTERWORTH AND COMPANY (Publishers) LIMITED.
- [14] White, Frank. M, (1999), “Fluid Mechanics”, Fourth edition, McGraw Hill.
- [15] Farokhi, Saeed, (2014), “Aircraft propulsion”, Second edition, John Wiley & Sons Ltd.
- [16] Edited by Glassman, Arthur J., (1972), “Turbine Design and application, Volume 1- NASA SP-290, Lewis Research Center.
- [17] Edited by Glassman, Arthur J., (1972), “Turbine Design and application, Volume 3-NASA SP-290, Lewis Research Center.
- [18] Burmeister, Louis C, (1983), “Convective Heat Transfer”, John Wiley & Sons Inc.
- [19] Turbine Blade description,” gas turbine cooling airfoil cooling images - Bing images”
- [20] Turbine Blade cooling effectiveness, “turbine airfoil cooling effectiveness heat load parameter images - Bing images”

- [21] Moustapha, Hany, Zelesky, Mark. F., Baines, Nicholas.C., Japikse, David, (2003), “Axial and Radial Turbines” Concepts NREC.
- [22] Denton, J.D., (1993), “Loss mechanisms in turbomachines”, ASME 93-GT-435
- [23] Jordal, Kristin; Doctoral Thesis Lund University, (2001) “Modeling and performance of Gas Turbine Cycles with various Means of blade cooling”, Lund University, Sweden.
- [24] Gere & Timoshenko, (1990), “Mechanics of materials”, Third edition, International Thomas Publishing.
- [25] Dally, James. W & Riley, William. F, (1978), “Experimental stress analysis”, Second Edition, McGraw-Hill, Inc.
- [26] Cook, Robert. D. & Young, Warren. C, (1985), “Advanced Mechanics of Materials” Macmillan Publishing Company.
- [27] Shigley, Joseph. Edward & Mischke, Charles. R, (1989), “Mechanical engineering Design” Fifth Edition, McGraw Hill
- [28] U.S. Environmental Protection Agency Energy Trends in Selected Manufacturing Sectors, Opportunities and Challenges for Environmentally Preferable Energy Outcomes Final Report (March 2007) “U.S. Environmental Protection Agency)”
- [29] INTERNATIONAL ENERGY OUTLOOK 2020,
 “http://www.eia.gov/forecasts/ieo/more_highlights.cfm”

[30] Natural Gas vs Coal,

[“http://www.global-greenhouse-warming.com/gas-vs-coal.html”](http://www.global-greenhouse-warming.com/gas-vs-coal.html)

[31] Gas Turbine Efficiency Calculation: Avoid Higher Cost in Fuel Consumption
(araner.com)

[32] Combined Cycle Power Plant “combined cycle power plant - Google Search”

[33] Timoshenko, S.P., Goodier, J.N., (1970), “Theory of Elasticity”, Third Edition,
McGraw Hill Inc.

[34] Harman, Richard T.C, “Gas Turbine Engineering”, (1981), John Wiley & Sons.

[35] Walsh, P.P. & Fletcher, P., “Gas Turbine Performance”, (1998), Blackwell
Science Ltd and ASME

[36] Cross section of the gas turbine:

land based gas turbine cross section - Bing images

12666_2014_398_Fig1_HTML.gif (600×448) (springernature.com)

[37] Gas Turbine simple cycle schematic:

Features of Closed Cycle Gas Turbine - Bing images

[38] U.S Energy information administration International Energy Outlook Executive
Summary (eia.gov) & Global Energy Consumption To Grow 53 Percent by 2035,
Report Says - Yale E360

[39] Gas Turbine Firing Temperature Evolution

https://www.google.com/search?q=GAS+TURBINE+FIRING+TEMPERATURE&tbm=isch&ved=2ahUKEwi9tYWPnNHtAhWUds0KHUCIBJsQ2-cCegQIABAA&oq=GAS+TURBINE+FIRING+TEMPERATURE&gs_lcp=CgNpbWcQAzIECAAQGDIECAAQGD0GCAAQBxAeUKpGWOdTYO9WaABwAHgAgAFeiAHyBpIBAjEymAEAoAEBqgELZ3dzLXdpei1pbWfAAQE&sclient=img&ei=X1HZX_2JBpTttQbAkJLYCQ#imgsrc=1Uhvpg1DbjWYmM&imgdii=khfD8X6k0nT8NM

[40] Kreith, Frank, (1967), Principles of Heat Transfer, second edition, International Text Book Company.

[41] Brooks, Frank J., “GER-3567H”, GE Gas Turbine Performance Characteristics
GE Power Systems Schenectady, NY,
[GER-3567H - GE Gas Turbine Performance Characteristics](#)

[42] Combustor images; “[nasa combustor burner images - Bing images](#)”

[43] Thermal Barrier Coatings; “[thermal barrier cross section Rensselaer - Bing images](#)”

[44] Sunden, B. & Faghri, M., (2001),” Heat Transfer in Gas Turbines” WIT Press.

[45] Taylor, J.R., “Heat Transfer Phenomena in Gas Turbines” (1980), ASME 80-GT-172.

[46] (a)Energy and the Environment, “[Learn about Energy and its Impact on the Environment | Energy and the Environment | US EPA](#)” & (b)[Better combustion for power generation -- ScienceDaily](#)

- [47] TODAY IN ENERGY,
Energy sources have changed throughout the history of the United States - Today in Energy - U.S. Energy Information Administration (EIA)
- [48] High Efficiency Gas Turbines will play a growing role in energy transition, “High-Efficiency Gas Turbines Will Play a Growing Role in the Energy Transition (ge.com)”
- [49] Combined Cycle Plant, (a) “Combined cycle power plant - Wikipedia” (b) A typical Combined Cycle Gas Turbine (CCGT) plant and can potentially achieve a approximate thermal efficiency of - Bing
- [50] Douglas, J F., Gasiorek, J M., Swaffield, J A., (1980), “Fluid Mechanics”, Pitman Books Limited
- [51] Gas turbine Performance Specifications, “Gas Turbine World”, (2020) Performance Specs; 36th Edition
- [52] Hansen, Kurt, Prof; Kantha, Lakshmi, (2009), “Land based Gas Turbines for Power Production” ASEN 5063; December 15th, 2009
- [53] Ajoko, Tolumoye John Department of Mechanical/Marine Engineering, Faculty of Engineering. Niger Delta University, Wilberforce Island, Bayelsa State, Nigeria, (2014) “Design Study for Single Stage High Pressure Turbine of Gas Turbine Engines” Department of Mechanical/Marine Engineering, Faculty of Engineering. Niger Delta University, Wilberforce Island, Bayelsa State, Nigeria, American Journal of Engineering Research (AJER).
- [54] Hill, Philip, Peterson, Carl, (1992), “Mechanics and Thermodynamics of Propulsion”, Adderson-Wesley Publishing Company,

[55] Thomson, L.M. Milne, (1972), “Theoretical Hydrodynamics, Macmillan Press LTD.

[56] GT Combined Cycle Power Plant Combined Cycle Power Plant - Bing images

[57] gas turbine combustion firing temperature images - Bing images

[58] higher turbine inlet temperature - Bing images

[59] Bertin, John. J. Smith, Michael. L, (1989), “Aerodynamics for engineers”,
Second edition, Prentice Hall, Inc

APPENDIX A:

**GAS TURBINE OVERALL THERMAL EFFICIENCY (UHPT PROCESS VS.
GT WORLD SIMPLE CYCLE SPECIFICATIONS EFFICIENCY DATA- (2020
36TH EDITION)**

Reference Material [51] Reference Gas Turbine World, 2020 Performance Specs; 36th Edition have been applied towards the assessments and comparisons to results from the Unified High Pressure Turbine Process.

This material from open literature has been leveraged towards calibration & validation of the Unified High Pressure Turbine formulation related to the HPT – Turbine efficiency.

Tables including heat rate values, compressor pressure ratio's gas turbine exhaust temperatures, generated from the overall Gas Turbine validation process that were based on the assumed bulk parameters-based engineering assumptions referenced from open literature, as aforementioned in the section above, are also depicted.

Table A.1: Gas Turbine Overall Thermal Efficiency (UHPT Process Vs. GT World Simple Cycle Specifications Efficiency data- (2020 36th Edition) [51]

| OEM-Compressor P-ratio (GTW 36th Edition) 2020 Performance Spec | Overall GT (cooled Turbine) η t% (UHPT) | Reference: OEM GTW SIMPLE CYCLE SPECS (GT WORLD) Actual overall GT η % |
|--|---|---|
| 12 | 37.69 | 36.30 |
| 18.3 | 42.57 | 36.40 |
| 35 | 50.45 | 41.00 |
| 4.5 | 23.31 | 30.00 |
| 13.1 | 39.42 | 34.60 |
| 13.3 | 39.70 | 37.00 |
| 22.8 | 46.47 | 42.90 |
| 23.8 | 48.07 | 44.00 |
| 18.6 | 41.29 | 34.30 |
| 25.8 | 47.37 | 40.30 |
| 10.5 | 34.23 | 28.40 |
| 17.4 | 39.96 | 35.80 |
| 12.2 | 38.06 | 32.10 |
| 12.7 | 38.94 | 32.70 |
| 12.7 | 38.95 | 33.80 |
| 10.3 | 34.32 | 29.10 |
| 13.9 | 42.76 | 32.40 |
| 13.8 | 42.39 | 31.00 |
| 13.8 | 37.92 | 34.20 |
| 15.5 | 41.46 | 34.50 |
| 16.8 | 42.30 | 34.80 |
| 18.9 | 44.12 | 35.40 |
| 13 | 39.63 | 33.90 |
| 16.7 | 39.86 | 38.60 |
| 19.2 | 39.82 | 37.80 |
| 21.6 | 43.94 | 42.00 |
| 23.1 | 47.64 | 42.60 |
| 23.7 | 49.87 | 43.30 |

APPENDIX B:

COMPARISON OF COMPRESSOR PRESSURE RATIO'S VS. HEATV

RATES (BTU/KW-HR.)

Table B.1: Comparison of Compressor Pressure Ratio's vs. Heat Rates (Btu/Kw-Hr.)

| OEM-(COMP-PR) GTW [51] | UHPT-HR | OEM- GTW HR [51] |
|---------------------------|----------|------------------|
| 12 | 9053.398 | 9400 |
| 18.3 | 8016.167 | 9374 |
| 35 | 6762.945 | 8322 |
| 4.5 | 11374 | 11374 |
| 13.1 | 8655.978 | 9860 |
| 13.3 | 8595.716 | 9210 |
| 22.8 | 7342.98 | 7960 |
| 23. 8 | 7098.732 | 7740 |
| 18.6 | 8263.287 | 9948 |
| 25. 8 | 7203.536 | 8460 |
| 10.5 | 9967.484 | 12025 |
| 17.4 | 8539.624 | 9517 |
| 12.2 | 8964.855 | 10644 |
| 12.7 | 8763.249 | 10417 |
| 12.7 | 8759.704 | 10094 |
| 10.3 | 9942.902 | 11747 |
| 13.9 | 7978.997 | 10631 |
| 13.8 | 8049.844 | 10973 |
| 13.8 | 8998.675 | 10526 |
| 15.5 | 8230.331 | 10831 |
| 16.8 | 8065.66 | 9815 |
| 18.9 | 7733.168 | 9647 |
| 13 | 8609.96 | 10060 |
| 16.7 | 8559.772 | 8840 |
| 19.2 | 8567.829 | 9019 |
| 21.6 | 7764.862 | 8120 |
| 23.1 | 7163.029 | 8009 |
| 23.7 | 6841.773 | 7884 |

APPENDIX C:

GAS TURBINE EXHAUST TEMPERATURE VS. COMPRESSOR

PRESSURE RATIO

Table C.1: Gas Turbine Exhaust Temperature Vs. Compressor Pressure Ratio

| T-Exhaust [51] | COMP PR [51] |
|----------------|--------------|
| 1022 | 12 |
| 1076 | 18.3 |
| 1157 | 35 |
| 518 | 4.5 |
| 1012 | 13.1 |
| 1007 | 13.3 |
| 1199 | 22.8 |
| 1184 | 23.8 |
| 1006 | 18.6 |
| 936 | 25.8 |
| 901 | 10.5 |
| 964 | 17.4 |
| 1016 | 12.2 |
| 995 | 12.7 |
| 1004 | 12.7 |
| 1031 | 10.3 |
| 923 | 13.9 |
| 997 | 13.8 |
| 940 | 13.8 |
| 966 | 15.5 |
| 1031 | 16.8 |
| 1004 | 18.9 |
| 1026 | 13 |
| 1151 | 16.7 |
| 1212 | 19.2 |
| 1158 | 21.6 |
| 1202 | 23.1 |
| 1217 | 23.7 |

APPENDIX D:

COMPARISON OF THE UNCOOLED TURBINE EFFICIENCY(UHPT) η_t

% VS. η_t -ADIABATIC % (BASED ON TURBINE (HPT) ISENTROPIC

EQUATION-NO TURBINE COOLING)

Table D.1: Comparison of the uncooled turbine efficiency (UHPT) η_t % Vs. η_t -Adiabatic % (Based on Turbine (HPT) Isentropic equation-No Turbine Cooling)

| Compressor P-ratio-GAS TURBINE WORLD [51] | UN-COOLED "HPT" TURBINE (UHPT)EFFICIENCY η_t % | η_t -Adiabatic-% (BASED ON "HPT" TURBINE ISENTROPICEQUATION-NO TURBINE COOLING) (Literature Search [4]) |
|---|---|--|
| 12 | 86.51156485 | 86.72503401 |
| 18.3 | 90.98560131 | 91.12780097 |
| 35 | 93.73277234 | 93.88306297 |
| 4.5 | 80.94496763 | 81.41528148 |
| 13.1 | 91.97235241 | 92.18488774 |
| 13.3 | 92.72522329 | 92.93680177 |
| 22.8 | 97.29229801 | 97.45889199 |
| 23.8 | 97.314106 | 97.47605778 |
| 18.6 | 90.99190536 | 91.14843934 |
| 25.8 | 98.62106528 | 98.76543462 |
| 10.5 | 83.04488036 | 83.2618888 |
| 17.4 | 90.32343553 | 90.48264258 |
| 12.2 | 86.93480569 | 87.1451262 |
| 12.7 | 87.78763073 | 87.98842671 |
| 12.7 | 87.78631974 | 87.98842671 |
| 10.3 | 82.97790037 | 83.22123352 |
| 13.9 | 93.88931665 | 94.06801094 |
| 13.8 | 93.14781413 | 93.338332918 |
| 13.8 | 93.15582355 | 93.338332918 |
| 15.5 | 90.00533594 | 90.177996614 |
| 16.8 | 90.7016517 | 90.8731928 |
| 16.9 | 91.72744936 | 91.88218237 |
| 13 | 88.60836071 | 88.79318194 |
| 16.7 | 91.91103168 | 92.09596214 |
| 19.2 | 91.71470768 | 91.90068668 |
| 21.6 | 96.28304006 | 96.45303325 |
| 23.1 | 97.61638836 | 97.78602918 |
| 23.7 | 97.94643818 | 98.11423521 |